Investigation of the Role of Thioredoxin-interacting Protein (TXNIP) in Cellular Senescence and Aging

Mohammed Abubaker

A thesis in conformity with the requirements for the degree of Doctor of Philosophy

Experimental Medicine

McGill University

Investigation of the Role of Thioredoxin-interacting Protein (TXNIP) in Cellular Senescence and Aging

Abstract

Thioredoxin-interacting protein (TXNIP), also known as Vitamin D upregulated protein (VDUP), is an alpha arrestin family member that acts as an endogenous inhibitor of the thiol oxidoreductase thioredoxin (TRX). TXNIP expression is heightened in response to hyperglycemia, vitamin D, and longevity-inducing factors such as calorie restriction and fasting. During studies of the role of TXNIP in diabetic nephropathy, it was observed that TXNIP KO cells were characterized by decreased cell number but also decreased apoptosis, reminiscent of cellular senescence. Thus this thesis aimed to investigate TXNIP's role in cellular senescence and organismal aging using a replicative model of senescence in mouse mesangial cells (MC) derived from wild-type (WT) and TXNIP knockout (KO) mice.

Serial passaging of WT MC revealed a senescence phenotype characterized by upregulation of P53, cyclin-dependent kinase inhibitor P16, and beta-galactosidase staining, along with significant downregulation of TXNIP mRNA and protein levels at passage 25 (late passage; LP). Notably, TXNIP is known to be transcriptionally induced by the glucose sensors as carbohydrate response element binding protein (ChREBP) and MondoA. Both were found to be downregulated in the LP cells which may account for the downregulation of TXNIP. Culturing the cells in high glucose was found to rescue the expression of TXNIP in LP cells.

TXNIP KO MC exhibited a comparable senescence phenotype at passage 5-7 (early passage; EP), associated with reduced PTEN phosphatase activity and increased activity of AKT. Pharmacological inhibition of AKT and its upstream activator PI3 kinase rescued the senescence

phenotype in TXNIP KO MC. Furthermore, TXNIP KO MC displayed increased reactive oxygen species (ROS) accumulation from NADPH oxidase (NOX4), increased resistance to apoptosis, and elevated oncogene RAS activity.

Lentivirus-mediated overexpression of wild-type TXNIP in TXNIP KO MC rescued the senescence phenotype, while thiol binding site mutant TXNIP (Cys to Ser at 247) was less effective underscoring the importance of TXNIP's thiol binding activity in mitigating cellular senescence. In vivo studies in aged mice (21 months old) confirmed reduced TXNIP expression in kidney cortex and brain hippocampal regions compared to young mice (6 months old). Additionally, TXNIP KO male mice showed impaired cognitive and motor functions (measured by spontaneous alteration behavior (SAB) in a Y-maze and latency to fall in a Rota-rod apparatus) respectively. Furthermore, TXNIP KO mice exhibited increased senescence markers and AKT activity in kidney cortex and hippocampus. TXNIP KO mice showed a significantly reduced longevity compared to WT mice.

These findings indicate that TXNIP is protective against cellular senescence and aging in murine models. Furthermore, these data support the involvement of the AKT pathway in these phenomena. These findings offer potential therapeutic strategies for aging and age-related disorders.

Résumé

La protéine d'interaction avec la thioredoxine (TXNIP), également connue sous le nom de protéine régulée à la hausse par la vitamine D (VDUP), est un membre de la famille des arrestines alpha qui agit comme un inhibiteur endogène de la thiol-oxydoréductase thioredoxine (TRX). L'expression de TXNIP est augmentée en réponse à l'hyperglycémie, à la vitamine D et à des facteurs induisant la longévité tels que la restriction calorique et le jeûne. Lors des études sur le rôle de TXNIP dans la néphropathie diabétique, il a été observé que les cellules KO TXNIP étaient caractérisées par une diminution du nombre de cellules mais aussi une diminution de l'apoptose, rappelant la sénescence cellulaire. Ainsi, cette thèse visait à étudier le rôle de TXNIP dans la sénescence cellulaire et le vieillissement des organismes en utilisant un modèle réplicatif de sénescence dans des cellules mésangiales de souris (MC) dérivées de souris de type sauvage (WT) et de souris knockout TXNIP (KO).

Le passage en série des MC WT a révélé un phénotype de sénescence caractérisé par une régulation à la hausse de P53, de l'inhibiteur de la kinase dépendante des cyclines P16 et de la coloration à la bêta-galactosidase, ainsi qu'une régulation à la baisse significative des niveaux d'ARNm et de protéine TXNIP au passage 25 (passage tardif; LP). Il est à noter que TXNIP est connu pour être induit transcriptionnellement par les capteurs de glucose tels que la protéine de liaison à l'élément de réponse aux glucides (ChREBP) et MondoA. Les deux ont été trouvés régulés à la baisse dans les cellules LP, ce qui pourrait expliquer la régulation à la baisse de TXNIP. La culture des cellules dans un milieu à haute teneur en glucose a permis de sauver l'expression de TXNIP dans les cellules LP.

Les MC KO TXNIP ont montré un phénotype de sénescence comparable au passage 5-7 (passage précoce; EP), associé à une activité réduite de la phosphatase PTEN et à une activité accrue d'AKT.

L'inhibition pharmacologique d'AKT et de son activateur en amont, la PI3 kinase, a permis de sauver le phénotype de sénescence dans les MC KO TXNIP. En outre, les MC KO TXNIP présentaient une accumulation accrue d'espèces réactives de l'oxygène (ROS) provenant de la NADPH oxydase (NOX4), une résistance accrue à l'apoptose et une activité élevée de l'oncogène RAS.

La surexpression médiée par lentivirus de TXNIP de type sauvage dans les MC KO TXNIP a sauvé le phénotype de sénescence, tandis que le mutant de site de liaison thiol TXNIP (Cys en Ser à 247) était moins efficace, soulignant l'importance de l'activité de liaison thiol de TXNIP dans la mitigation de la sénescence cellulaire. Des études in vivo chez des souris âgées (21 mois) ont confirmé une expression réduite de TXNIP dans le cortex rénal et les régions hippocampiques du cerveau par rapport à des souris jeunes (6 mois). De plus, les souris mâles KO TXNIP ont montré des fonctions cognitives et motrices altérées (mesurées par le comportement de modification spontanée (SAB) dans un labyrinthe en Y et la latence à la chute dans un appareil Rota-rod) respectivement. En outre, les souris KO TXNIP présentaient des marqueurs de sénescence accrus et une activité AKT dans le cortex rénal et l'hippocampe. Les souris KO TXNIP ont montré une longévité significativement réduite par rapport aux souris WT.

Ces résultats indiquent que TXNIP est protecteur contre la sénescence cellulaire et le vieillissement dans les modèles murins. De plus, ces données soutiennent l'implication de la voie AKT dans ces phénomènes. Ces découvertes offrent des stratégies thérapeutiques potentielles pour le vieillissement et les troubles liés à l'âge.

Acknowledgments

I would like to express my deepest gratitude to my supervisor, Professor Dr. I. George Fantus, for his unwavering patience, trust, and invaluable support throughout this thesis. His guidance and insights have been instrumental in shaping this research.

I am also immensely grateful to our lab research associate, Ling Xia, for her kindness, support, and dedicated guidance. Her expertise and willingness to share knowledge have greatly contributed to the success of this work.

I extend heartfelt thanks to my thesis committee members, Dr. Jose Morais, Dr. Stephane Laporte, and Dr. Simon Wing, for their invaluable contributions, feedback, and encouragement at every stage of this study.

Lastly, I want to express my deepest appreciation to my parents and family for their unwavering love, support, and understanding throughout this journey. Their encouragement has been my motivation.

Thank you all for believing in me and supporting me during this challenging yet rewarding endeavor.

Contribution to original knowledge

This thesis makes several significant contributions to the field of cellular senescence, aging, and the role of thioredoxin-interacting protein (TXNIP), thereby adding to the body of original knowledge in these areas. The key contributions are as follows:

Novel Insights into TXNIP Function in Senescence

The project provides new evidence demonstrating the crucial role of TXNIP in mitigating cellular senescence. By comparing wild-type (WT) and TXNIP knockout (KO) mouse mesangial cells (MC) at various passages, it was shown that TXNIP deficiency leads to early onset of senescence. This extends the understanding of TXNIP's regulatory functions beyond its known role as an endogenous inhibitor of thioredoxin (Trx).

In Vivo Confirmation of TXNIP's Role

The in vivo studies presented here are the first to document the impact of TXNIP deficiency on lifespan and age-related phenotypes in mice. The significant reduction in longevity and increased incidence of tumors in TXNIP KO mice provide strong evidence of TXNIP's importance in aging and as a tumor suppressor. These findings contribute to the understanding of how TXNIP influences organismal aging.

Mechanistic Insights into ROS and AKT Pathways

This research elucidates the mechanistic pathways involving reactive oxygen species (ROS) and AKT signaling in the context of TXNIP deficiency. The study demonstrates that loss of TXNIP leads to increased ROS production and hyperactivated AKT pathway, contributing to cellular

senescence and resistance to apoptosis. These insights add a new dimension to the understanding of redox regulation and senescence pathways.

Differential Effects in Male and Female Mice

The project uniquely identifies sex-specific differences in the aging phenotypes of TXNIP KO mice. The findings that male and female TXNIP KO mice exhibit distinct patterns of cognitive decline, motor coordination, and body composition with aging add a novel aspect to the study of TXNIP, highlighting the importance of considering sex as a biological variable in aging research.

Role of Nrf2 in TXNIP-Deficient Cells

The discovery that TXNIP KO MC have upregulated Nrf2, which suggests a pivotal role for Nrf2 in maintaining cellular survival and resisting apoptosis in TXNIP-deficient cells, through its regulation of antioxidant genes like catalase and SOD2, provides new insights into the interplay between TXNIP and Nrf2. This contributes to the broader understanding of how cells adapt to oxidative stress in the absence of TXNIP.

Therapeutic Implications

The thesis also explores potential therapeutic strategies, such as the use of AKT and PI3K inhibitors to rescue the senescence phenotype in TXNIP KO cells. This offers a promising avenue for developing interventions aimed at modulating TXNIP activity to combat aging and related diseases.

Identification of Tumor Suppressor Functions

The findings reinforce the role of TXNIP as a tumor suppressor, with its downregulation observed in various cancers. By linking TXNIP deficiency to increased AKT activation and oncogene Ras

activity, the study provides a mechanistic basis for TXNIP's involvement in tumor suppression, thereby contributing to cancer biology.

In summary, this project significantly advances the understanding of TXNIP's role in cellular senescence, organismal aging, tumor formation and longevity. The findings not only provide mechanistic insights but also open up new research directions and potential therapeutic strategies, making a substantial contribution to the field of aging and age-related diseases.

Contributions of the authors

My supervisor, Dr. I. George Fantus, was instrumental in conceiving the study and played a crucial role in training me in experimental design and result interpretation. Under his guidance, I developed the skills necessary to carry out rigorous scientific research.

Ling Xia provided invaluable assistance in teaching me the practical aspects of working in a research laboratory. She patiently guided me through numerous techniques, including cell culture, Western blotting, microscopy, cellular imaging, and the collection and treatment of mice tissues. Her support was essential in helping me acquire the technical expertise needed for this project.

I took primary responsibility for designing and executing most of the experiments, organizing and analyzing the data, interpreting the results, and presenting the original ideas that drove our research forward. This hands-on experience was crucial in honing my research skills and deepening my understanding of the scientific process.

The thesis was authored by me, with Dr. I. George Fantus providing critical editorial feedback to refine and enhance it. His mentorship and editorial guidance were invaluable in shaping the final document.

Table of Contents

List of Tables

List of Figures

Chapter 1 Introduction and Literature Review

Chapter 3 Results

List of Abbreviations

2-DG	2-deoxy glucose
Ab	Antibody
ADP	Adenosine diphosphate
AGR	Agouti-related protein
AKT	Protein kinase B
AML	Acute myeloid leukemia
ANOVA	Analysis of variance
AOs	Antioxidants
AP-1	Activator protein 1
ARRDC	Arrestin Domain Containing proteins
ASK1	Apoptosis signal-regulating kinase I
ATM	Ataxia-Telangiectasia mutated
ATP	Adenosine triphosphate
Bcl-2	B-cell lymphoma 2
BSA	Bovine serum albumin
CD45	Lymphocyte common antigen

C. elegans	Caenorhabditis elegans
CDKI	Cyclin dependent kinase inhibitor
ChoRE	Carbohydrate response element
ChREBP	Carbohydrate response element-binding protein
CK20	Cytokeratin 20
CLS	Chronological lifespan
CoQ	Ubiquinone
COX-2	Cyclooxygenase-2
CPP	Cell-penetrating peptide
CRM 1	Chromosome maintenance region 1
CUL3	Cullin-3
CXCL1	C-X-C motif chemokine ligand 1
DCF	2′,7′-di- chlorofluorescein
DDIT4	DNA damage-inducible transcript 4
DDR	DNA damage response
DMEM	Dulbecco's modified Eagle's medium
DSBs	DNA double-strand breaks

ECL	Enhanced chemiluminescence
EDTA	Ethylenediaminetetraacetic acid
EP	Early passage
ER	Endoplasmic reticulum
ES	Embryonic stem cells
ETC	Electron transport chain
F6P	Fructose-6-Phosphate
FAD	Flavin adenine dinucleotide
FBS	Fetal bovine serum
FOXO1	Forkhead box protein O1
FOXO3	Forkhead box protein O3
FRT	Free radical theory
G6P	Glucose-6-Phosphate
GCL	Gamma cysteine ligase
GDP	Guanosine diphosphate
GFP	Green fluorescent protein
GLUT	Glucose transporter

GPCRs	G protein-coupled receptors
GPx	Glutathione peroxidase
GR	Glutathione reductase
Grx	Glutaredoxin
GSEA	Gene Set Enrichment Analysis
GSH	Glutathione
GTEx	Genotype Tissue Expression
GTP	Guanosine triphosphate
H_2O	Water
H_2O_2	Hydrogen peroxide
HEPES	4-(2-hydroxyethyl)-1-piperazine ethanesulfonic acid
HFD	High-fat diet
HG	High glucose
HIF-1α	Hypoxia inducible factor 1-α
IgG	Immunoglobulin G
IL	Interleukin
IR	Ionizing radiation

HNE	4-hydroxynonenal
$HO^{\bullet}$	Hydroxyl
HO-1	Heme oxygenase-1
$HO_2^{\bullet}$	Hydroperoxyl
HRE	Hypoxia-response element
HSCs	Hematopoietic stem cells
IHC	Immunohistochemistry
ITIM	Immunoreceptor tyrosine-based inhibition motif
Keap1	Kelch-like ECH associating protein 1
KO	Knockout
LIF	Leukemia-inhibitory factor
LP	Late passage
MAPK	Mitogen-activated protein kinase
MC	Mesangial cells
Mclk1	Mammalian clk1
MEF	Mouse embryonic fibroblasts
MnSOD	Manganese superoxide dismutase

MOI	Multiplicity of infection
MRI	Magnetic resonance imaging
mRNA	Messenger RNA
MRS	Magnetic resonance spectroscopy
MS	Multiple sclerosis
mTORC1	Mechanistic target of rapamycin complex 1
mut.	Mutant
NAC	N-acetyl cysteine
NAD	Nicotinamide adenine dinucleotide
NADPH	Nicotinamide adenine dinucleotide phosphate
NF-κB	Nuclear factor kappa-light-chain-enhancer of activated B cells
NG	Normal glucose
NLRP3	Nucleotide-binding oligomerization domain (NOD)-like receptor (NLR) protein 3
NK	Natural killer cells
NO	Nitric Oxide
NOX	Nicotinamide dinucleotide phosphate (NADPH) oxidase

NOX4	NADPH oxidase 4
Nrf2	Nuclear factor (erythroid-derived 2)-like 2
NUO-6	Ubiquinone Oxidoreductase
$O_2^{\bullet -}$	Superoxide
O_2	Oxygen
OIS	Oncogene-induced senescence
OS	Osteosarcoma
OXPHOS	Oxidative phosphorylation
p	Observed significance level
PCR	Polymerase chain reaction
PD	Parkinson disease
PFC	Prefrontal cortex
PGCs	Pprimordial germ cells
PHD	Prolyl hydroxylase domain
PI3K	Protein kinases (MAPK), phosphoinositide 3-kinase
PRDX	Peroxiredoxin
PTEN	Phosphatase and TENsin homolog deleted on chromosome 10

PTP1B	Protein tyrosine phosphatase 1B
pVHL	von Hippel- Lindau protein
Ras	Rat sarcoma virus
RNS	Reactive nitrogen species
$RO_2^{\bullet-}$	Peroxyl
$RO^{\bullet}$	Alkoxyl radicals
ROS	Reactive Oxygen Species
RPE	Retinal pigment epithelium
RPM	Rotation per minute
RTKs	Receptor tyrosine kinases
SA-β-gal	Senescence associated beta galactosidase staining
SASP	Senescence associated secretory phenotype
SCD	Standardchow diet
SDS-PAGE	Sodium dodecyl sulfate polyacrylamide gel electrophoresis
sMAF	Small musculoaponeurotic fibrosarcoma
SMS	Senescence messaging system
SOD	Superoxide dismutases

STZ	Streptozotocin
TAFs	Telomere-associated foci
TBP2	Thioredoxin-binding protein 2
TCA cycle	Tricarboxylic acid cycle
TGF-β	Transforming growth factor beta
TIFs	Telomere dysfunction-induced foci
TNF-α	Tumor necrosis factor-alpha
Trx	Thioredoxin
TrxR	Thioredoxin reductase
TSP1	Thrombospondin 1
TUNEL	Terminal deoxynucleotidyl transferase-mediated dUTP nick-end labeling
TXNIP	Thioredoxin Interacting Protein
UV	Ultraviolet
VSMCs	Vascular smooth muscle cells
VDUP1	Vitamin D upregulated protein 1
VEGF	vascular endothelial growth factor

WT	Wildtype
XIAP	X-linked inhibitor of apoptosis protein

Amino Acid Abbreviations

Cys	Cysteine
Thr	Threonine
Ser	Serine

Methodological Abbreviations

%	Percent
°C	Degree celsius
BW	Body weight
g	gram
h	hour(s)
l	liters
M	molar
m	month
min	minute(s)
mol	moles
sec	second(s)

Chapter 1 Introduction and Literature Review

1.1 Aging: Epidemiology and Consequences

Aging is a biological process that impacts the majority of living organisms. However, some primitive species, such as *hydra* and other cnidarians, may be the only exceptions to this natural rule, as they do not possess post-mitotic cells [1, 2]. Aging was defined by Herman and Denham as "the progressive accumulation of changes with time that are associated with or responsible for the ever-increasing susceptibility to disease and death which accompanies advancing age" [3]. Aging demographics have shifted dramatically in recent decades. With rising life expectancy, populations, especially of the developed countries have increased the proportion of older age people (65 years and above) compared to younger ages in a phenomenon known as population aging [4].

The aging population is an escalating global challenge and is set to become one of the most significant social changes of the twenty-first century. According to the United Nations World Population Prospects: 2022 Revision, by 2050, it is projected that 16% of individuals worldwide will be over the age of 65, an increase from 10% in 2022 [5]. By mid-century, 25% of the population in Europe and North America could be 65 years or older. In 2018, for the first time ever, the global population of people aged 65 and above surpassed the number of children under five. Furthermore, the number of individuals aged 80 and over is expected to triple, rising from 143 million in 2019 to 426 million by 2050 [5].

As documented in the most recent publication by Statistics Canada in July 2023, more than 7 million Canadians were 65 years or older, accounting for 18.9 percent of the country's population [6]. By 2030, this senior population is projected to exceed 9.5 million, making up 23.8 percent of all Canadians. Additionally, by 2036, the average life expectancy at birth is expected to increase

to 87.3 years for women, up from 83.95 years in 2020, and to 84.0 years for men, up from 79.84 years in 2020 [7, 8].

The aging of the population brings forth adverse consequences and repercussions that impact nearly every facet of society. These include but are not limited to:

1- Functional decline: With aging, there is a decline in physical and cognitive function. Activities of daily living (ADLs), such as dressing, bathing, and eating, may become challenging, leading to increased dependency on caregivers [9].
2- Economic burden: The healthcare costs associated with aging are substantial. Older adults often require more medical services, prescription medications, and long-term care, which can strain healthcare systems and individual finances [10].
3- Social isolation: Older adults may experience social isolation due to factors such as the loss of friends and family, limited mobility, and retirement. Social isolation can have adverse effects on mental health and overall well-being [11].
4- Healthcare System Challenges: An aging population places pressure on healthcare systems to adapt to the specific needs of older adults, including geriatric care, specialized medical services, and age-friendly infrastructure [12].

1.2 Aging and age-associated diseases

Aging is a major risk factor for many chronic diseases [13-15], including cardiovascular diseases [16, 17], cancer, diabetes, and neurodegenerative disorders such as Alzheimer's disease [18, 19]. These conditions have a significant impact on the health and quality of life of older adults. Approximately 100,000 individuals across the globe die of age-related ailments daily [20].

1.3 Pathophysiology of aging:

Mitochondrial dysfunction, increased Reactive Oxygen Species (ROS) production and oxidative stress, emerge as pivotal mechanisms that bridge aging with a myriad of age-associated diseases [21]. There are multiple intricate mechanisms that link age-associated diseases with mitochondrial dysfunction and oxidative stress including:

1. ROS production: As cells utilize oxygen to produce energy through aerobic metabolism, they generate ROS as natural byproducts [22]. Unopposed excess ROS, including superoxide radicals and hydrogen peroxide, can cause damage to cellular macromolecules, such as DNA, proteins, and lipids. Over the lifespan, ROS accumulation and production has been found to be increased, leading to oxidative stress in aged mouse brains [23, 24], human fibroblasts [25] and several other tissues and cells in animals and humans [26, 27].
2. Antioxidant Defense Decline: Aging is associated with a gradual decline in the efficiency of the body's antioxidant defense mechanisms, which normally counteract ROS. In the elderly, Ferric (Fe^{+++}) reducing ability of the plasma, an indicator of antioxidant capacity, was found to be significantly decreased as a factor of age [28].This imbalance between ROS production and antioxidant capacity contributes to ROS accumulation and oxidative stress associated with aging.
3. Cellular Consequences: Oxidative stress can trigger a cascade of cellular events, including DNA damage, protein oxidation, and lipid peroxidation, which promote the development of age-related pathologies [29].
4. Energy Decline: Age-related mitochondrial dysfunction can lead to decreased ATP production, affecting cellular energy levels and overall tissue function. This energy decline is particularly significant in highly energy-demanding tissues like muscle [30].

1.4 Theories of aging

Aging is a multifactorial process influenced by a combination of genetic, environmental, and lifestyle factors. In the context of genetic determinants of aging, progeroid syndromes are classified as human genetic disorders characterized by a markedly reduced lifespan and the premature onset of a distinct set of biological changes typically associated with advanced age [31]. Despite their rarity in humans, numerous progeroid mouse models have been generated to study these syndromes and gain mechanistic insights into the aging process. For instance, the Hutchinson-Gilford progeria mouse model, which carries the G608G mutation in the human Lamin A/C (LMNA) gene. This mutation, although synonymous (Gly608Gly) and not altering the amino acid sequence, activates a cryptic splice site. This activation leads to the production of an aberrant, truncated form of lamin A, termed progerin. In the wild-type LMNA gene, the nucleotide sequence at the relevant position is GGT GGC CAG GAG CGC AGT, where the codon GGC encodes for glycine at position 608. In the Hutchinson-Gilford Progeria Syndrome (HGPS) G608G mutation, the sequence is altered to GGT GGT CAG GAG CGC AGT, where the codon GGT still encodes for glycine. This mouse model is specifically used to mimic the human condition. Additionally, more generalized progeroid mouse models exhibit defects in DNA repair mechanisms, such as Terc-/-, Ku86-/-, Ercc1-/-, and Dna-pkcs−/− mutants. These models demonstrate accelerated aging phenotypes due to compromised DNA repair capabilities [31].

Environmental factors such as diet, physical activity, exposure to pollutants, and socioeconomic status have a significant impact on the rate of aging [32].

To understand what underlies the aging process, several theories have been proposed, with the free radical theory of aging being the oldest.

1.4.1 Free radical theory of aging (FRT)

One prominent theory of aging is the "free radical theory" of aging, which posits that cumulative damage from reactive oxygen species (ROS) contributes to aging [33].

According to the FRT of aging, the age-related decline in physiological function results from molecular damage caused by oxidative stress, as proposed by Harman in 1956. This oxidative stress can lead to cellular damage, DNA mutations, and the activation of inflammatory pathways [33]. The significance of defending against this damage induced by free radicals is underscored by the presence of antioxidant defense systems in all living organisms [34].

Support for the FRT is substantial and includes key findings such as the correlation of shorter lifespan with increased production of mitochondrial oxidants, as demonstrated by multiple studies in different mammalian and bird species [35-39]. Genetic intervention studies have provided compelling evidence that augmenting the activity of antioxidant enzymes, which reduce oxidative stress, can extend lifespan in various organisms. In yeast, all mutants that exhibit an extended chronological lifespan (CLS) indicate that maintaining manganese superoxide dismutase (MnSOD) activity is necessary to achieve the extension of longevity [40-42]. Furthermore, co-expressing SOD1 and SOD2 led to a 30% increase in CLS, whereas expressing each SOD individually had a noticeable but less substantial impact [41, 43]. Knockout mutations of yeast SOD2 result in reduced chronological and replicative lifespan [44, 45].

In Caenorhabditis elegans (*C. elegans*), the imposition of peroxide stress resulted in the manifestation of aging-associated phenotypes, including diminished mobility, a slowed growth rate, and reduced ATP levels. Notably, the genetic ablation of the antioxidant protein peroxiredoxin 2 (PRDX-2) mirrored the effects observed under chronic peroxide exposure, displaying a comparable phenotype and a notable reduction in lifespan [46]. Additional

corroborative evidence in *C. elegans* lends support to the proposition that augmentation of antioxidant enzyme activity holds potential for extending longevity [47-51].

In studies involving various models, the beneficial impact of extending lifespan through the overexpression of SODs has been consistently demonstrated in *Drosophila melanogaster*. For example, in a transgenic system employing flippase (FLP recombinase) to facilitate the overexpression of transgenes, it was noted that elevating the levels of either SOD1 or catalase provided resistance to H_2O_2-induced damage. However, only the overexpression of SOD1 had the capacity to extend lifespan [52]. In another study that also applied the FLP recombinase, the act of overexpressing SOD2 has likewise been found to boost the mean lifespan by an average of approximately 16%, with certain lines exhibiting increases of 30-33%. The maximum lifespan, on average, saw an increase of about 15%, with one line even demonstrating a remarkable 37% extension [53].

In another study, employing the introduction of DNA through P-element mediation, transgenic flies that exhibited overexpression of both SOD1 and catalase were found to have decreased oxidative damage and extension in their lifespan [54]. In a separate investigation, the GAL4-UAS system was employed to selectively overexpress human SOD1 in motor neurons. This led to enhanced protection against oxidative stress and an elongation of lifespan [55].

In mice, the absence of SOD2 in the brain resulted in increased mitochondrial superoxide and fatality within a period of 3 to 4 weeks after birth [56], while SOD1 knockout mice exhibited substantial oxidative damage in the cytoplasm that was accompanied by approximately 30% reduction in their lifespan [57]. Moreover, various investigations conducted in mice have identified a correlation between the loss of SOD1 and the onset of numerous age-related ailments. These include age-related skeletal muscle atrophy, delayed wound healing, hearing impairment,

heightened cellular senescence, motor axonopathy, locomotor issues, compromised motivational behavior, accelerated age-related macular degeneration, impaired olfactory sexual signaling in males, and reduced female fertility [57-67].

One of the most extensively studied methods to enhance longevity is caloric restriction, which limits metabolic activity and thereby reduces the production of ROS and age-related diseases in flies [68], rats [69], mice [66, 70-72], monkeys [73] and humans [74].

The evidence linking oxidative stress and ROS accumulation to age-related health decline also supports the FRT theory of aging. Oxidants have been implicated in various health issues, e.g. multiple sclerosis (MS), an autoimmune neurological disorder characterized by disrupted nerve conduction. The onset of MS is triggered by activated microglia/macrophages, which generate ROS that lead to lipid peroxidation, resulting in the demyelination of the neurons [75]. Furthermore, protein oxidation and reduced SOD levels were also reported in patients with MS [76]. Cataract, a leading cause of visual impairment affecting approximately 25 million individuals globally [77], is largely attributed to oxidative stress [78]. In cataract lenses, there is evidence of oxidation affecting proteins, lipids, and DNA [79]. Notably, oxidative stress gives rise to the formation of harmful lipid peroxidation products, such as 4-hydroxynonenal (HNE), which in turn leads to the breakdown of lens proteins, ultimately contributing to the clouding of the lens and the development of opacity [80-82]. In Parkinson's disease (PD), reports have found that the disturbance in redox balance results in oxidative harm to dopaminergic neurons, particularly those located in the substantia nigra. This disturbance also initiates modifications in the synthesis and metabolic pathway of dopamine, which subsequently amplifies oxidative stress due to the formation of quinones [83].

1.4.2 Redox stress theory of aging

Despite the notable importance and substantial evidential support for the FRT theory of aging, divergent findings challenging this theory have emerged from various studies. One such example is the naked mole-rat, an exceptionally long-lived rodent species exhibiting a lifespan that surpasses 37 years [84, 85]. However, numerous investigations have demonstrated that naked mole-rats manifest a heightened degree of oxidative damage compared to mice [86-88].

Mammalian clk1 (Mclk1) is a pivotal mitochondrial enzyme essential for ubiquinone (CoQ) biosynthesis [89, 90]. CoQ facilitates the transfer of electrons from complex I or II to complex III within the mitochondrial inner membrane. Notably, the primary site of superoxide generation occurs at the CoQ site [91].

In mice, heterozygosity for Mclk1 (Mclk1+/−) results in markedly elevated mitochondrial oxidative stress, paradoxically accompanied by increased lifespan compared to their wild-type littermates [92].

Several long-lived mutants in *C. elegans* exhibit associations with heightened oxidative stress and/or compromised mitochondrial enzyme activity. Notably, knockout mutations targeting the mitochondrial superoxide dismutase SOD-2 result in elevated oxidative stress levels, yet the impact on lifespan varies, showing either no difference or an extension [93, 94]. Clk-1 mutants, characterized by reduced electron transport and oxygen consumption, paradoxically demonstrate increased longevity [95-97]. The gene isp-1 encodes the Rieske iron-sulfur protein, a constituent of complex III in the Electron Transport Chain (ETC) [98]. Isp-1 mutants display diminished resistance to oxidative stress, reduced oxygen consumption, and notably, an extended lifespan [99]. Additionally, mutant strains featuring NADH Ubiquinone Oxidoreductase (NUO-6) (complex I) mutations manifest heightened mitochondrial superoxide levels in isolated mitochondria,

concomitant with increased longevity compared to their wild-type counterparts. Intriguingly, the observed longevity in this mutant is contingent upon increased oxidative stress, as the introduction of the antioxidant NAC effectively suppresses the observed lifespan extension [100].

These data have necessitated the development of a refined theoretical framework that offers a more intricate understanding of the involvement of free radicals in the aging phenomenon. Thus these paradoxical results have spurred the evolution of the free radical theory of aging, leading to the formulation of the redox stress theory of aging, as proposed by Sohal and Orr [101]. This theory posits that, if free radicals induce a stress response within cells that the cellular mechanisms can effectively manage, ensuing damage is averted due to the overwhelming capability of antioxidant defenses to counteract the stress. This theory stems from contemporary insights into the pivotal physiological functions of ROS across a spectrum of cellular actions, encompassing signal transduction, gene regulation, redox homeostasis, cellular proliferation, differentiation, and migration [102-104]. ROS possess several attributes that render them effective second messengers. These include tightly regulated production and elimination mechanisms, as well as reversible signaling effects characterized by specificity towards signaling targets [105]. ROS play a crucial role in modulating the intensity and duration of specific signals within redox-sensitive pathways through the oxidation and reduction cycle of cysteine residues in kinases and phosphatases. This function is essential for preserving cellular homeostasis [105-107].

The concept of hormesis supports the redox theory of aging and aids in comprehending the advantageous outcomes of heightened ROS levels on longevity. Hormesis is defined as “a beneficial response to a sub-threshold dose of a stimulus that at a higher dose is toxic or detrimental” [108]. Hormesis-induced advantages have been observed in various organisms such as *C. elegans* and mice. In a study conducted by Cypser and Johnson, it was observed that exposing

C. elegans worms to 100% oxygen for 24 hours led to a mortality rate of 70-90%. However, when the worms were pretreated with 100% oxygen for 8 hours, the mortality rate decreased to 10-50%, and their lifespan was extended [109]. In another investigation, subjecting worms to a low dose (40μM) of the superoxide-generating compound juglone led to a slight extension in lifespan [110]. In a separate study, a strategy was employed to induce hormesis by imposing a diminished cellular energy state as a form of low-level stress. This was achieved by administering 2-deoxy glucose (2-DG) to inhibit glycolysis and reduce ATP production. As a compensatory response, oxidative phosphorylation increased, leading to elevated ROS levels. Remarkably, worms treated with 2-DG exhibited resistance to paraquat-induced oxidative stress and demonstrated an extension in lifespan [111]. In mice, Caldeira de Silva and colleagues have found that administering low doses of the mild mitochondrial uncoupler protonophore 2,4-dinitrophenol (ranging from 30 to 105 μg/kg/day) resulted in improved tissue respiration rates (enhanced oxygen utilization), as well as favorable changes in serological insulin and glucose levels, ultimately leading to increased lifespan [112]. These outcomes were linked to changes in energy metabolism and the redox state [112]. In another investigation, it was observed that the depletion of SOD2 during embryonic development led to heightened mitochondrial biogenesis and decreased ROS levels in the livers of the adapted adult mice. Additionally, at the cellular level, transient SOD2 depletion in fibroblasts from mice that were exposed to SOD2-knockdown during embryonic development prompted mitochondrial adaptation, leading to an improved antioxidant capacity [113].

The elucidation of these findings underscores a nuanced perspective on the role of free radicals in the aging process and age-associated diseases. Contrary to the notion that free radicals are exclusively detrimental, their positive contributions to cellular processes are evident. However, a

pivotal revelation emerges: there exists a critical threshold wherein the quantity of reactive oxygen species (ROS) transitions from being beneficial to becoming deleterious.

This intricate interplay between ROS quantity and its dual impact—positive and detrimental—is visually encapsulated in (Figure 1.1). The figure serves as a graphical representation of the hormetic response associated with ROS. This biphasic phenomenon highlights that, within a certain range, ROS function as essential signaling molecules, contributing positively to cellular processes. Yet, upon surpassing a critical threshold, ROS shift their role, exerting damaging effects that underpin aging and associated pathologies. This conceptual framework emphasizes the delicate equilibrium between the beneficial and harmful facets of ROS, thus providing a comprehensive portrayal of their dynamic involvement in cellular homeostasis and aging.

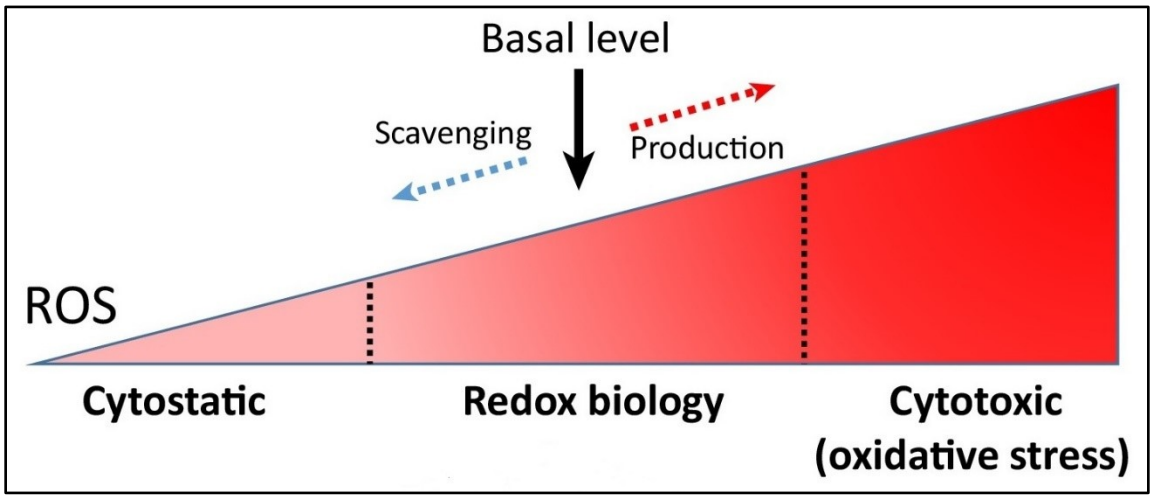

Figure 1.1: Maintaining an appropriate baseline level of ROS within cells is crucial for ensuring proper cellular function, adapted from Mittler R. (2017). [103]

1.5 Cellular senescence

1.5.1 Definition

Cellular senescence is defined as a state in which the cell enters a permanent cell cycle arrest in response to damaging stimuli [114]. Cyclin dependent kinase inhibitors (CDKI) such as P15, P16 and P21 were reported to mediate cell cycle arrest seen in senescent cells [115]. In particular, P16 is considered unique for the senescence phenotype [116-118]. In addition to the irreversible cell cycle arrest, senescent cells manifest a distinctive secretory profile comprising cytokines, chemokines, and proteinases recognized as the Senescence-Associated Secretory Phenotype (SASP) [115], alternatively denoted as the Senescence Messaging System (SMS) [119]. An underlying feature of the senescence phenotype seen in all models of senescence (described below) is the activation of the DNA Damage Response (DDR), primarily triggered by DNA double-strand breaks (DSBs), leading to the recruitment of ATM kinase [120, 121]. Morphologically, senescent cells are enlarged and flattened. These senescence-mediated changes in cell size and shape are attributed to different mechanisms including mTORC1 activation [122] and rearrangement of cytoskeleton filaments such as vimentin [123, 124]. Senescent cells have an increased number of dysfunctional mitochondria [125-127] and increased lysosomal activity which can be detected with increased senescence associated beta-galactosidase staining (SA-β-gal) [128, 129]. Accumulation of senescent cells is considered a hallmark of organismal aging and age-associated diseases [130, 131]. Accumulation of these non-dividing cells was reported to negatively affect the regenerative potential of various cell types as β-cells [132], skeletal muscle [133, 134], intestinal and renal cells [135]. Furthermore, SASP secretion from senescent cells contributes to the chronic mild inflammatory state seen in the elderly that is known as inflammaging [136] and these inflammatory mediators have been proposed to initiate the onset and promote the progression of various age-related diseases [136, 137].

1.5.2 Models of cellular senescence

Cellular senescence can be induced in in vitro systems via different stimuli [138], with activation of the DNA damage response (DDR) being involved in the majority of these models [139]. The DDR process is activated as a response to any DNA damage, and it encompasses the recruitment of ATM kinase, phosphorylation of histone H2AX, and subsequent activation of the transcription factor P53, which serves as a mediator of the induction of cellular senescence [120, 121, 140, 141].

The most extensively studied in vitro senescence models are:

1.5.2.1 Replicative senescence

This model relies on passaging cells to a late passage number which is associated with decreased replicative potential that ultimately leads to total cell cycle arrest [142]. Multiple studies have linked induction of senescence in late cell passages to telomere shortening with each cell division [143-146]. Telomeres are repetitive DNA sequences situated in terminal loops at the ends of chromosomes [147]. The process of cellular proliferation involves the gradual shortening of telomeres, leading to the destabilization of telomeric DNA loops and the uncapping of telomeres. This phenomenon results in the formation of telomere dysfunction-induced foci (TIFs) and activation of the DDR and ultimately causes cell-cycle arrest [148]. Additionally, another type of DNA damage referred to as telomere-associated foci (TAFs) can occur at telomeres due to oxidative damage at these G-rich repeats, regardless of telomere length [147].

1.5.2.2 DNA damage-induced senescence

DNA damage that is beyond the ability of the cell to repair can cause either apoptosis or senescence depending on the impact of the damage [138]. Different DNA damaging agents are used in vitro to induce cellular senescence. These include radiation and chemotherapy [138, 149]. Ionizing radiation (IR) is a documented insult that induces cell cycle arrest in virtually all eukaryotic cells, and this

effect is sensitive to as low a radiation dose as under 1 gray (Gy) [150]. The mechanism underlying IR-mediated cell cycle arrest is the activation of ATM as an early responder to DNA damage. Once activated, ATM kinase activity is enhanced resulting in phosphorylating downstream targets involved in cycle arrest such as P53 and P21[151, 152]. In support of this crucial role of ATM in radiation-induced senescence, Correia-Melo et al. exposed human MRC5 fibroblasts to X-ray irradiation at 20 Gy to induce senescence. Treating the cells with an ATM inhibitor (KU55933) at 10 μM concentration was able to rescue the radiation-induced senescence phenotype [153]. Multiple anticancer drugs (chemotherapy) are also known to induce cellular senescence that is referred to as chemotherapy-induced senescence [115]. The mechanisms underlying chemotherapy-induced senescence depend largely on the drug used. Some of these drugs such as bleomycin and doxorubicin induce DNA damage and activate the DDR, while others such as palbociclib and abemaciclib inhibit cell proliferation by inhibiting cyclin dependent kinases (CDKs) [149].

1.5.2.3 Oncogene-induced senescence (OIS)

OIS is triggered by the activation of certain oncogenes such as Ras and BRAF or inactivation of tumor suppressors such as PTEN phosphatase [138, 154].

This phenomenon was first observed in Ras oncogene activation in primary cells of human lung fibroblasts IMR90 [155]. Unlike replicative senescence, OIS operates independently of telomere erosion and can activate both P53 and p16 [156]. Oncogene activation induces DNA replication stress and a collapsed replication fork that actives the DDR pathway [157]. The replication fork is an important structure that arises during the process of DNA replication within the helical DNA molecule. This formation is facilitated by helicase enzymes, which disrupt the hydrogen bonds linking the two DNA strands, resulting in the unwinding of the helix. The replication fork consists of two diverging "prongs," each composed of a single DNA strand. The activation of oncogenes,

which can modify the replication timing program, may elevate the likelihood of replication fork collisions, consequently increasing the risk of fork stalling and collapse [158].

The involvement of ATM and p53 play a pivotal role in orchestrating OIS [157, 159]. Studies indicate that in mice, the loss of P53 induces invasive behavior in Ras-induced cancer cells. Conversely, the reactivation of P53 not only suppresses tumor growth but also induces common senescence markers [160-162].

Oncogene-induced senescence (OIS) represents a multifaceted cellular response initially recognized for its role in halting unregulated cell growth, thereby acting as a safeguard against the unchecked proliferation of aberrant cells. This process is vital for maintaining cellular homeostasis and preventing the development of malignancies. OIS is triggered by the activation of oncogenes, which paradoxically induce a stable and irreversible growth arrest, serving as a critical mechanism to inhibit tumorigenesis. [163]. Furthermore, the SASP may also trigger tumor-suppressive reactions, potentially by aiding in the removal of senescent cells and curbing tumor progression. [164]. Nevertheless, investigations have uncovered that SASP can induce responses that are both tumor-suppressive and tumor-promoting, contingent on the specific array of secreted factors. For instance, components such as vascular endothelial growth factor (VEGF), interleukin-8 (IL-8), interleukin-6 (IL-6), and C-X-C motif chemokine ligand 1 (CXCL1) have shown the capacity to advance tumor progression by promoting endothelial cell division [165], contributing to angiogenesis [166], facilitating tumor cell invasion [167], or promoting the formation of cancer stem cells [168]. Additionally, factors like CXCL12 and extracellular matrix-degrading enzymes [169] have been implicated in recruiting immune cells such as macrophages and natural killer (NK) cells, establishing an immunosuppressive microenvironment around senescent cells, thereby aiding tumor cells in evading immune detection and destruction [170].

1.5.2.4 Paracrine senescence

Paracrine senescence, also referred to as bystander senescence [171], describes the phenomenon in which senescent cells release various SASP factors, including pro-inflammatory cytokines, chemokines, into their microenvironment. These signals influence neighboring cells, triggering a cascade of events that mirror the senescent phenotype [172]. Mechanistically, investigations have demonstrated that binding of IL-6 (a member of SASP) to its receptor IL-6R initiates signaling cascades, particularly the induction of the STAT3/P53 pathway in a ROS/DDR-dependent manner, leading to senescence in human fibroblasts [173, 174].

The transfer of senescence-inducing signals can occur through direct cell-cell contact, which is termed juxtacrine senescence, or through secretion that affect cells in remote tissues [171]. Extracellular vesicles, such as exosomes, have emerged as potential mediators in the paracrine transmission of senescence signals [175].

1.5.2.5 Oxidative stress-mediated senescence

Oxidative stress can be defined as a condition characterized by an imbalance between the production of ROS and the ability of the cell's antioxidant defenses to neutralize these harmful molecules [176]. The correlation between elevated ROS levels and cellular senescence is associated with the detrimental impact of ROS on different cellular components such as proteins [177], nucleic acids, and lipids [153, 157, 178]. ROS are implicated in inducing DNA double-strand breaks [179], a robust trigger for initiating the DDR [115]. As noted above, the DDR is a common activator of senescence. In addition, DDR activation by ROS plays a significant role in stimulating nuclear factor kappa-B (NF-kB) [115], a pivotal transcription factor that, in part, stimulates the secretion of the senescence-associated secretory phenotype (SASP) [180].

1.6 Regulation of cellular redox homeostasis

The regulation of cellular redox homeostasis refers to the maintenance of a balanced and controlled environment within cells, specifically the balance of the levels of ROS and antioxidants [181]. Cellular redox homeostasis is crucial for normal cell function and survival. It involves intricate regulatory mechanisms that ensure a dynamic equilibrium between the generation of ROS and the defense mechanisms that counteract their harmful effects. Key components regulating cellular redox homeostasis are the antioxidants (AOs). AO can be defined as a compound, whether enzymatic or non-enzymatic, that competes with an oxidative substrate, leading to a substantial inhibition or reversal of oxidation. This action shifts the equilibrium away from ROS action and toward the scavenging of ROS [182]. Among enzymatic AOs, superoxide dismutases (SODs) stand out as particularly crucial, given their ability to convert the highly reactive superoxide radical (O_2•−) into hydrogen peroxide (H_2O_2), a less potent yet still oxidative compound [183]. SOD facilitates the electron transfer through two redox reactions, utilizing transition metals in its active site [184]. In the initial reaction, superoxide undergoes oxidation to molecular oxygen, resulting in the reduction of the transition metal in the active site. In the subsequent reaction, oxygen is reduced to H_2O_2, and the transition metal within the active site reverts back to its oxidized form [185]. Humans exhibit three distinct forms of SOD: SOD1, situated in the cytosol, possesses a Cu/Zn active site; SOD2, located in the mitochondria, has an active site composed of Mn; and SOD3, positioned extracellularly, features a Cu/Zn active site [185, 186]. Subsequently, two parallel enzyme pathways come into play to neutralize H_2O_2: Catalase facilitates the conversion of H_2O_2 into water (H_2O) and oxygen (O_2), while Glutathione (GSH) peroxidase (GPx) orchestrates a reaction involving H_2O_2 and glutathione producing 2 water molecules and oxidized glutathione disulfide (GSSG) [182]. The enzymatic AOs of the glutaredoxin (Grx) and thioredoxin (Trx) families are

essential for protecting thiol-containing proteins and repairing oxidative damage. These enzymes transfer electrons to the disulfide bonds in their target proteins, effectively reducing and restoring the proteins to their functional state. [187]. The process involves a sequence of reactions, commencing with the reduction of the target residue and the oxidation of the Grx or Trx active site, which comprises cysteine residues [188]. Subsequently, each enzyme requires reduction to revert to its active form: Grx undergoes reduction by two GSH molecules, leading to the oxidation of these GSH molecules into GSSG. In parallel, thioredoxin is reduced by an enzyme known as thioredoxin reductase (TrxR) [188]. TrxR utilizes electrons provided by NADPH to reactivate the Trx thiol-containing active site, returning it to its functional state. Similarly, glutathione reductase (GR) reduces GSSG back to two glutathione (GSH) molecules by also utilizing electrons from NADPH. [187].

Non-enzymatic AOs can be endogenous or supplied exogenously through diet [189]. Glutathione (GSH) plays an important role in the functionality of the GPx and Grx systems. In these systems, GSH functions to restore each enzyme to its active state [190, 191]. Additionally, GSH itself acts as an antioxidant, utilizing its sulfhydryl group to contribute electrons and thereby reducing and detoxifying ROS [191].Active GSH levels can be replenished through the conversion of oxidized GSH to its reduced form by the action of GR and NADPH or through dietary supplementation [192]. Another important non-enzymatic AO is N-acetyl cysteine (NAC). NAC serves a dual role as both a precursor in GSH formation and an active participant in redox reactions due to its thiol group. This enables NAC to donate electrons for the detoxification of ROS and safeguard sulfhydryl-containing proteins against oxidative damage [193]. The levels of NAC are regulated through the intake of cysteine, found abundantly in high-protein foods [194]. Vitamin C, also known as ascorbic acid, is a water-soluble antioxidant located both within cells and in the extracellular matrix. It

operates by neutralizing oxygen free radicals in watery environments, thereby protecting against the oxidation of cholesterol. Conversely, Vitamin E includes various forms such as alpha-, beta-, gamma-, delta-tocopherols, and alpha-, beta-, gamma-, delta-tocotrienols. Being a lipid-soluble antioxidant, Vitamin E resides in cell membranes and lipoproteins, where it acts to prevent the peroxidation of lipids caused by oxidative stress. [185].

1.7 TXNIP structure and function

TXNIP was identified in 1994 by DeLuca's team in HL-60 cells (human promyeloblasts) treated with 1,25-dihydroxyvitamin D-3. Initially termed vitamin D3 upregulated protein 1 (VDUP1), this research demonstrated the upregulation of TXNIP mRNA in response to 1,25 dihydroxyvitamin D3 treatment [195]. The human TXNIP gene encodes a protein of 391 amino acid residues. TXNIP exhibits a high degree of conservation among species, and the mouse TXNIP shares a 94% homology with its human counterpart [196]. TXNIP is categorized within the α-arrestin family of proteins. Notably, TXNIP is distinct in that the active cysteine residues essential for binding to Trx and modulating the redox environment are absent in other members of this protein family [197-199].

1.7.1 α-arrestin domain-related functions of TXNIP (non-thioredoxin dependent functions)

TXNIP exhibits distinctive α-arrestin, SH3 and PPxY domains. At the N-terminus, two SH3-binding domains with PxxP sequences facilitate interaction with the non-receptor tyrosine kinase Src and a MAPKKK-ASK1 binding domain. The C-terminus harbors three SH3-binding domains and two PPxY motifs [200, 201]. The C-terminal PPxY motifs play a crucial role in interacting with the E3 ubiquitin ligase, ITCH, leading to the polyubiquitination of TXNIP and marking it for proteasomal degradation [202]. Additionally, TXNIP features an immune-receptor tyrosine-based inhibition (ITIM) domain and a chromatin maintenance region 1 (CRM1) domain. The ITIM domain facilitates interactions with tyrosine phosphatases, regulating nuclear-to-plasma

membrane signal transduction [203]. The CRM1 domain is responsible for mediating interactions between TXNIP and hypoxia-inducible factor 1-α (HIF1-α) and the ubiquitin ligase von Hippel-Lindau protein (pVHL), promoting the nuclear export and cytosolic degradation of HIF1-α [204]. See Figure 1.2.

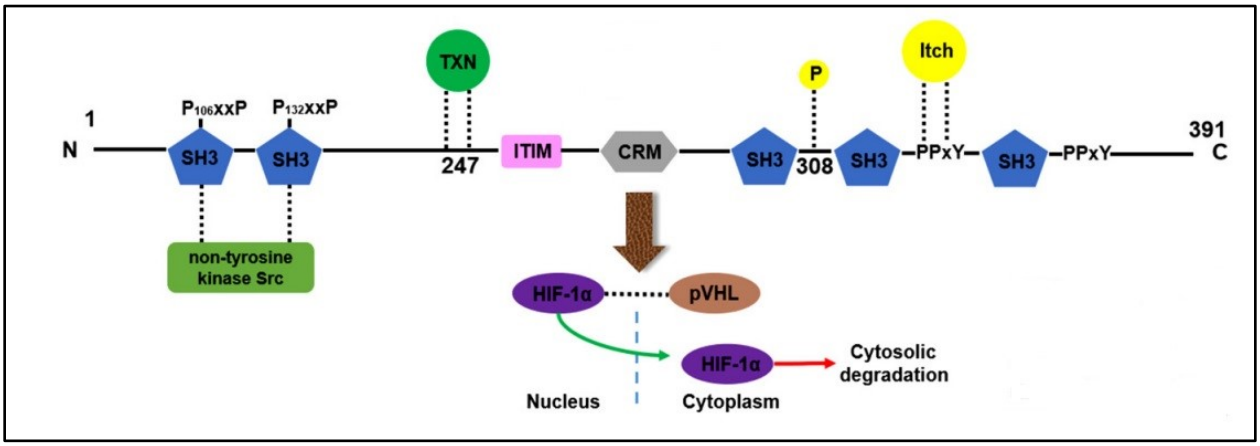

Figure 1.2: A proposed model for the TXNIP structure binding domains, adapted from Xiankun et al. (2020) [205]

1.7.2 Thioredoxin (Trx) domain-related functions of TXNIP

Trx1 and Trx2 play distinct roles in regulating cytoplasmic and mitochondrial redox state, respectively by reducing oxidized proteins generated in response to elevated ROS. This redox process involves the continuous oxidation and reduction of Trx, facilitated by the NADPH-dependent Trx reductase (TrxRD). In this dynamic interplay, Trx cycles between its reduced and oxidized forms, exchanging hydrogen ions [205].

The antioxidant function of Trx is modulated by TXNIP, which acts as an inhibitor. Specifically, TXNIP binds exclusively to the reduced (active) form of Trx at its catalytic site. The interaction relies on essential cysteine residues, particularly cysteine 247 and cysteine 63 on TXNIP, which interact with cysteine 32 of Trx [199]. Trx has a characteristic motif of 2 cysteine residues separated

by 2 amino acids. Mutations of these cysteine residues disrupt the interaction between TXNIP and Trx, underscoring their critical role in this molecular interplay [199, 206, 207]. Notably, these cysteine residues are unique to TXNIP and are not conserved in the broader α-arrestin family of proteins, emphasizing the distinctive nature of the interaction [208].

Apart from inhibiting the antioxidant actions of Trx, other proapoptotic and inflammatory effects of TXNIP have been documented. Trx exerts antiapoptotic effects by binding to and inhibiting the pro-apoptotic protein ASK1. However, when cells encounter various stressors, such as oxidative stress, TXNIP undergoes translocation to the mitochondria, where it competes with ASK1 for binding to Trx2. The binding of TXNIP to Trx2 facilitates the activation of ASK1 through phosphorylation, initiating the apoptotic pathway. This pathway includes key events such as the release of cytochrome-c and the cleavage of caspase-3 [208-210]. Supporting the involvement of TXNIP in apoptosis, our lab has previously shown that Hcb-19 mice, a mouse model lacking TXNIP, exhibits relative protection against streptozotocin-induced diabetes. This protection is attributed to decreased apoptosis and consequently, an increased beta cell mass [211].

Furthermore, other studies highlight the significant involvement of TXNIP in modulating the innate immune system: TXNIP binds to and activates the nucleotide-binding oligomerization domain (NOD)-like receptor (NLR) protein 3 inflammasome (NLRP3) in a redox-dependent manner [212, 213]. This activation results in the maturation of the proinflammatory cytokine IL-1β from pro-IL-1β [212, 213]. Increased ROS levels facilitate the dissociation of TXNIP from Trx [212, 214], allowing TXNIP to directly associate with and activate NLRP3. This activation process leads to the release of active caspase-1 and the production of IL-1β [212]. Moreover, the activation of NLRP3 by TXNIP leads to endoplasmic reticulum (ER) stress-induced cleavage of caspase-2 and the pro-apoptotic factor, Bid. This process results in the release of mitochondrial contents and the

initiation of the canonical inflammasome, highlighting a TXNIP-NLRP3-caspase-2 dependent mechanism that transmits ER stress to the mitochondria, promoting inflammation [215].

1.8 Cellular Reactive Oxygen Species (ROS)

1.8.1 Overview

Reactive oxygen species (ROS) encompass a diverse range of intracellular molecules characterized by high reactivity, originating from the incomplete reduction of molecular oxygen within the cell [216, 217], that can oxidize lipid, DNA and protein [216]. ROS can manifest as free radicals, possessing unpaired electrons that render them unstable and highly reactive [185, 218]. Due to their reactivity, free radicals are typically short-lived and often confined to the subcellular locales of their generation until undergoing reduction. Free radical ROS include superoxide ($O_2^{\bullet -}$), hydroxyl ($HO^{\bullet}$), peroxyl ($RO_2^{\bullet -}$), hydroperoxyl ($HO_2^{\bullet}$), and alkoxyl radicals ($RO^{\bullet}$) [219, 220].

Superoxide can interact with nitric oxide, generating highly reactive nitrogen species (RNS) that function in a manner analogous to ROS [221]. ROS that are not free radicals lack unpaired electrons, making them less reactive and facilitating their movement across subcellular compartments as well as membrane penetration [219]. Examples of non-free radical ROS include hydrogen peroxide (H_2O_2), the hydroxide ion (OH^-), and organic peroxides (ROOH) [220].

Various stimuli, including hormones, growth factors, pro-inflammatory cytokines, UV radiation, nutrients, and endoplasmic reticulum (ER) stress, can instigate ROS production [222-225]. The ability of non-free radical ROS, such as hydrogen peroxide, to traverse within the cell becomes important when considering the redox state for cell signaling in diverse subcellular compartments and the distribution of antioxidants within the cell. [226, 227].

Under normal physiological conditions, the oxidation of cellular macromolecules induces structural, interactional, and functional modifications, playing pivotal roles in cellular processes

such as gene and protein regulation, cell proliferation and differentiation, intracellular signaling, and the regulation of adaptive and innate immunity [216, 221]. Endogenous antioxidants typically maintain ROS at balanced levels within cells. However, the compromised functionality of these antioxidants can lead to abnormally high ROS levels, contributing to various pathophysiological conditions, including aging-related diseases such as cancers, atherosclerosis, obesity, and diabetes [216].

1.8.2 Sources of ROS

The production of reactive oxygen species (ROS) is a byproduct of aerobic metabolism. However, when ROS levels exceed the capacity of antioxidants to neutralize them, it becomes detrimental to cells, impacting cell signaling and causing damage to cellular compartments. Various intracellular systems and processes contribute to ROS production, including mitochondrial electron transfer, the NADPH oxidase family, xanthine oxidase, cytochrome P450 systems, and uncoupled endothelial nitric oxide synthase [228]. The primary contributors to intracellular ROS are the mitochondria and the NADPH oxidase system [229], and their interplay exacerbates the gradual development of oxidative stress [230]. ROS generated by mitochondria and NADPH oxidase are of special significance in the context of aging, cellular senescence, and age-related diseases [231-236], forming the central focus of this thesis. Therefore, the subsequent section will delve into the specifics of ROS generation by these two sources.

1.8.2.1 Mitochondrial source of ROS

The mitochondrial electron transport chain (ETC), essential for respiratory processes that transfer electrons from NADH and $FADH_2$ to molecular oxygen while establishing an electrochemical gradient across the inner mitochondrial membrane, stands as a prominent origin of ROS production [237, 238]. Oxidative phosphorylation (OXPHOS), which is responsible for converting O_2 into H_2O

through a four-electron reduction process is imperfect and results in a minor fraction of O_2 (0.2-2%) undergoing reduction by single prematurely leaked electrons from the ETC, resulting in the generation of superoxide anion radicals [239]. This electron leakage predominantly occurs at complexes I and III of the ETC [240, 241]. In complex I, electrons escape from the iron-sulfur cluster N_2 (Fe-S cluster N2), leading to the production of superoxide radicals, which are then released into the mitochondrial matrix. Meanwhile, at complex III, electrons diffuse from ubiquinol, occurring at the Qo site, and release on both sides of the inner mitochondrial membrane [241]. A well-documented example of increased mitochondrial ROS is exposure to high glucose (hyperglycemia), that results in increased flux through the TCA cycle and ETC [242]. The intricate association between mitochondrial ROS and the processes of aging and age-related diseases has been outlined in Section 1.3.1 of this thesis.

1.8.2.2 NADPH oxidase

NADPH oxidases are membrane-bound multisubunit enzymatic complexes, which are responsible for transferring electrons from the cytosolic donor NADPH to the acceptor, O_2, thereby generating superoxide and H_2O_2 [243]. Presently, seven isoforms of NADPH oxidase (NOX) have been identified—NOX1 through NOX5 and Duox1 and Duox2. NOX5 is expressed in humans, but not in mice [243]. These isoforms exhibit distinct patterns of tissue distribution, as outlined in Table 1.1.

Table 1.1: The various isoforms of NADPH oxidase and their corresponding sites of expression, adapted from Paik, Y. et al. (2014) [244].

Catalytic subunit	*Major tissue/cell distribution*
NOX1	Colon, vessel, heart, uterus, prostate, liver
NOX2	Neutrophil, phagocyte, vessel, heart, liver
NOX3	Fetal tissue, inner ear
NOX4	Kidney, vessel, heart, lung, liver
NOX5	Testis, spleen, lymph node, heart, vessel
DUOX1/ DUOX2	Thyroid tissue

Each NOX homolog comprises six remarkably conserved transmembrane domains, and two heme-containing domains [245]. The cytoplasmic COOH terminus is characterized by highly preserved flavin adenine dinucleotide (FAD) and NADPH binding domains [245]. The activation of most NOX enzymes is triggered by the binding of particular protein subunits of the complex like p22phox, P47, P67 and Rac. However, NOX4 stands out as the sole isoform believed to be constitutively active and concurrently subject to negative regulation through ATP binding [246-248]. In the context of this thesis, it is noteworthy that kidney and mesangial cells predominantly express NOX4/renox (renal NOX), with minimal levels of NOX1 and 2 [249, 250].

Substantial data have shown that overexpression of various NOX members in different tissues has been linked with cellular senescence, aging, and age-related diseases. In a study conducted by McCrann et al., it was observed that the expression of NOX4 is heightened in vascular smooth muscle cells (VSMCs) from the aortas of aged rats [251]. Additionally, they found that NOX4 levels are elevated in polyploid VSMCs compared to diploid cells in vivo [251]. In the same investigation, primary VSMCs were transduced with NOX4 adenovirus, resulting in a consistent buildup of polyploid cells. Concurrently, there was a reduction in the percentage of diploid cells observed in the NOX4-overexpressing cells compared to control cells or those overexpressing dominant negative Nox4 [251]. It is important to highlight that the presence of polyploidy in aortic VSMCs is indicative of aging, and this polyploid state is associated with an increased occurrence of senescence in vivo [251]. In humans, examination of data from the Genotype Tissue Expression (GTEx) database also revealed age-related elevations in NOX4 expression levels in human lung tissues, which was linked to changes in genes associated with TGF-β signaling and extracellular matrix remodeling, suggesting a potential involvement of NOX4 in age-related pulmonary fibrosis [252, 253]. Endothelial senescence triggered by thrombospondin 1 (TSP1), a matricellular protein

implicated in vascular aging, was observed to coincide with the induction and activation of NOX1, and targeted inhibition of NOX1 was shown to mitigate this process [254, 255]. Elevated NOX4 level in endothelial cells during aging has been associated with endothelial dysfunction, mediated by endoplasmic reticulum (ER) stress that ultimately led to eNOS uncoupling [256]. Additionally, NOX4-induced senescence has been observed in various cell types. For instance, oncogenic H-Ras has been shown to increase NOX4 expression, inducing DNA damage and senescence in human thyrocytes [257]. Similarly, it has been reported that the Ras oncogene signaling enhanced the expression of Nox1 in rat REF52 cells and Nox4 in primary human lung TIG-3 cells, resulting in elevated intracellular ROS levels. Activation of the DDR and p38MAPK signaling by NOX isoforms in both cell types further promoted cellular senescence [258]. In a study conducted by Kim et al., which aimed to identify pathways implicated in oncogenic Ras-induced senescence, they found that Akt activation played a crucial role. Akt was observed to stimulate the NF-κB-dependent elevation in NOX4 transcription, resulting in oxidative stress and subsequent senescence [259]. Various transcription factors, such as NF-κB, HIF-1α, and Nrf2, have been associated with the upregulation of NOX4 expression [260-263].

1.8.3 ROS in cellular signaling

Under physiological conditions, ROS serve as pivotal signaling molecules in various cellular signaling pathways including mitogen-activated protein kinases (MAPK), phosphoinositide 3-kinase (PI3K)/protein kinase B (AKT), and ASK1, orchestrating physiological responses to environmental cues [264-266]. ROS have the ability to modify cysteine residues within proteins, inducing structural changes that affect the protein's function. These modifications can either activate or deactivate kinase signaling pathways. When ROS oxidize cysteine residues, they can inhibit phosphatases. Conversely, ROS can also inactivate kinases. Reduction of oxidized cysteine

residues, restores the original function of the protein, however, under severe oxidative stress, the oxidation process can be irreversible [185, 267]. Additionally, ROS can activate redox-sensitive transcription factors such as NF-κB, AP-1, HIF-1α and Nrf_2, which in turn regulate the expression of genes involved in cell survival, antioxidant defense, and inflammation [264, 266, 268-270]. Furthermore, ROS produced by the ETC might serve as a means for cells to relay information about the nutritional status of the cell promoting appropriate cellular responses [185]. It should be noted that the cysteine residues in different proteins or sites may display a differential sensitivity to oxidation [271]. In this manner, the cell can detect mild, moderate, or severe changes in redox state to initiate the appropriate signaling response, e.g cell growth and proliferation versus apoptosis [272, 273].

1.8.4 Role of redox state in cell growth and apoptosis

The intricate balance between ROS production and detoxification mechanisms within the cell is meticulously regulated to uphold redox equilibrium. This equilibrium serves as a protective mechanism against the deleterious consequences of heightened ROS levels on crucial macromolecules such as nucleic acids, lipids, and proteins [265]. The redox state of a cell influences various signaling pathways involved in cell growth, proliferation, and apoptosis. PI3K serves as a prominent downstream mediator of signaling cascades initiated by both receptor tyrosine kinases (RTKs) and G protein-coupled receptors (GPCRs) [274]. The generation of ROS has the capability to activate protein tyrosine kinases and impede protein tyrosine phosphatase [266, 275]. H_2O_2 oxidizes the cysteine residue at the active site of protein tyrosine phosphatase 1B (PTP1B), consequently hindering the dephosphorylation process of RTKs [276]. Furthermore, ROS oxidize the cysteine residues of the negative regulator of AKT, PTEN, causing its inactivation, which ultimately results in the activation of the PI3K/Akt signaling pathway [277]. Upon activation, AKT phosphorylates a

diverse array of cellular substrates, thereby modulating their activity and function. This activity facilitates cellular growth, survival, and proliferation [266]. One of the downstream effects of Akt activation is the inhibition of FoxO transcription factors through phosphorylation, leading to their exclusion from the nucleus and subsequent degradation. This process favors cell survival and proliferation [274, 278]. Additionally, the activated PI3K/Akt signaling pathway suppresses apoptosis and promotes tumorigenesis, including growth, invasion, metastasis, and angiogenesis. Dysregulation of the PI3K/Akt pathway results in the upregulation of the antiapoptotic protein Bcl-2, which confers resistance to apoptosis in cancer cells [274]. Moreover, Akt activation inhibits apoptosis by phosphorylating and inactivating the proapoptotic protein Bad, thus blocking apoptotic signaling. Furthermore, Akt impedes apoptosis by preventing the translocation of Bax to mitochondria and by increasing the expression of the X-linked inhibitor of apoptosis protein (XIAP), which in turn inhibits the activation of caspase-3 [266, 274].

The cellular redox state also regulates apoptosis by modulating the activation of apoptosis signal-regulating kinase 1 (ASK1). Upon exposure to oxidants such as H_2O_2, ASK1 undergoes transient activation via autophosphorylation at threonine (Thr845) [279]. Furthermore, the oxidation of the active cysteine residues within Trx, an inhibitor of ASK-1, specifically cysteine 32 and cysteine 35, results in the dissociation of Trx from ASK1, leading to the formation of an oligomeric complex. This process facilitates the autophosphorylation of the Thr845 residue, which is essential for the kinase activity of ASK1 [266]. Additionally, oxidants have the capacity to induce tumor necrosis factor-alpha (TNF-α) signaling through the TNF receptor (TNFR), culminating in the release of ASK1 from Trx [280].

Nrf2 functions as a central regulator in cellular responses to oxidative stress, orchestrating the antioxidant defense mechanisms, playing a crucial role in cellular proliferation and differentiation

[281-283]. Under normal (balanced redox) conditions, Nrf2 is bound and kept inactive in the cytoplasm by Kelch-like ECH associated protein 1 (Keap1). Keap1 facilitates the ubiquitination of Nrf2 primarily via the cullin-3 (CUL3)-based E3 ubiquitin ligase pathway, leading to its proteasomal degradation [281]. ROS, specifically H_2O_2 leads to modifications of specific cysteine residues (Cys226, Cys613, Cys622 and Cys624) in Keap1, resulting in a conformational change that reduces its affinity for Nrf2 [282, 284]. Consequently, Nrf2 is stabilized and translocates to the nucleus, where it forms a heterodimer with one of the small musculoaponeurotic fibrosarcoma (sMAF) proteins [282, 285]. This Nrf2-sMAF complex binds to antioxidant response elements (AREs), initiating the transcription of various target genes involved in cellular defense mechanisms [281, 285]. These genes include those encoding antioxidant enzymes such as manganese superoxide dismutase (MnSOD), catalase, peroxiredoxins (Prxs), glutathione peroxidases (GPxs), gamma cysteine ligase (GCL), and heme oxygenase-1 (HO-1) [286].

HIF-1 is a heterodimeric transcription factor composed of a constitutive subunit, HIF-1β, and a regulatory oxygen-dependent subunit, HIF-1α. Under normal oxygen conditions (normoxia), HIF-1α is typically unstable, undergoing degradation. However, under hypoxic conditions or in the presence of ROS, HIF-1α becomes stabilized [287]. Normoxic conditions maintain proline hydroxylation of HIF-1α by prolyl hydroxylase domain (PHD) proteins. The tumor suppressor protein Von Hippel-Lindau (VHL) plays a crucial role in regulating HIF-1α stability by facilitating its ubiquitination and subsequent degradation via the proteasomal system. VHL mediates ubiquitination and proteasomal degradation of HIF-1α by interacting with hydroxylated proline residues (P402 and P564) [266]. Hypoxic conditions inhibit proline hydroxylation, which consequently prevents the degradation of HIF-1α [266]. Moreover, ROS have been implicated in the regulation of HIF-1α activity, as evidenced by studies demonstrating that moderate hypoxia (1.5%

O_2) triggers a burst of mitochondrial ROS production, leading to HIF-1α stabilization [288-290]. At oxygen levels of 1.5%, mitochondria functioned as oxygen sensors, triggering the stabilization of HIF-1α by releasing ROS from complex III into the cytosol [290]. Additionally, the introduction of exogenous H_2O_2 inhibited the activity of PHD proteins, by oxidizing cysteine residues in the catalytic domain of PHD protein 2, leading to reduced degradation and subsequent stabilization of HIF-1α [291]. Oxidative modifications result in the accumulation of HIF-1α and its translocation into the nucleus. There, it combines with HIF-1β to form the HIF-1αβ complex, which binds to the hypoxia-response element (HRE), initiating a hypoxia-resistant adaptive response in cells to promote cell survival [291]. This involves a shift towards ATP production via glycolysis, independent of oxygen availability [291]. This adaptation inhibits oxidative phosphorylation and reduces ROS in hypoxic conditions [292, 293], suggesting a negative feedback mechanism wherein ROS-mediated control of HIF-1 plays a pivotal role [291]. Various mechanisms have been suggested for decreased mitochondrial ROS production during hypoxia, including HIF-1α's ability to activate the gene encoding pyruvate dehydrogenase kinase 1, which inactivates pyruvate dehydrogenase and redirects glucose metabolite pyruvate away from mitochondria [291]. Thereby, HIF-1α can reduce ROS production by inhibiting the mitochondrial tricarboxylic acid cycle [287].

1.9 Effects of TXNIP on metabolism

In recent years, TXNIP has garnered significant interest owing to its multifaceted role in regulating various facets of energy metabolism. TXNIP serves as a major regulator of glucose and lipid metabolism, exerting pleiotropic effects such as modulating β-cell function, hepatic glucose production, peripheral glucose uptake, adipogenesis, and substrate utilization [294]. In addition to its roles related to thioredoxin and alpha arrestin, TXNIP exhibits high expression levels in specific areas of the hypothalamus and brainstem, which are critical centers for regulation of metabolism.

This suggests that neuronal TXNIP plays a significant role in maintaining metabolic homeostasis and energy balance [295, 296]. Supporting this proposed function, a study by Blouet et al. has shown that hypothalamic TXNIP responds to hormonal and nutrient signals, thereby regulating metabolism of adipose tissue and maintaining glucose balance [297]. Subsequent studies have demonstrated the function of TXNIP in Agouti-related protein (AGRP) neurons in mediation of diet-induced obesity by regulating energy expenditure and metabolism of adipose tissue, however the underlying mechanisms are not fully understood. Mice with overexpressed TXNIP in AGRP neurons are prone to diet-induced obesity due to heightened adipogenesis and diminished energy expenditure. Conversely, targeted deletion of TXNIP in AGRP neurons shields animals from diet-induced obesity by increasing energy expenditure and decreasing fat storage in adipose tissue [298]. TXNIP expression is notably upregulated during fasting-induced and natural torpor, a condition characterized by reduced body temperature and metabolic rate. Based on these findings, TXNIP is believed to act as a key nutrient sensor, regulating energy homeostasis within the brain during prolonged periods of hypothermia and fasting [299].

1.9.1 TXNIP and glycolysis

In a study employing DNA microarrays in human islets, TXNIP emerged as the gene showing the highest upregulation in response to glucose stimulation [300]. Mechanistically, it was demonstrated that TXNIP is transcriptionally induced by a carbohydrate response element (ChoRE) binding transcription factor complex, MondoA-MLX and/or ChREBP-MLX. This suggests that TXNIP acts as a glucose-responsive gene and plays a significant role in glucose metabolism [301, 302]. TXNIP negatively modulates glucose uptake from the extracellular space in human skeletal muscles, both in an insulin-dependent and insulin-independent manner [303]. Mechanistically, it has been observed that TXNIP-mediated suppression of glucose uptake involves the clathrin-mediated

endocytosis of GLUT1 [304] and GLUT4 [305]. This indicates that the expression of TXNIP induced by glucose works to inhibit glucose uptake, thereby restoring energy homeostasis, particularly during conditions of rapid glucose influx mediated by GLUT1 and GLUT4 in insulin-independent and insulin-dependent contexts, respectively. Furthermore, studies have elucidated the role of AMP-activated protein kinase (AMPK) signaling in the regulation of TXNIP levels in response to energetic stress. Activation of AMPK signaling leads to phosphorylation of TXNIP on the Ser308 site, enhancing its susceptibility to proteasomal degradation mediated by the ITCH ubiquitin ligase [304]. This degradation of TXNIP by AMPK alleviates its inhibition of GLUT1, thereby promoting glucose uptake [304]. Similarly, in 3T3-L1 adipocytes, TXNIP was found to modulate GLUT4 transporters in a similar manner. Interestingly, in this system, AKT phosphorylation of the same AMPK site induces proteasomal degradation of TXNIP, leading to AKT-dependent glucose influx via GLUT4 in response to growth factor stimulation [305]. Moreover, TXNIP deficiency has been associated with inactivation of phosphatase and tensin homolog (PTEN), a PI3K/AKT negative regulator, resulting in increased PI3K/AKT signaling via a redox-sensitive mechanism. Loss of TXNIP inhibits the reduction of cysteine71 and cysteine124 on the active site of PTEN, primarily due to an increased NADH/NADPH ratio, which prevents the Trx-mediated reductive activation of PTEN [306, 307].

Concomitant with diminished mitochondrial activity, heightened glucose uptake, and elevated lactate accumulation, the absence of TXNIP also triggers metabolic reorganization favoring aerobic glycolysis [308]. Under normoxic conditions, TXNIP plays a crucial role in modulating the activity of the hypoxia-induced transcription factor, HIF1α, thereby inhibiting the metabolic shift towards glycolysis. Specifically, TXNIP destabilizes HIF1α by facilitating its association with the β-domain of von Hippel-Lindau protein (pVHL), thereby enhancing the interaction between pVHL

and HIF1α. This interaction promotes the nuclear export and subsequent degradation of HIF1α [204, 309]. As a key regulator of glycolytic gene expression, HIF1α transcriptionally upregulates numerous glycolytic enzymes [310, 311]. In line with these findings, TXNIP knockout (KO) mice exhibit heightened glycolytic activity in oxidative tissues, particularly the heart and skeletal muscles. Moreover, under fasting conditions, KO mice display increased plasma lactate levels, indicating an augmented reliance on anaerobic glycolysis for energy following the loss of TXNIP [306].

1.9.2 TXNIP and Tricarboxylic Acid (TCA) cycle

TXNIP has been identified as a crucial regulator that governs the conversion of pyruvate into acetyl-CoA for mitochondrial glucose oxidation via the TCA cycle and electron transport, indicating its role as a "gatekeeper" in this metabolic process [312]. A study conducted by Yoshioka et al. revealed that cardiomyocytes lacking TXNIP exhibit heightened glycolysis and augmented lactate production, a Warburg-like effect [312]. In line with this observation, our lab has documented that Hcb-19 mesangial cells lacking TXNIP, when subjected to high glucose conditions, exhibited a notable increase in lactate concentrations detected in the culture medium compared to control C3H cells. Moreover, in control cells, the addition of high glucose led to an elevation in mitochondrial membrane potential, unlike in TXNIP deficient cells, indicating that mitochondrial glucose metabolism was not enhanced in the absence of TXNIP [313]. These findings provide support for the concept that TXNIP plays a crucial role in enhancing glucose metabolic flux via the TCA cycle.

The precise mechanism by which TXNIP regulates the TCA cycle remains unclear [209], but evidence suggests that HIF-1α plays a pivotal role in this metabolic regulation. TXNIP is essential for mediating the degradation of HIF-1α, and the absence of TXNIP is associated with the

accumulation of HIF-1α and metabolic reprogramming towards anaerobic glycolysis. HIF-1α plays a crucial role in orchestrating this metabolic shift by inducing the expression of various glycolytic enzymes such as aldolase A and pyruvate kinase M [314, 315]. Furthermore, HIF-1α reduces mitochondrial oxygen consumption by activating pyruvate dehydrogenase kinase 1 and inhibiting the TCA cycle [293].

1.10 Effects of TXNIP on growth, proliferation, and apoptosis

Cellular growth, proliferation, and apoptosis are tightly regulated processes essential for maintaining tissue homeostasis and organismal development. TXNIP has been implicated in these important cellular processes through interactions with signaling pathways, metabolic processes, and apoptotic machinery. TXNIP has been shown to suppress Akt activation, via maintaining the activity of PTEN phosphatase, thereby inhibiting downstream signaling events involved in cell growth and survival [306, 307]. Moreover, TXNIP modulates cellular growth by regulating the expression of genes involved in metabolic processes, such as glucose metabolism as previously discussed in Section 1.8 of this thesis.

TXNIP has been proposed as a significant suppressor of tumorigenesis. While Trx is frequently upregulated in different cancer types [316], TXNIP expression is notably decreased in various tumor tissues and cancer cell lines [200, 317]. The reduction in TXNIP expression has been demonstrated to confer increased proliferative capacity, heightened glucose uptake, and augmented estrogen-induced cell growth in breast cancer cell lines [318]. In addition, TXNIP knockout (KO) mice have shown an increased susceptibility to Helicobacter pylori-induced gastric carcinogenesis due to chronic inflammation and preneoplastic alterations, accompanied by increased activation of TNFα-induced NF-κB and expression of cyclooxygenase-2 (COX-2) [319]. Moreover, the loss of TXNIP markedly increases the incidence of hepatocellular carcinoma in mice by significantly

enhancing TNFα production and secretion, leading to amplified activation of NF-κB [320]. Additionally, ectopic overexpression of TXNIP can interact with HDAC1 and HDAC3 to inhibit TNFα-induced activation of NF-κB and suppress hepatocarcinogenesis [320]. In a study conducted by Yuan et al., it was observed that human osteosarcoma (OS) tissues and cells exhibited reduced expression of TXNIP, a finding that was significantly associated with poor survival rates. TXNIP was found to exert inhibitory effects on the proliferation, migration, and invasion of OS cells, while promoting their apoptosis [321]. Additionally, the study revealed that the tumor-suppressive role of TXNIP was mediated by its ability to upregulate DNA damage-inducible transcript 4 (DDIT4), an inhibitor of mechanistic target of rapamycin complex 1 (mTORC1). This, in turn, inhibits the phosphorylation of the mTORC1 downstream substrate S6, thereby contributing to the observed antitumor effects of TXNIP [321]. Another potential mechanism by which the loss of TXNIP may contribute to tumorigenesis is through the induction of metabolic alterations resembling a glycolytic phenotype and the Warburg effect. In cancer cells, which often exhibit a dependence on glucose, diminished or absent expression of TXNIP markedly amplifies glucose uptake, thus promoting the progression of tumorigenesis [322].

Several studies have provided evidence supporting the role of TXNIP as a tumor suppressor, demonstrating its ability to attenuate tumorigenesis across various cancer types. For instance, overexpression of TXNIP in the human hepatocellular carcinoma cell line, SMMC-7221, resulted in tumor cell growth arrest and apoptosis [323]. Similarly, TXNIP exhibited anti-proliferative and pro-apoptotic effects in lung carcinoma cells in an in vivo tumor xenograft model [320]. Moreover, the reactivation of TXNIP expression in acute myeloid leukemia (AML) cells was shown to induce leukemia cell apoptosis through an ASK1-MAPK dependent mechanism [324]. In HTh74 anaplastic thyroid cancer cells, overexpression of TXNIP reduced glucose uptake and cell proliferation in

vitro, and also hindered tumor growth and metastasis in an orthotopic thyroid cancer mouse model in vivo [325]. Additionally, overexpression of TXNIP alone in HEp-2 cells, a human head and neck squamous cell carcinoma cell line, was sufficient to inhibit tumor growth of xenotransplants in vivo in immunocompromised mice [326].

1.11 TXNIP knockout mice-in vivo characteristics

Efforts to gain deeper insights into the role of TXNIP in vivo have involved targeted deletion of the TXNIP gene, resulting in the creation of total and conditional TXNIP knockout (KO) mouse models by various research groups [306, 327-329]. These knockout mice exhibit fasting-related metabolic alterations, including elevated ketone bodies, increased levels of free fatty acids, and reduced glucose levels. Notably, these metabolic changes are apparent in both the fasting and fed states of TXNIP KO mice. However, prolonged fasting poses a challenge for these animals, leading to hypoglycemia, ultimately culminating in death [330]. This phenomenon may be attributed to an extreme Warburg effect observed during fasting, characterized by heightened levels of pyruvate, lactate, and ketones, coupled with impaired mitochondrial fuel oxidation, a consequence of TXNIP loss [187]. Furthermore, decreased hepatic gluconeogenesis, specifically due to a deficiency in the supply of glucose-6-phosphate (G6P) and fructose-6-phosphate (F6P) in the terminal steps of gluconeogenesis, has also been documented as a contributing factor [308].

The TXNIP KO mice used in this doctoral project were procured from Jackson Laboratories and were originally generated by Dr. Richard Lee at Harvard University, USA. Further information regarding the generation of these mice can be found in the publication by Yoshioka et al [328]. As for their phenotype, the TXNIP KO mice do not show alterations in Trx activity, have normal lipid profiles, exhibit hypoglycemia, and demonstrate enhanced myocardial glucose uptake [328].

1.11.1 TXNIP knockout mice and diabetes

Induction of TXNIP in the pancreatic islets of both human diabetic patients and diabetic mice, presumably by hyperglycemia has been associated with β-cell apoptosis [331-333]. Notably, TXNIP-deficient mice exhibit increased beta cell mass and are protected from streptozotocin-induced beta cell destruction and subsequent diabetes development [334] as well as diabetes progression in obese db/db mice [335]. Moreover, TXNIP deficiency attenuates glucose toxicity-induced β-cell apoptosis and prevents mitochondrial β-cell death by activating antiapoptotic AKT/Bcl-xL signaling, thereby preserving β-cell mass and function in both type 1 and type 2 diabetes [333, 334]. In addition, TXNIP knockout mice demonstrate improvements in glucose tolerance and insulin sensitivity compared to wild-type counterparts following an eight-week high-fat diet regimen [212]. Furthermore, our lab's research findings indicate that TXNIP deletion mitigates functional and structural kidney damage associated with STZ-induced diabetes in mice, characterized by reductions in albuminuria, glomerular fibrosis, podocyte foot process effacement, glomerular basement membrane thickening, and IL-1β-mediated inflammation [336].

1.12 TXNIP and senescence

The age-related dysregulation of the Trx/TXNIP redox systems has been linked to cellular senescence and the aging process [337]. While the precise effects and underlying mechanisms remain incompletely understood, research suggests that the regulation of cellular redox by Trx's antioxidant activities may confer protection against aging and age-related diseases in *C. elegans* and mice [338-341]. Conversely, studies have revealed a decrease in TXNIP expression in several carcinoma types, including hepatocellular carcinoma, breast cancer, renal cancers, and melanoma [342].

In a study conducted by Huy et al. [343], mouse embryonic fibroblasts (MEF) cells derived from TXNIP knockout mice exhibited elevated ROS production, upregulation of senescence markers such as P16 and P53, and increased staining for senescence-associated beta-galactosidase compared to cells from wild-type mice. The senescence phenotype observed in TXNIP-deficient cells was associated with heightened AKT activation. Another investigation aimed at elucidating the role of TXNIP in age-related macular degeneration revealed that under oxidative stress, TXNIP expression was promptly downregulated in retinal pigment epithelium (RPE) cells. This downregulation was accompanied by decreased cell proliferation and increased expression of P21. Knockdown of TXNIP showed that the inhibited proliferation was a result of TXNIP depletion-induced p53 activation [344].

In a study conducted by Jung et al., it was demonstrated that the deletion of TXNIP significantly reduced mouse survival under paraquat-mediated oxidative stress [345]. Hematopoietic stem cells (HSCs) isolated from 22-month-old TXNIP KO mice displayed elevated levels of ROS and impaired hematopoiesis. This was associated with a significant upregulation of P53-target genes P21 (CDKN1A), BAX, and PUMA. Importantly, the re-expression of TXNIP in TXNIP KO bone marrow cells rescued the redox imbalance and partially restored the survival rate of mice following oxidative stress [345].

In a subsequent investigation using the same model, the authors observed that the premature aging of HSCs resulting from the loss of TXNIP was due to increased ROS production and the expression of aging-associated genes via enhanced p38 MAPK activity. They found that TXNIP inhibited p38 MAPK activity through a direct docking interaction with p38 in HSCs under oxidative stress conditions. Moreover, utilizing a cell-penetrating conjugated peptide (CPP) derived from the TXNIP-p38 interaction motif, it was shown that the inhibition of p38 activity significantly

rejuvenated aged HSCs both in vitro and in vivo [346]. Furthermore, a recent study conducted by Lim et al. revealed that the loss of TXNIP was not correlated with any significant alterations in cell proliferation among MDA-MB-231 cells. However, upon further analysis using Gene Set Enrichment Analysis (GSEA), it was observed that the absence of TXNIP was associated with increased enrichment of pathways related to transforming growth factor beta (TGF-β) signaling and fatty acid metabolism [347]. In a separate investigation targeting the elucidation of TXNIP's role in the development and functionality of human natural killer (NK) cells, models involving the knockdown and overexpression of TXNIP in cord blood hematopoietic stem cells were employed, followed by their in vitro differentiation. The downregulation of TXNIP was observed to correlate with diminished protein synthesis, reduced proliferation during early differentiation stages, and a substantial decline in the overall count of NK cells. Conversely, TXNIP overexpression yielded only modest effects in this context [348].

Embryonic stem (ES) cells cultured in low glucose medium with leukemia-inhibitory factor (LIF) retained pluripotency and could differentiate into primordial germ cells (PGCs) within 3-5 days upon exposure to high glucose medium without LIF. This suggests a potential role for high glucose in promoting ES cell differentiation into PGCs. In a study by Mizuno et al., TXNIP was one of the more highly expressed genes during in vitro differentiation in high glucose medium compared to low glucose medium. Additionally, TXNIP was expressed in specific cell types within developing gonads and adult testes. Notably, TXNIP expression showed the most significant increase in response to high glucose concentration and was specifically observed in Sertoli cells of the testis, that serve as supportive cells, providing essential nutrients and regulatory factors for the growth and differentiation of spermatogenic cells [349].

Lastly, Caloric restriction and fasting are widely recognized methods for extending longevity [350-352]. Intriguingly, studies have shown that TXNIP expression is strongly upregulated in mice subjected to fasting compared to those in a fed state [299, 305, 353]. This suggests a potential contribution of TXNIP to the longevity effects of calorie restriction.

1.13 Hypothesis and Rationale

Rationale:

The rationale behind this project stems from two observations. First, in my early studies of renal mesangial cells (MC) from both wildtype (WT) and TXNIP knockout (KO) mice, it was observed that TXNIP KO cells exhibited reduced viability in comparison to wild-type (WT) cells. Furthermore, the KO cells demonstrated a lower rate of apoptosis relative to the WT cells. (these data are shown in chapter 3 of this thesis). Second, previous studies have implicated the involvement of TXNIP in senescence and aging. These were primarily focused on hematopoietic stem cells and mouse embryonic fibroblasts. Chronic activation of AKT, which is known to promote cellular senescence and increased ROS production was implicated. It has also been reported that the metabolic effects of TXNIP deficiency that result in increased glycolysis versus TCA cycle glucose metabolism results in increased NADH/NADPH ratio and inhibition of the lipid phosphatase PTEN. It remains unclear whether TXNIP deficiency elicits senescence in other cell types, organs and in vivo. Cellular senescence is known to be associated with aging, however, the effect of lack of TXNIP in vivo on longevity has not been investigated.

Hypothesis:

I hypothesize that TXNIP plays a crucial role in regulating cellular senescence and organismal aging through mechanisms involving PTEN inhibition, AKT activation, and ROS production. I

propose that optimal levels of TXNIP expression protect against cellular senescence and aging, while loss of TXNIP leads to increased susceptibility to these processes (Figure 1.3)

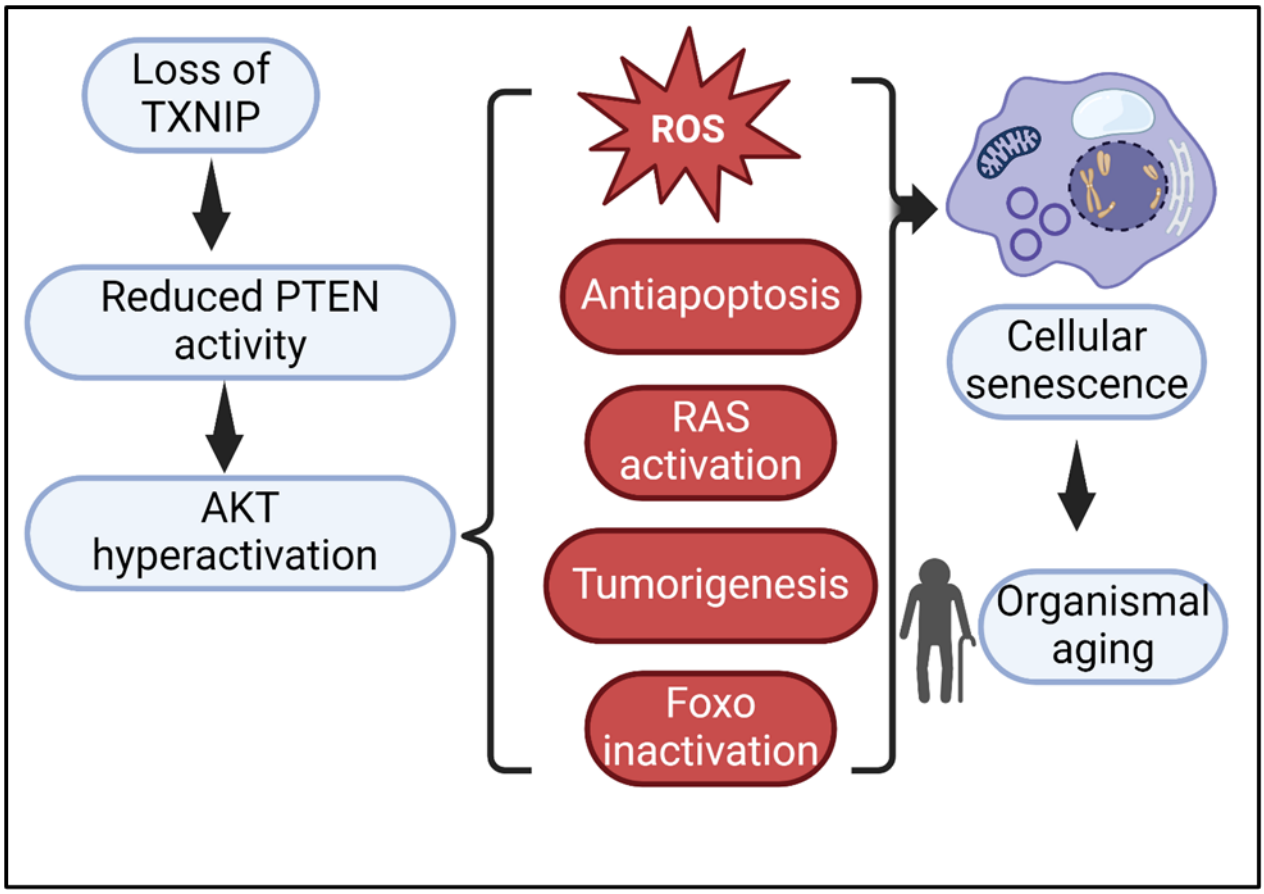

Figure 1.3: Illustration of the proposed hypothesis.

Chapter 2 Materials and methods

2.1 In vitro studies

2.1.1 Cell culture

2.1.1.1 Replicative senescence

Primary mouse mesangial cells (MC) from B6;129-SF2/J (wild-type TXNIP) and B6;129-TXNIPtm1.1Rlee/J (strain number 018313, Jackson Laboratory) (TXNIP- knockout) mice were isolated and characterized as described [354, 355]. MC were grown in low glucose Dulbecco's Modified Eagle Medium (DMEM) supplemented with 10% FBS, 2mM 4-(2-hydroxyethyl)-1-piperazineethanesulfonic acid (HEPES) and 1% penicillin-streptomycin at 37°C with fresh medium change every 48 hours until 70%-80% confluency. Cells were then passaged until late passage (P25) by trypsinizing the cells and culturing 100000 cells in 10cm plates and grown to 70%-80%. Each cycle of trypsinizing the cells and growing to 70%-80% confluency was considered a passage. Cells were harvested at the passage numbers used for further analysis (Early passage (EP (between P5 and P7)), and Late passage (LP (P25)).

2.1.1.2 AKT and PI3K inhibition

The AKT inhibitor (GSK 690693, Santa Cruz Biotechnology, Cat# sc-363280) and PI3K inhibitor (LY 294002, Santa Cruz Biotechnology, Cat# sc-201426) were dissolved in dimethyl sulfoxide (DMSO) and applied to 100,000 cells of EP WT and TXNIP KO MC cultured in 10% FBS-supplemented DMEM medium. The AKT inhibitor was administered at a concentration of 5μM and PI3K inhibitor was administered at a concentration of 25 μM for a duration of 72 hours. An equal volume of DMSO was added to the control samples. Following treatment, cells were lysed and kept at -80°C for further analysis.

2.1.1.2.3 High glucose

EP WT, LP WT and EP KO MC were grown in the standard medium condition until 70-75% confluency. High glucose (HG) (25mM) was added to the medium and the cells were grown for 48h. The cells were then lysed and kept at -80°C for further analysis.

2.1.1.4 NOX4 inhibition

25,000 cells were plated in 200 µL of medium supplemented with 10% FBS in individual wells of a 96-well plate and cultured for a duration of 24 hours. Subsequently, NOX Inhibitor IV, GKT136901 (Sigma Aldrich, Cat# 534032), was solubilized in DMSO and introduced to the cells at concentrations of 0.1 and 1 µM. Following incubation for 48 hours, quantification of reactive oxygen species (ROS) was performed utilizing the below-described DCF method (section 2.1.9).

2.1.2 Western blotting

Following the collection of total cell lysates, the protein concentration was determined using a modified Lowry microassay kit (Bio-rad, Hercules, CA). To ensure equal loading of protein for subsequent immunoblotting, the protein concentration was adjusted to be uniform across all samples of each experiment. Subsequently, the samples were boiled in 4X sample buffer, and 10-20µg of protein was separated on 10-15% SDS-PAGE gels and transferred onto either nitrocellulose or PVDF membranes. The membranes were then blocked using either 5% milk-Tris buffered saline containing 0.1% Tween 20 (for non-phosphorylated proteins) or 5% bovine serum albumin (BSA)-Tris buffered saline containing 0.1% Tween 20 (for phosphorylated proteins). Primary antibodies were used at concentrations of 1:500 to 1:1000, while secondary antibodies were used at 1:4000 concentration. The primary and secondary antibodies used are summarized in Table 2.1. β-actin was used as a loading control housekeeping protein (1:10000). To visualize the immunoblots, ECL detection system was used and to quantify the bands, NIH image J software

was used for densitometric analyses. In all experiments, the protein/β-actin ratios were determined. The control samples were normalized to a value of 1.0, and the ratios for the experimental samples were expressed as fold changes relative to the control.

Table 2.1: List of antibodies

Antibody	Manufacturer	Catalog number
P53	Cell signaling	9282
P16	Santa Cruz	sc 1661
TXNIP	Cell signaling	14715
Ser139 phosphorylated Histon H2AX	Cell signaling	9718
Histon H2AX	Cell signaling	2595
Ser 473 phosphorylated AKT	Cell signaling	9271
AKT	Cell signaling	9272
Ser 256 phosphorylated FoxO1	Cell signaling	9461
FOXO1	Cell signaling	2880
Ser 253 phosphorylated FoxO3	Cell signaling	9466
FoxO3	Cell signaling	2497
ChREBP	Cell Signaling	58069
MondoA	Servicebio	GB114701-100
PTEN	Cell signaling	9559
Nrf2	Cell signaling	12721
NOX4	Novus biologicals	NB110-58849
SOD2	Cell signaling	13194
Catalase	Cell signaling	8841
β-actin	Invitrogen	MA5-15739, PA1-183

2.1.3 Senescence associated beta galactosidase staining (SA-β-gal)

Cell staining was conducted following the manufacturer's guidelines (Abcam, Toronto, Canada, Cat# ab65351). In brief, 100,000 cells were seeded in 6-well plates and cultured for 48 hours. The culture medium was then aspirated, and the cells were fixed using 4% paraformaldehyde before staining at pH 6. After staining, the plates were covered with nylon foil to prevent pH change upon exposure to CO_2 in the incubator. Cells were incubated overnight at 37°C. Ten random fields of view were captured using a light microscope (Evos XL-core, life technologies) at 20X magnification. The total cell count and the number of SA-β-gal-positive cells (appearing blue) were determined per field (100-200 cells/field in each experiment. With n=10, total cell count was 1000-2000/condition), and the percentage of β-galactosidase-positive cells was calculated.

2.1.4 Quantitative reverse transcription polymerase chain reaction (RT-qPCR) for TXNIP

WT MC at passages 5, 10, and 25 were cultured in DMEM supplemented with 10% FBS until reaching 70%-80% confluency. RNA extraction was carried out by homogenizing the cells in 1 ml of Tri-reagent RNA/DNA protein extraction reagent (Sigma, Cat# TR-118). The concentration and purity of the extracted RNA were determined using a Nanodrop spectrophotometer (Thermo Fisher Scientific). Subsequently, cDNA was synthesized from 1 µg of total RNA using the M-MLV reverse transcription kit (Invitrogen). Real-time PCR analysis was performed using the Taqman gene expression system (Applied Biosystems) with gene-specific primers for mouse TXNIP (Mm00452393_m1) and the housekeeping gene Actb (Mm02619580_g1). The PCR reaction mixture (25 µl) comprised 10 µl of 300 ng/ml cDNA, 1.25 µl of double-distilled water, 1.25 µl of Taqman Gene Expression Primers, and 12.5 µl of Taqman Fast Advanced Master Mix (Cat# 4444556). The samples were loaded into a 96-well reaction plate and then analyzed on an ABI Prism 7900HT sequence detection system. The obtained values were normalized to Actb for

all samples. The final results were calculated as fold changes relative to wildtype EP (P5) MC, which served as controls. Fold changes were calculated using the $2^{(-\Delta\Delta Ct)}$ method.

2.1.5 MTT assay

EP and LP WT and KO MC were seeded at a density of 7000 cells per well in 96-well plates and cultured for 24 hours. The MTT assay was conducted according to the manufacturer's instructions (Abcam, Toronto, Canada, Cat# ab211091). Briefly, after 24 hours of cell culture, the medium was aspirated, and 50 µl of serum-free DMEM medium along with 50 µl of MTT reagent were added to each well. The cells were then incubated at 37°C for 3 hours. Subsequently, the MTT mixture was removed, and 150 µl of MTT solvent was added to each well. The plate was covered with aluminum foil to protect it from light and placed on a shaker for 5 minutes. Absorbance was measured using a plate reader at a wavelength of 590 nm. Cell-free culture media was used as a background control.

2.1.6 Relative telomere length

EP and LP WT and KO MC were cultured in DMEM medium supplemented with 10% FBS until reaching 70-80% confluency. Genomic DNA was extracted from the cells using 1 ml of Tri-reagent RNA/DNA protein extraction reagent (Sigma, Cat# TR-118). The concentration and purity of the isolated DNA were assessed using a Nanodrop spectrophotometer (Thermo Fisher Scientific). Relative telomere length to a standard sample WT (EP) was determined following the manufacturer's protocol (ScienCell, Cat# M8918, Carlsbad, CA, USA). Briefly, 1 ng of genomic DNA from each sample was mixed with telomere or single-copy reference primer and master mix (ScienCell, Cat# MB6018a-1) provided in the kit to create a reaction volume of 20 µl. The qPCR program included an initial denaturation step at 95°C for 10 minutes, followed by denaturation at 95°C for 20 seconds, annealing at 52°C for 20 seconds, and extension at 72°C for 45 seconds,

repeated for 32 cycles. All experimental reactions were performed in duplicate, and calculations were conducted according to the manufacturer's instructions.

2.1.7 Terminal deoxynucleotidyl transferase biotin-dUTP nick end labeling (TUNEL) assay

The TUNEL assay was conducted to detect apoptotic cells following the manufacturer's instructions (DeadEnd Fluorometric assay, Promega, Madison, USA, Cat# G3250). In brief, 100,000 cells were cultured on glass coverslips for 48 hours at 37°C. The cells were then fixed with 4% paraformaldehyde for 25 minutes and permeabilized with 0.2% Triton X-100. Subsequently, the cells were incubated with the TUNEL reaction mix in a humidified incubator at 37°C for 1 hour, followed by staining of the nuclei with DAPI. The samples were prepared for microscopic examination by mounting the coverslips onto microscopic slides. Apoptotic cells were visualized under a fluorescence microscope at 20x magnification, with apoptotic cells appearing green. The percentage of apoptotic cells was calculated relative to the total cell count in a specific field (minimum 80 cells/field. With n=10, a total cell count was 800-1500/condition).

2.1.8 Intracellular ROS imaging

50,000 MC were seeded in each well of an 8-well glass bottom microslide (Ibidi, USA) containing 300 µl of DMEM medium supplemented with 10% FBS and cultured for 24 hours at 37°C. Following incubation, the cells were washed three times with PBS and then incubated in the dark with carboxymethyl-H2-dichlorofluorescein diacetate (CM-H2-DCF-DA) in FBS-free medium for 30 minutes at 37°C. To visualize intracellular ROS production, a Zeiss LSM 780 laser scanning confocal microscope was utilized with excitation/emission wavelengths set at 488 nm/515 nm while maintaining the cells at 37°C.

2.1.9 Intracellular ROS quantification

Intracellular ROS levels were quantified using the DCFDA / H2DCFDA - Cellular ROS Assay Kit (Abcam, cat # ab113851), adhering to the manufacturer's protocol. Briefly, 25,000 MC (both WT and KO at the tested passages) were seeded in 200 µL of medium supplemented with 10% FBS in a 96-well plate and cultured for 24 hours. Following this incubation period, the medium was aspirated, and each well was treated with 20 µM of DCF diluted in 100 µL of PBS. The cells were then incubated with the DCF solution at 37°C for 45 minutes while protected from light. After the incubation period, the DCF solution was removed, and 100 µL of fresh medium was added to each well. The plate was immediately measured on a fluorescence plate reader with excitation/emission wavelengths set at 485/535 nm.

2.1.10 Mitochondrial ROS (Mitosox assay)

50,000 MC (both WT and KO at the tested passages) were seeded in 300 µl of DMEM medium supplemented with 10% FBS in an 8-well glass bottom microslide (Ibidi, USA) and incubated for 48 hours. Following incubation, the cells were treated with 3 µM Mitosox (Invitrogen, Cat# M36008, Canada) in PBS for 10 minutes to assess mitochondrial ROS production. Mitochondrial ROS were visualized using a Zeiss LSM780 Laser Scanning Confocal Microscope with excitation/emission wavelengths set at 488 nm/515 nm while maintaining the cells at 37°C. Mean intensity fluorescence was determined using NIH image J software.

2.1.11 Activated Ras pull down assay

Active Ras-GTP detection was conducted utilizing the Active Ras Detection Kit (Cell Signaling, Cat# 8821) in accordance with the manufacturer's instructions. In brief, cells were cultivated under standard medium conditions until reaching 70-80% confluency, after which they were lysed. Following lysis, the lysate was centrifuged at 13,000 × g for 15 minutes, and aliquots of the

resulting supernatant were utilized for immunoprecipitation. Glutathione Agarose resins were used for the affinity purification of GST-bound Ras. To ensure the efficacy of the immunoprecipitation procedures, GTPγS (positive control) and GDP (negative control) were included. Subsequently, the abundance of Ras was assessed via Western blot analysis.

2.1.12 TXNIP reconstitution

To reintroduce TXNIP expression in TXNIP KO MC, Lentiviral ORF particles containing human WT TXNIP (Origene, Cat# RC210804L2V) and 247 Cys to Ser mutant TXNIP (Origene Cat# RC210804L4) with mGFP tagging and mGFP cDNA (Origene Cat# CW309959) were utilized following the manufacturer's guidelines. Initially, 25,000 cells were cultured in a standard growth medium in a 24-well plate for 24 hours to allow for cell attachment. Subsequently, lentivirus particles were added to the cells at a multiplicity of infection (MOI) of 2, supplemented with polybrene (Sigma Cat# TR-1003-G) at a concentration of 16 μL/mL. The cells were then incubated with the lentivirus particles for a duration of 48 hours. Following incubation, the medium containing lentivirus was aspirated, and fresh lentivirus-free medium was added. The cells were cultured for an additional 72 hours before being lysed, with the lysates stored at -80°C for subsequent analysis. Transfection efficiency was confirmed by visualizing the cells under a fluorescence microscope to detect green GFP fluorescence.

2.2 In vivo studies

2.2.1 The animals

B6129SF2/J mice (strain number 101045), which represent the WT genotype controls for the TXNIP KO, and B6;129-TXNIPtm1.1Rlee/J mice (strain number 018313), known as TXNIP KO mice, were obtained from the Jackson Laboratories and bred in the animal facility of the Research Institute of McGill University Health Center (RI-MUHC). The animals were housed under

standard animal facility conditions with a 12-hour light-dark cycle and regular health monitoring. Female and male mice aged 21 months were used for the experiments unless specified otherwise. All experimental procedures were conducted in compliance with the guidelines of the Canadian Council on Animal Care (CCAC) and were approved by the local McGill University Animal Care Committee.

Mice were provided with regular chow (Harlan Laboratories). Body composition analysis of 21-month-old male and female mice was conducted using EchoMRI (Echo Medical Systems).

2.2.2 The behavioral tests

2.2.3.1 Y-maze

Spontaneous alteration behavior (SAB) was evaluated to measure working memory function in both WT and TXNIP KO mice aged 15 and 21 months. The assessment was conducted using a Y-maze from the San Diego Y maze Instrument model (7001-0307) following a standardized protocol [356, 357]. During an 8-minute test period, SAB, defined as choosing a different arm than the two previous choices, was quantified. The SAB score was calculated as the total number of alternations during the 8-minute test period (total arm entries -2). Results are shown as the percentage of SAB (%SAB).

2.2.3.2 Rota-rod

To evaluate motor learning and coordination, both WT and TXNIP KO mice aged 15 and 21 months underwent a 60-minute acclimatization period in the testing room. Subsequently, the mice received three training sessions lasting 5 minutes each on the Rota-rod apparatus (MED-Associates) set at a constant speed. One hour after the training, the mice were placed on the rotating rod, which increased in speed from 4 RPM to 40 RPM over 300 seconds. The latency to fall off

the rotarod was recorded for each mouse. The mean latency of two consecutive trials was used for the analysis. This method was adapted from the study conducted by Dai et al [358].

2.2.3 Tissue collection

Mice were euthanized by exposure to carbon dioxide (CO_2) while under anesthesia with Isoflurane. The kidney cortex and brain were carefully dissected and promptly snap-frozen on dry ice, then stored at -80°C for subsequent analysis. The hippocampal region was meticulously isolated from the brain following established protocol [359]. For Western blotting analysis, approximately 50 mg of frozen kidney cortex and hippocampal region samples from both WT and TXNIP KO mice were pulverized in liquid nitrogen and homogenized in 1 ml of lysis buffer. The samples were then centrifuged to remove any residual tissue debris. Protein concentration determination, separation on SDS-PAGE gel and subsequent immunoblotting were all done following the procedures outlined in the in vitro western blotting section of the methods (2.1.2).

2.2.4 Senescence associated beta galactosidase staining (SA-β-gal)

The experimental procedure followed the protocol Cazin et al [360]. In summary, kidney samples preserved in optimal cutting temperature (OCT) compound were sectioned into 10 µm slices using a cryostat. Prior to staining, the slides containing tissue sections were fixed in ice-cold phosphate-buffered saline (PBS) solution containing 1% paraformaldehyde for 10 minutes. Subsequently, the slides were rinsed and washed twice with PBS for 10 minutes each. Following this, the tissue sections were incubated in PBS for 30 minutes. The sections were then exposed to X-gal solution at pH of 6 and incubated at 37°C for 24 hours to facilitate beta-galactosidase staining. After the staining period, the slides were washed three times with PBS for 10 minutes each. Finally, the tissue sections were counterstained with 0.2% eosin.

2.2.5 Immunohistochemistry (IHC)

2.2.5.1 P16 IHC in kidney glomeruli

Tissues were extracted and fixed in formalin for 48 hours before processing with a tissue processor to create formalin-fixed paraffin-embedded (FFPE) blocks. Sections of 4 μm thickness were cut, deparaffinized, and rehydrated. Immunohistochemistry (IHC) was performed using the Discovery Ultra instrument from Roche. Following antigen retrieval treatment with Tris-EDTA for 32 minutes, the sections were incubated for 24 minutes at 37°C with an anti-p16 antibody (Abcam, Cat# ab241543) at a 1:500 dilution. This was followed by incubation with an OmniMap anti-Rt HRP secondary antibody (Roche, Cat# 7604457) at room temperature for 20 minutes. Detection was carried out using the ChromoMap DAB Kit (Roche, Cat# 7604304).

The slides were then counterstained with hematoxylin, dehydrated, cleared, and coverslipped. Digital scanning of the slides was performed at 40X magnification using an Aperio scanner for morphometric analysis with Imagescope software. Quantitative analysis was conducted on a minimum of 50 glomeruli per kidney section using QuPath 0.5.5 software.

2.2.5.2 CD45 and CK20 dual IHC staining of tumors

Sections of 4 μm thickness were cut from FFPE blocks, then deparaffinized and rehydrated.

For CK20 detection, sections underwent antigen retrieval with Tris-EDTA for 32 minutes, followed by incubation with an anti-CK20 antibody (Abcam, Cat# ab9754) at a 1:300 dilution for 24 minutes at 37°C. The sections were then incubated with OmniMap anti-Rb HRP secondary antibody (Roche, Cat# 760-4311) at room temperature for 20 minutes. Detection was achieved using the Discovery Purple Kit (Roche, Cat# 760-229). Subsequently, antibody denaturation was performed before incubation with an anti-CD45 antibody (Cell Signaling, Cat# 70527) at a 1:300 dilution for 24 minutes at 37°C. This was followed by a secondary antibody incubation with

OmniMap anti-Rb HRP (Roche, Cat# 760-4311) at room temperature for 20 minutes. Detection was performed using the Discovery Green Kit (Roche, Cat# 760-271).

Slides were counterstained with hematoxylin, dehydrated, cleared, and coverslipped. Digital scanning of the slides was performed at 40X magnification using an Aperio scanner. Morphometric analysis was conducted using Imagescope software.

2.2.6 Longevity (lifespan) study

The animals were housed under standard animal facility conditions until they either reached the end of their natural lifespan (deceased) or displayed severe illness and/or lost 20% of their original weight necessitating euthanasia under veterinary recommendation. The age of each animal was carefully documented and recorded throughout the study duration. Lifespan analysis was conducted using the Kaplan-Meier survival curve method to compare survival rates and assess longevity outcomes across different experimental groups. The log-rank (Mantel-Cox) statistical test was utilized for pairwise comparisons to ascertain the statistically significant differences.

2.3 Statistical analyses

Results are shown as mean ± standard error of the mean (SEM). Graphpad Prism software, version 9.0 (Graphpad Prism, San Diego, CA) was used to calculate the statistical difference. Comparing two sets of samples was performed by t-test analysis, while multiple comparisons were assessed by one-way ANOVA. $p< 0.05$ was considered statistically significant.

Chapter 3 Results

3.1 In vitro studies

3.1.1 Serial passaging induces cellular senescence

Cells have a definite number of divisions after which they stop dividing permanently and acquire a senescence phenotype. This division limit is known as the Hayflick limit [361]. Here, we passaged WT MC in standard medium conditions to induce replicative senescence and compared early passage (EP) (P5-7) to late passage (LP) (P25) for a panel of senescence biomarkers. Late passage (P25) MC showed a significantly higher protein expression of senescence biomarker P53 compared to EP (Figure 3.1A). Cyclin dependent kinase (CDK) inhibitor (P16) is an important mediator of cell cycle arrest and senescence induction [362, 363]. LP MC demonstrated a significant increase in P16 protein expressions than EP (Figure 3.1B). Senescence phenotype in LP MC was further confirmed by significantly higher senescence associated β-galactosidase staining (SA-β-gal) (Fig 3.1C). These findings demonstrate that serial passaging of WT MC to late passages (25) induces cellular senescence.

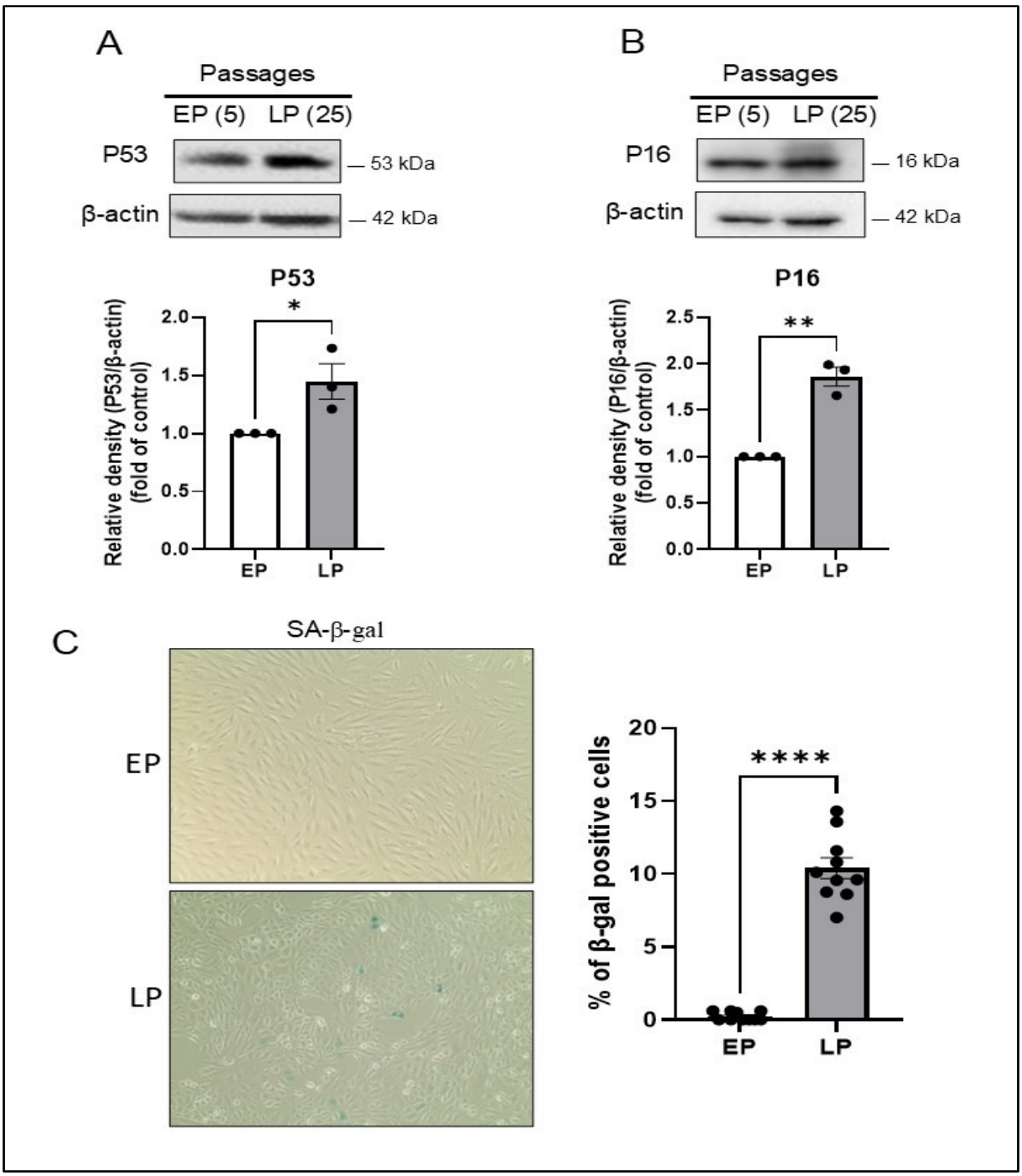

Figure 3.1: Passaging the cells induced cellular senescence. Representative western blots of total cell lysates of EP and LP WT MC LP show (A) increased P53, (B) P16 and (C) β-gal staining (as described in methods). Graphs depict mean values ± SEM (n=3 for A,B and 10 for C). *p<0.05, **p<0.01, ****p<0.0001

3.1.2 Replicative senescence induction in WT MC is associated with TXNIP downregulation

To investigate whether TXNIP has a role in the WT MC senescence phenotype induced by passaging the cells, we measured TXNIP expression at different cell passages (P5, P10 and P25). Surprisingly, both TXNIP protein and mRNA expression were found to be gradually downregulated as cell passage number increased (Figure. 3.2 A,B). MC at P10 showed significantly reduced TXNIP protein and mRNA compared to P5. Moreover, MC TXNIP protein amount and mRNA expression at P25 were further downregulated compared to P10. These data suggest that TXNIP transcription and protein synthesis are significantly downregulated in MC late passage and this downregulation is associated with senescence induction.

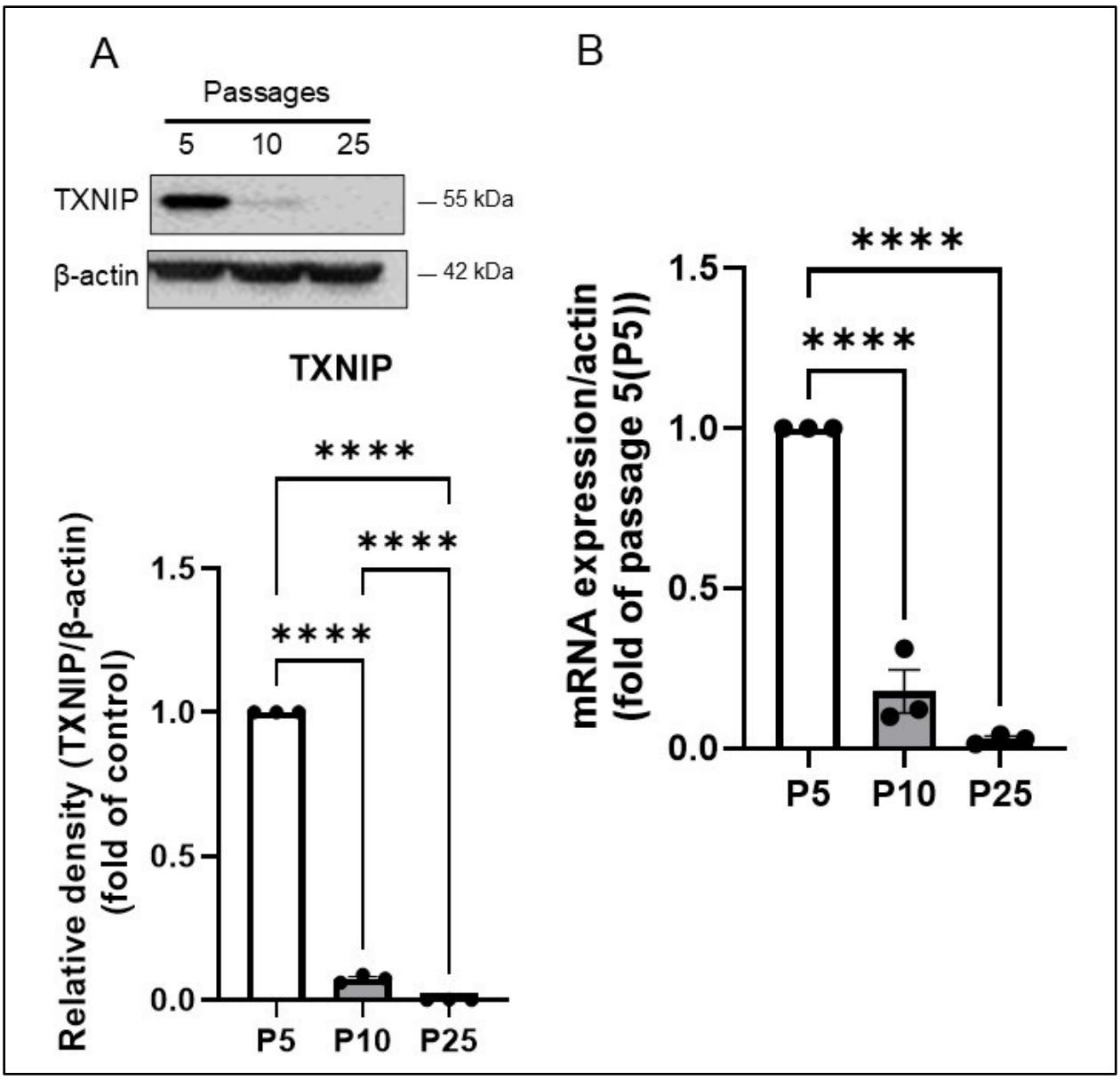

Figure 3.2: Replicative senescence induction in MC is associated with TXNIP downregulation. (A) Representative western blots of total cell lysates of WT MC at P5, P10, P25 showing significant reduction of TXNIP protein level. (B) RT-qPCR analysis of WT MC showing significant downregulation of TXNIP mRNA level at P5, P10, P25. Graphs depict mean values ± SEM (n=3). ****p<0.0001

3.1.3 ChREBP and MondoA downregulation in late passage MC contribute to TXNIP downregulation

To begin to probe the underlying mechanism of TXNIP downregulation, we tested a possible role for carbohydrate element binding protein (ChREBP) and MondoA that are known transcriptional activators of TXNIP gene expression. ChREBP and its paralog MondoA are glucose sensors that bind the TXNIP promoter, enhancing its mRNA expression in response to glucose uptake [301, 364]. Of note, in a recent investigation by Yamamoto-Imoto et al., it was revealed that MondoA exerts a protective function against cellular senescence, with loss of MondoA exacerbating senescence in human retinal pigment epithelial (hRPE) cells under conditions of DNA damage-induced senescence [365]. Interestingly, both ChREBP and MondoA protein levels were found to be significantly reduced in LP compared to EP MC (Figure. 3.3A, B). Moreover, exposure of cells to high glucose (HG) conditions (25 mM for 48 hours) resulted in a notable increase in TXNIP expression in both early and late passage MC (Figure 3.3 C). Of interest, glucose was able to increase TXNIP in both EP and LP cells, its action was more potent in EP consistent with the lower level of ChREBP in LP cells. Intriguingly, despite the lesser potency, late passage MC exposed to high glucose exhibited a significant decrease in the senescence marker P53, coinciding with elevated TXNIP expression induced by high glucose (Figure 3.3 D). These collective observations suggest that the decrease of ChREBP and MondoA in late passage MC contributes, at least in part, to the reduced TXNIP expression observed in these cells. Furthermore, glucose-induced re-expression of TXNIP mitigated the P53 senescence marker in late passage MC, supporting a potential role of ChREBP and MondoA in TXNIP regulation and cellular senescence.

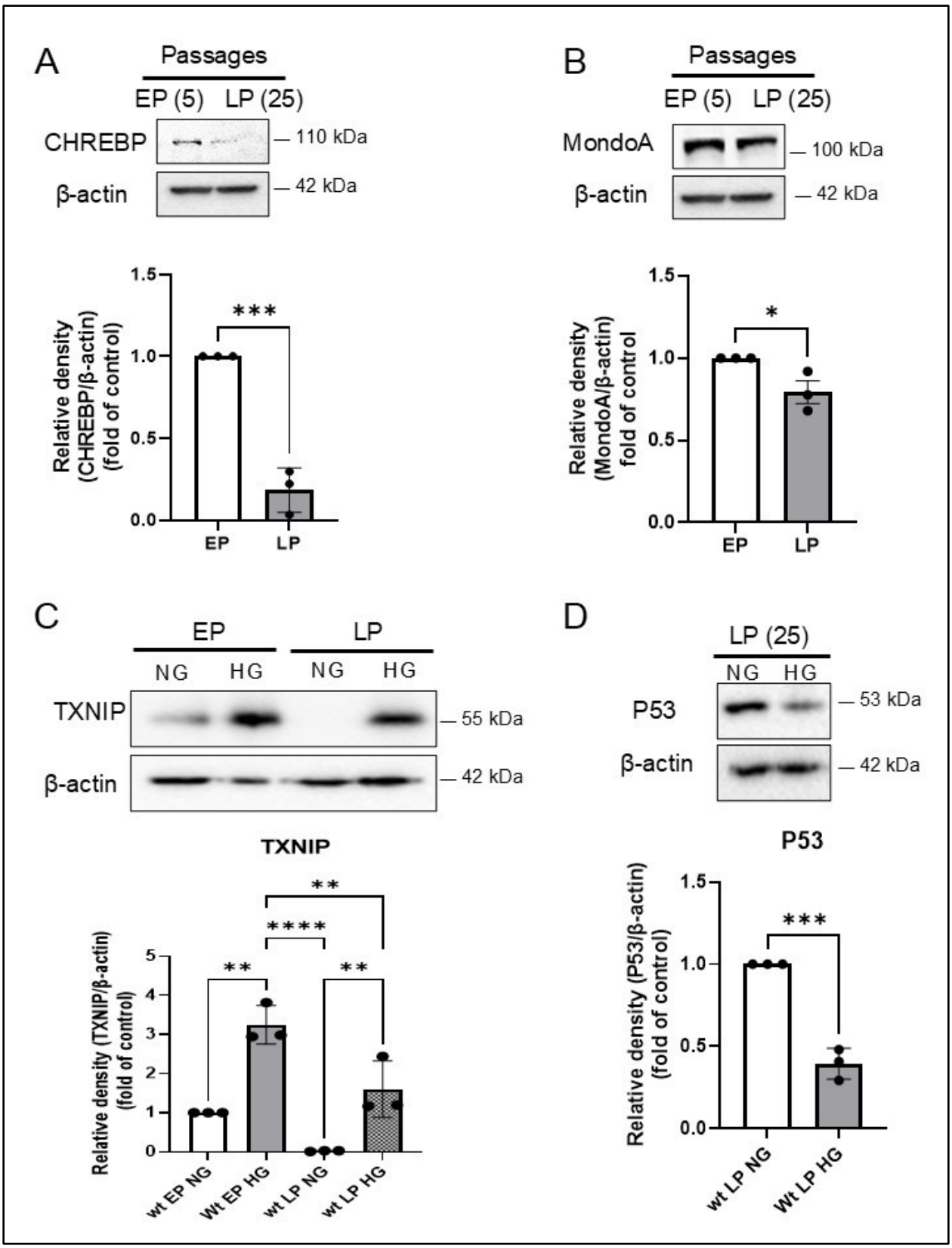
A
Passages
EP (5) LP (25)
CHREBP
— 110 kDa
β-actin
— 42 kDa
Relative density (CHREBP/β-actin) (fold of control)
1.5
1.0
0.5
0.0
***
EP
LP
B
Passages
EP (5) LP (25)
MondoA
— 100 kDa
β-actin
— 42 kDa
Relative density (MondoA/β-actin) fold of control
1.5
1.0
0.5
0.0
*
EP
LP
C
EP
LP
NG HG NG HG
TXNIP
— 55 kDa
β-actin
— 42 kDa
TXNIP
Relative density (TXNIP/β-actin) (fold of control)
5
4
3
2
1
0
**
****
**
**
wt EP NG
Wt EP HG
wt LP NG
wt LP HG
D
LP (25)
NG HG
P53
— 53 kDa
β-actin
— 42 kDa
P53
Relative density (P53/β-actin) (fold of control)
1.5
1.0
0.5
0.0
***
wt LP NG
Wt LP HG

Figure 3.3

Figure 3.3: Glucose sensors ChREBP and MondoA downregulation contribute to TXNIP downregulation in LP WT MC and glucose-mediated TXNIP overexpression downregulates P53 in LP WT MC. (A) Representative western blots of total cell lysates of WT MC at P5, P25 showing significant reduction of ChREBP and (B) MondoA protein levels. (C) High glucose (HG) treatment at 25mM for 48h upregulates TXNIP in both EP and LP WT MC. (D) HG treatment in LP WT MC downregulates P53 expression. Graphs depict mean values ± SEM (n=3). *p<0.05, **p<0.01, ***p<0.001, ****p<0.0001

3.1.4 The absence of TXNIP in primary MC from TXNIP KO mice is sufficient to induce senescence in EP MC

As TXNIP was shown to be downregulated in association with replicative senescence in WT MC, this raised the question of whether loss of TXNIP can be considered an inducer of senescence even at early passage MC. To answer this question, we used primary MC that were obtained from TXNIP knockout mice (KO MC) (Figure. 3.4 A). We measured senescence biomarkers in KO MC versus WT MC both at EP. KO MC showed significant upregulation of the senescence biomarkers P53 and P16 (Figure. 3.4 A, B). The senescence phenotype of EP KO MC was further confirmed by significantly more SA-β-gal-positive cells in KO compared to WT MC (Figure.3. 4 C). Moreover, the levels of (ChREBP) and MondoA were notably elevated in EP TXNIP KO MC compared to control EP WT MC (Figure 3.4 D). The upregulation of ChREBP and MondoA may reflect absence of negative feedback by TXNIP. Consistent with KO of TXNIP, exposure of these cells to high glucose conditions had no effect on the P53 protein level (Figure 3.4 E). These findings indicate that the absence of TXNIP is associated with the induction of cellular senescence even at the EP stage, thus supporting the pivotal role of TXNIP as a downstream effector of senescence regulation, potentially via the ChREBP and/or MondoA pathway.

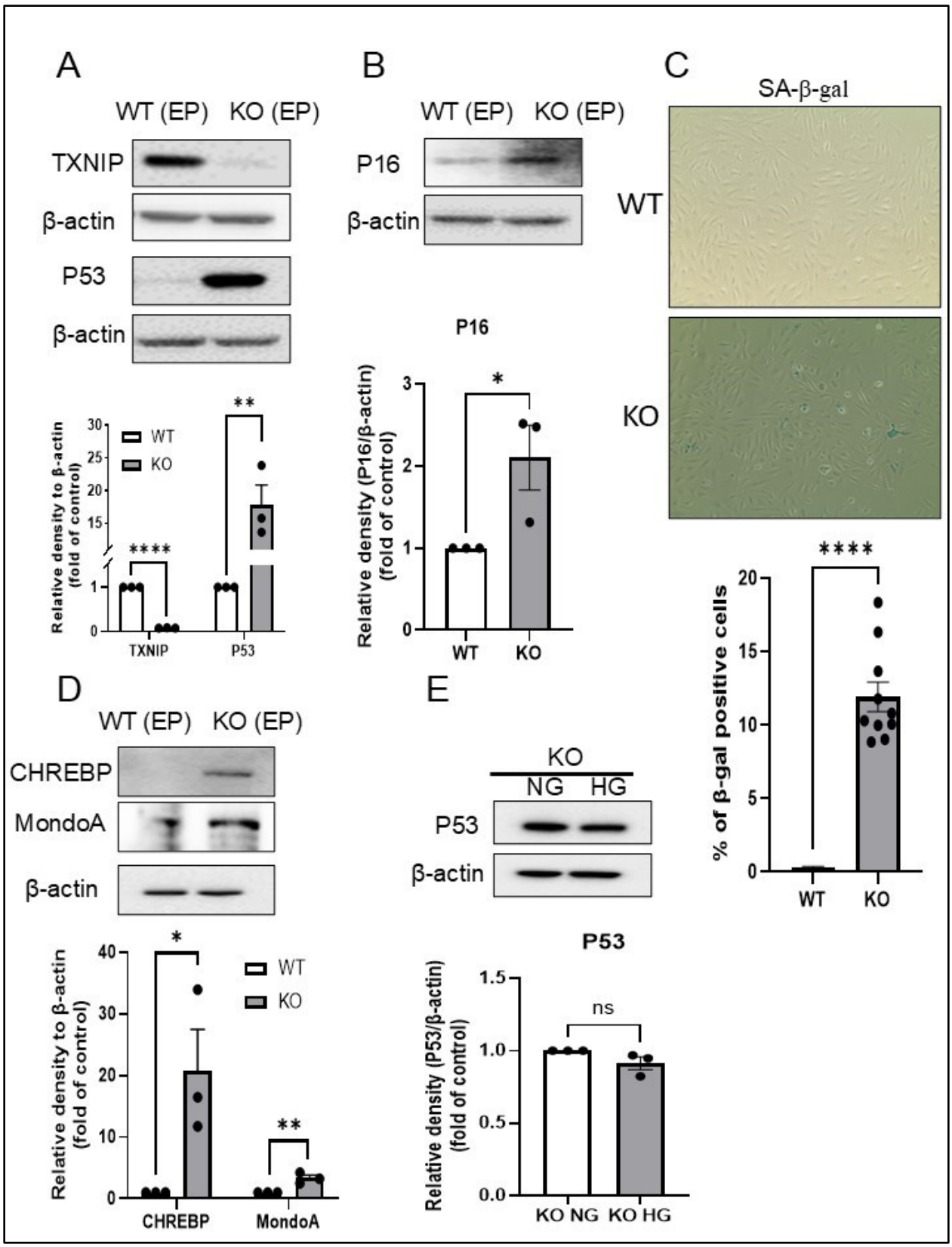
A
WT (EP) KO (EP)
TXNIP
β-actin
P53
β-actin
Relative density to β-actin (fold of control)
WT
KO
TXNIP
P53
B
WT (EP) KO (EP)
P16
β-actin
P16
Relative density (P16/β-actin) (fold of control)
WT
KO
C
SA-β-gal
WT
KO
% of β-gal positive cells
WT
KO
D
WT (EP) KO (EP)
CHREBP
MondoA
β-actin
Relative density to β-actin (fold of control)
CHREBP
MondoA
E
KO
NG HG
P53
β-actin
P53
Relative density (P53/β-actin) (fold of control)
ns
KO NG
KO HG

Figure 3.4

Figure 3.4: The absence of TXNIP in MC from TXNIP KO mice induces senescence in early passage in association with accumulation of ChREBP and MondoA. (A) Representative western blots of total cell lysates of WT MC and TXNIP KO MC at EP showing lack of TXNIP in TXNIP KO MC. (A,B) Lack of TXNIP in EP KO MC significantly upregulates P53, P16 and (C) SA-β-gal staining (as described in methods). (D) TXNIP EP KO MC show significant increase in ChREBP and MondoA compared to EP WT MC. (E) HG treatment at 25mM for 48h did not change expression of P53 in TXNIP EP KO MC compared to TXNIP EP KO MC cultured at NG condition. Graphs depict mean values ± SEM (n=3 for A, B, D, E, and n=10 for C). *$p<0.05$, **$p<0.01$, ****$p<0.0001$

3.1.5 The absence of TXNIP expression at early passage (EP) MC is linked to decreased cell proliferation in telomere length- independent manner

MC lacking TXNIP (TXNIP KO), exhibit significantly lower cell viability compared to WT cells at the corresponding passage number (comparison in both EP and LP) indicated by percentage of viable cells by MTT assay (Figure 3.5 A). Cellular senescence was suggested by observable morphological changes, with LP WT cells and EP KO cells displaying flattened and enlarged characteristics under light microscope, contrasting with the smaller, spindle-shaped morphology of EP WT cells (Figure. 3.5 B). Replicative senescence is associated with telomere shortening [366-368]. Despite the induction of replicative senescence, the loss of TXNIP did not notably impact relative telomere length in EP KO cells. This contrasts with the significant reduction observed in telomere length between LP versus EP cells, in both WT and KO MC (Figure 3.5 C).

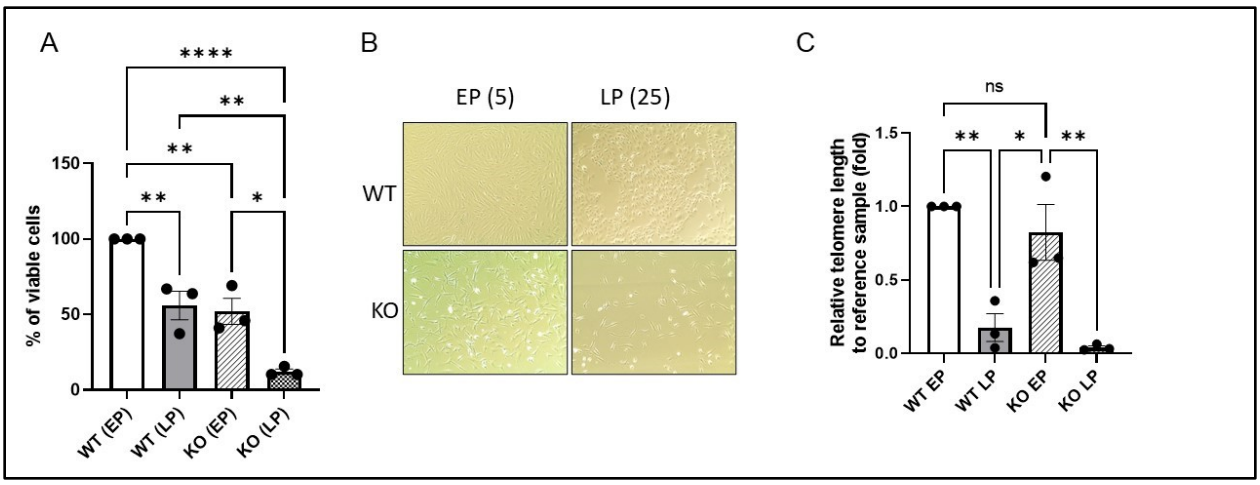

Figure 3.5: TXNIP KO MC demonstrate shorter replicative lifespan and telomere attrition-independent senescence at EP. (A) TXNIP KO MC have significant reduction in percentage of viable cells measured in MTT assay at both EP and LP compared to the corresponding passage of WT MC. (B) Representative light microscope images (20x) showing unique flattened and enlarged senescent cells-associated morphological changes in TXNIP KO EP MC cells compared to the spindle-shaped morphology of WT EP MC. (C) Relative telomere length is significantly reduced in LP vs EP of both WT and TXNIP KO MC, but non-significantly changed in TXNIP KO EP versus WT EP MC. Graphs depict mean values ± SEM (n=3). *p<0.05, **p<0.01, ****p<0.0001

3.1.6 ROS accumulation and DDR activation drive the senescence in LP and TXNIP KO MC

Senescence can be triggered by diverse stimuli, often involving increased production of ROS and subsequent oxidative stress, which play pivotal roles in induction and maintenance [369]. The accumulation of ROS and resulting oxidative stress-induced senescence are closely linked to the activation of the DDR, characterized by histone H2AX phosphorylation. To measure elevated ROS levels and DDR activation, we quantified ROS levels in LP WT MC and EP TXNIP KO MC using live-cell DCF fluorescence. LP WT MC exhibited significantly higher ROS levels compared to EP (Figure 3.6 A), confirmed by laser confocal imaging (Figure 3.6 B). Moreover, LP WT MC displayed increased histone H2AX phosphorylation (Figure 3.6 C), indicative of DDR activation. Similar observations were obtained in TXNIP KO MC at EP, with significant increases in ROS production (Figure 3.6 D, E) and histone H2AX phosphorylation (Figure 3.6 F). These findings demonstrate the association of ROS accumulation and DDR activation in replicative senescence in LP WT MC and TXNIP deficiency-induced senescence in KO EP MC.

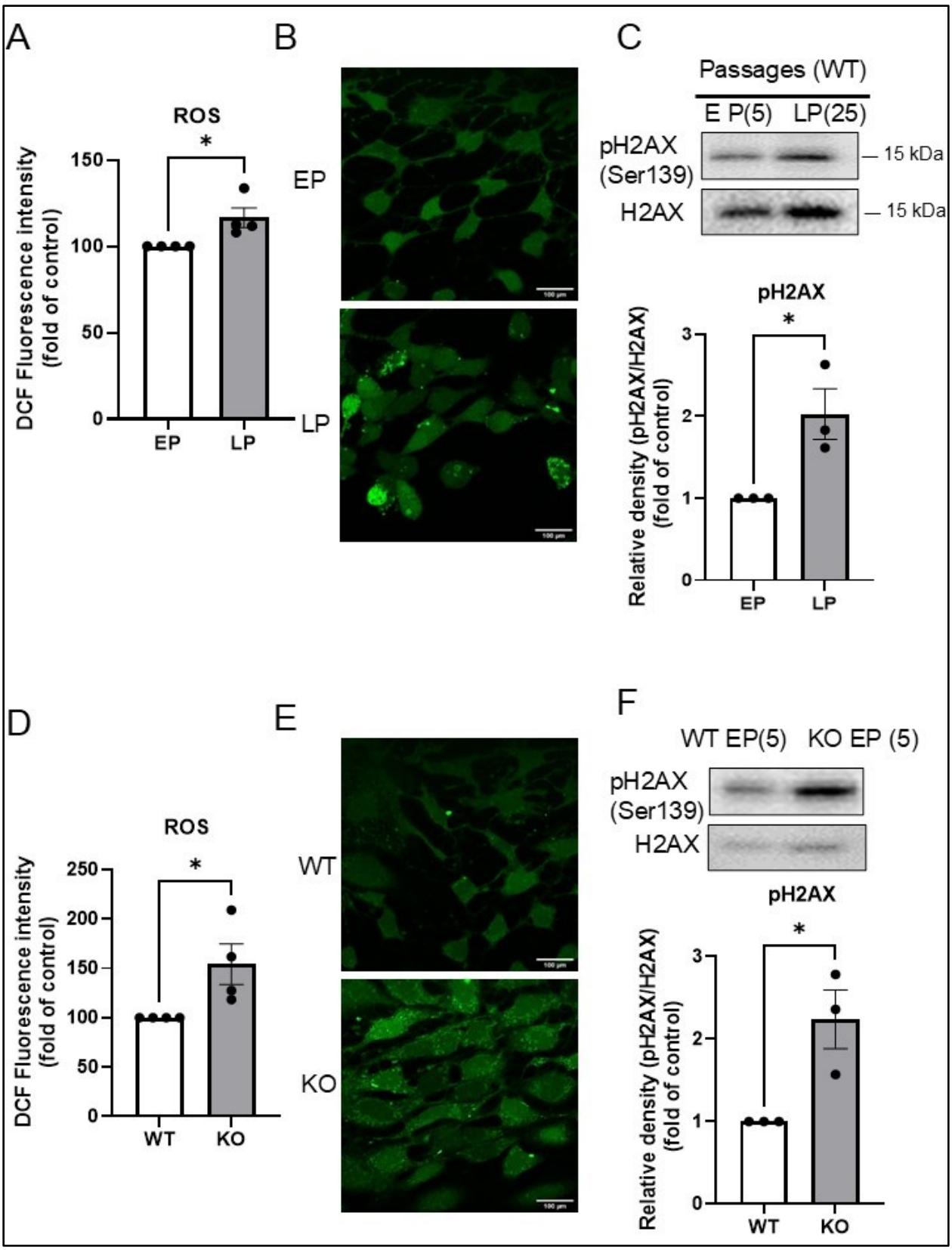
A
ROS
*
DCF Fluorescence intensity (fold of control)
150
100
50
0
EP
LP
B
EP
LP
C
Passages (WT)
E P(5)
LP(25)
pH2AX (Ser139)
H2AX
15 kDa
15 kDa
pH2AX
*
Relative density (pH2AX/H2AX) (fold of control)
3
2
1
0
EP
LP
D
ROS
*
DCF Fluorescence intensity (fold of control)
250
200
150
100
50
0
WT
KO
E
WT
KO
F
WT EP(5)
KO EP (5)
pH2AX (Ser139)
H2AX
pH2AX
*
Relative density (pH2AX/H2AX) (fold of control)
3
2
1
0
WT
KO

Figure 3.6

Figure 3.6: ROS production and DDR activation are increased in LP WT and EP TXNIP KO MC (A) ROS is significantly increased in WT LP MC measured by DCF fluorescence compared to WT EP MC. (B) Representative image by confocal microscopy showing increased fluorescence (indicative of ROS) in LP versus EP WT MC (DCF). (C) Representative western blot of total cell lysates showing significantly increased histone H2AX phosphorylation in LP WT MC compared to EP WT MC. (D,E). EP TXNIP KO MC show significantly increased ROS production and (F) increased histone H2AX phosphorylation compared to EP WT MC. Graphs depict mean values ± SEM (n=3-4), *$p<0.05$

3.1.7 AKT activation is an important driver of senescence in both LP WT and EP KO MC

The activation of the PI3K/AKT pathway has been widely implicated in the triggering of senescence via various pathways, including increased ROS production, replicative senescence, DDR-induces senescence and OIS [370]. To investigate a potential relationship between AKT activation and TXNIP deficiency in senescence, we assessed AKT phosphorylation in LP WT and EP TXNIP KO MC. AKT phosphorylation at serine 473 was significantly elevated in LP WT and EP KO MC compared to EP WT MC (Figure 3 .7 A, C). This activation of AKT was confirmed by enhanced phosphorylation of its substrates, the longevity transcription factors, FOXO 1 and 3 in both LP WT MC (Figure 3.7 B) and EP KO MC (Figure 3.7 D). Cellular senescence is characterized by resistance to apoptosis, a process regulated by pathways including AKT signaling and the antiapoptotic proteins, Bcl-xL and Bcl-W [371, 372]. Both KO EP and WT LP MC exhibited significantly fewer apoptotic cells (measured by TUNEL assay) compared to WT EP MC (Figure 3.7 E).

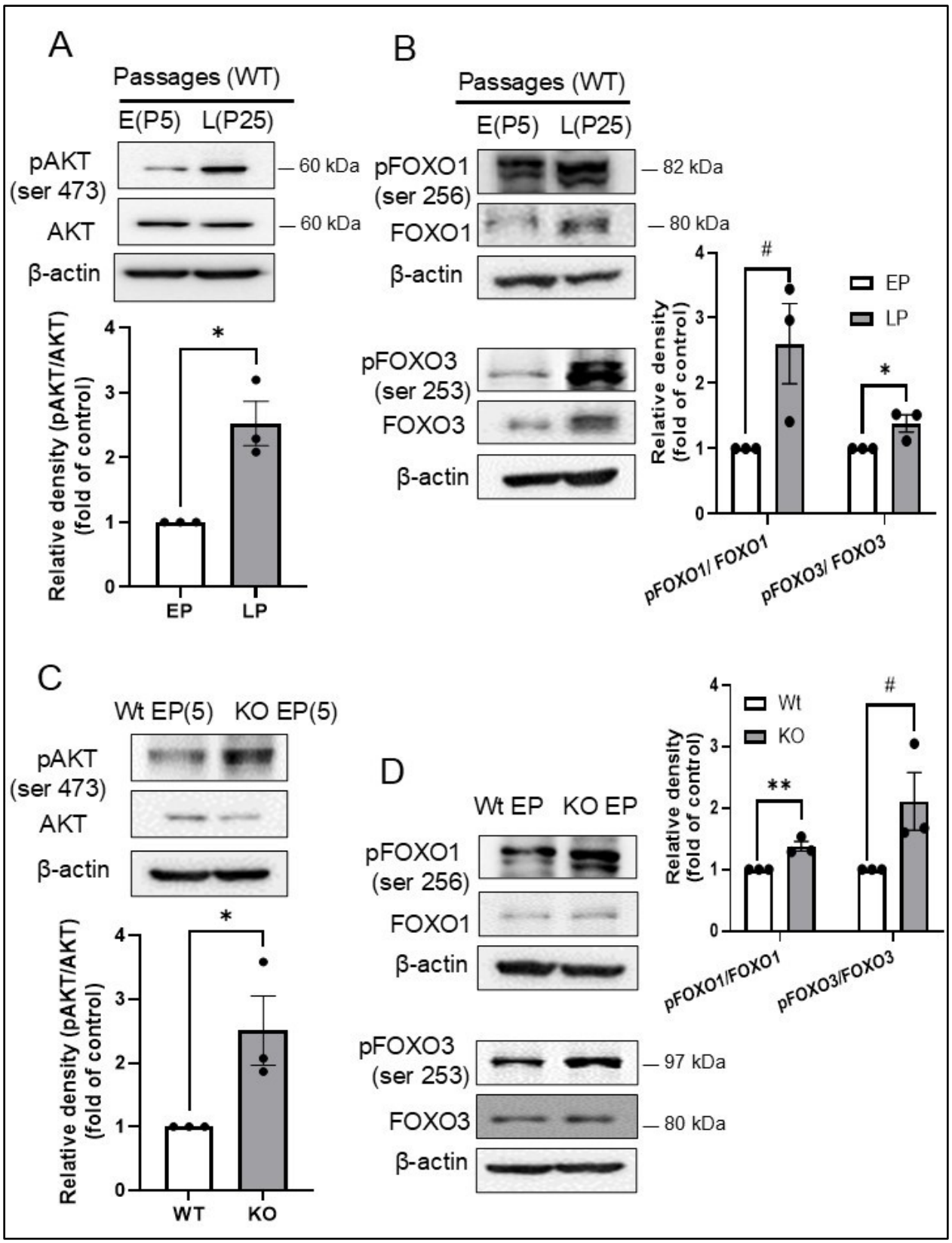
A
Passages (WT)
E(P5) L(P25)
pAKT (ser 473)
AKT
β-actin
60 kDa
60 kDa
Relative density (pAKT/AKT) (fold of control)
EP
LP
B
Passages (WT)
E(P5) L(P25)
pFOXO1 (ser 256)
FOXO1
β-actin
82 kDa
80 kDa
pFOXO3 (ser 253)
FOXO3
β-actin
Relative density (fold of control)
EP
LP
pFOXO1/ FOXO1
pFOXO3/ FOXO3
C
Wt EP(5) KO EP(5)
pAKT (ser 473)
AKT
β-actin
Relative density (pAKT/AKT) (fold of control)
WT
KO
D
Wt EP KO EP
pFOXO1 (ser 256)
FOXO1
β-actin
pFOXO3 (ser 253)
FOXO3
β-actin
97 kDa
80 kDa
Relative density (fold of control)
Wt
KO
pFOXO1/FOXO1
pFOXO3/FOXO3

Figure 3.7

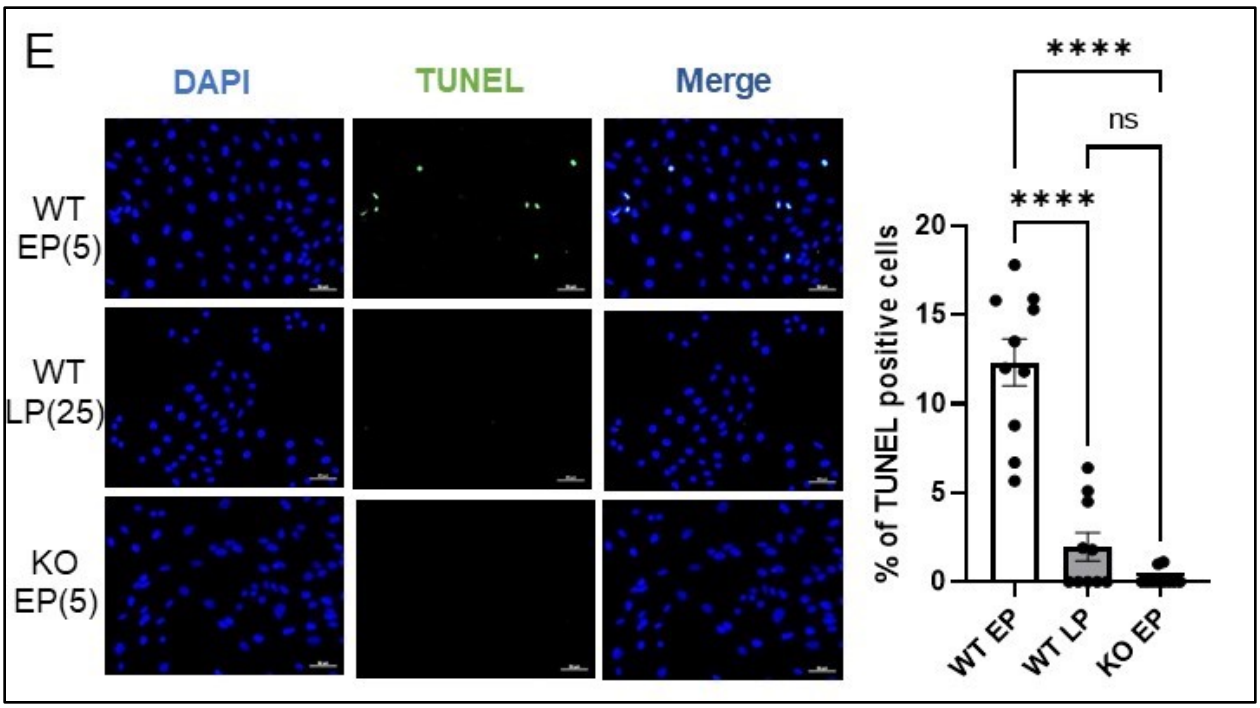

Figure 3.7: Increased AKT activation is associated with senescence in LP MC and TXNIP ko MC. (A) Representative western blot of total cell lysate showing that activated AKT (phosphorylated at Ser 743) is significantly increased in LP WT MC. (B) Representative western blot of total cell lysates showing increased phosphorylation of FOXO1 and FOXO3 (phosphorylated at Ser 256 and Ser 253 respectively) in WT LP MC versus EP WT MC. (C) Increased AKT phosphorylation in EP TXNIP KO MC. (D) FOXO1 and FOXO3 are significantly more phosphorylated in EP TXNIP KO MC compared to EP WT MC. (E) Representative image (20X) taken by fluorescence microscope showing a significantly reduced percentage of apoptotic cells (green fluorescence) in both LP WT MC and TXNIP KO EP MC compared to WT EP MC (as described in methods). Graphs depict mean values ± SEM (n=3, n=10 for TUNEL assay), *p<0.05, **p<0.01, ****p<0.0001, # p<0.05 (one tail t-test)

3.1.8 TXNIP-deficient MC exhibit features of oncogene-induced senescence

While DCF fluorescence was increased in the senescent LP WT MC as well as EP KO MC, the source of ROS was not clear. It is documented that TXNIP KO cells display decreased TCA cycle and ETC flux and increased glycolysis in comparison to WT cells [312, 313], we therefore tested whether ROS were derived from mitochondria or other sources. Using the Mitosox assay no significant difference was observed between WT EP and TXNIP KO EP MC. However, mitochondrial ROS levels were notably higher in WT LP MC. (Figure 3.8 A). Another significant source of ROS that has been implicated in various senescence models is NADPH oxidase (NOX). Furthermore, AKT is known to induce NOX expression [373, 374]. To determine if NOX upregulation was responsible for the observed ROS increase in EP TXNIP KO MC, we quantified NOX4 levels in KO (EP) MC and WT LP MC. Both EP KO MC and LP WT MC exhibited significantly increased NOX4 expression compared to WT EP MC (Figure 3.8 B,C). Of note, incubating TXNIP KO EP MC with the NOX4 inhibitor, GKT136901 at 0.1 and 1 μM concentrations for 48h was found to significantly decrease the amount of ROS (Figure 3.8 D), indicating that in these cells upregulated NOX4 appeared to be the primary source of the increased ROS.

Phosphatase and tensin homolog (PTEN) is a known tumor suppressor phosphatase that regulates AKT activation by dephosphorylating phosphatidylinositol-3-triphosphate [375]. To measure the active form of PTEN (reduced form), cell lysates of LP WT and EP KO MC were separated in non-reducing gel (absence of 2-mercaptoethanol) and immunoblotted. TXNIP KO EP MC exhibited a significant decrease in the amount of active (reduced) PTEN (Figure 3.8 E). Surprisingly, LP WT MC showed no significant difference in the amount of active PTEN (Figure 3.8 F). These results suggest that AKT activation may mediate TXNIP deficiency-induced senescence in EP KO MC through reduced PTEN activity.

The unique senescence phenotype observed in TXNIP KO EP MC includes hyperactivation of AKT (Figure 3.7), independence of telomere attrition (Figure 3.5), decreased PTEN activity, and upregulation of NOX4 (Figure 3.8), all characteristic of Oncogene-Induced Senescence (OIS) [257, 258, 373, 374, 376]. This is consistent with TXNIP's role as a tumor suppressor and its downregulation linked to the growth of various cancers (e.g., breast, renal, gastric) [342]. To further confirm an OIS senescence phenotype in TXNIP KO EP MC, levels of activated (GTP-bound) RAS were quantified and found to be significantly elevated in TXNIP KO EP, but not in LP WT MC, compared to WT EP MC (Figure 3.8 G, H). These findings demonstrate, for the first time, that loss of TXNIP is associated with the emergence of an OIS phenotype, at least in the tested mouse primary MC.

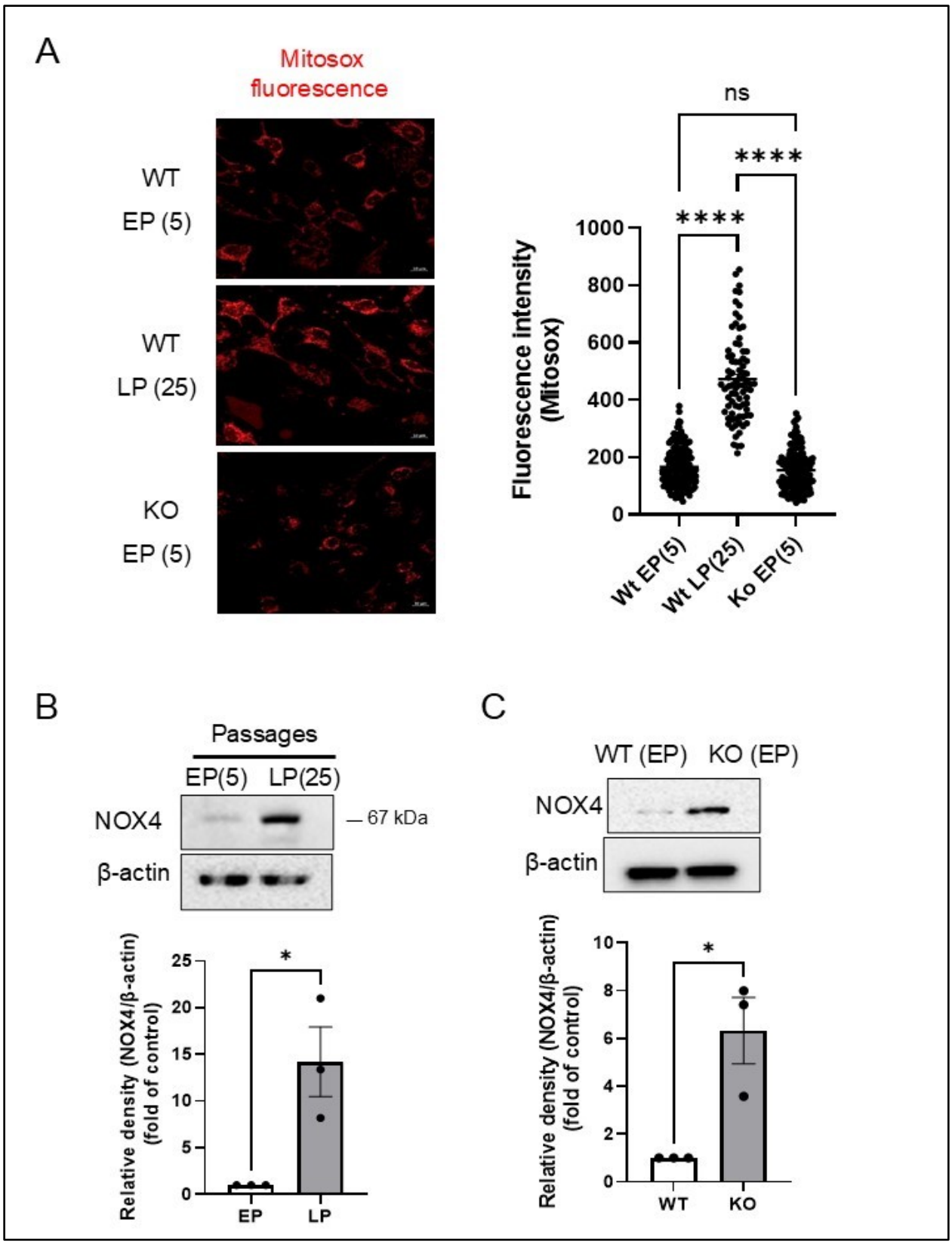
A
Mitosox fluorescence
WT EP (5)
WT LP (25)
KO EP (5)
ns
****
****
Fluorescence intensity (Mitosox)
1000
800
600
400
200
0
Wt EP(5)
Wt LP(25)
Ko EP(5)
B
Passages
EP(5) LP(25)
NOX4
— 67 kDa
β-actin
Relative density (NOX4/β-actin) (fold of control)
25
20
15
10
5
0
*
EP
LP
C
WT (EP) KO (EP)
NOX4
β-actin
Relative density (NOX4/β-actin) (fold of control)
10
8
6
4
2
0
*
WT
KO

Figure 3.8

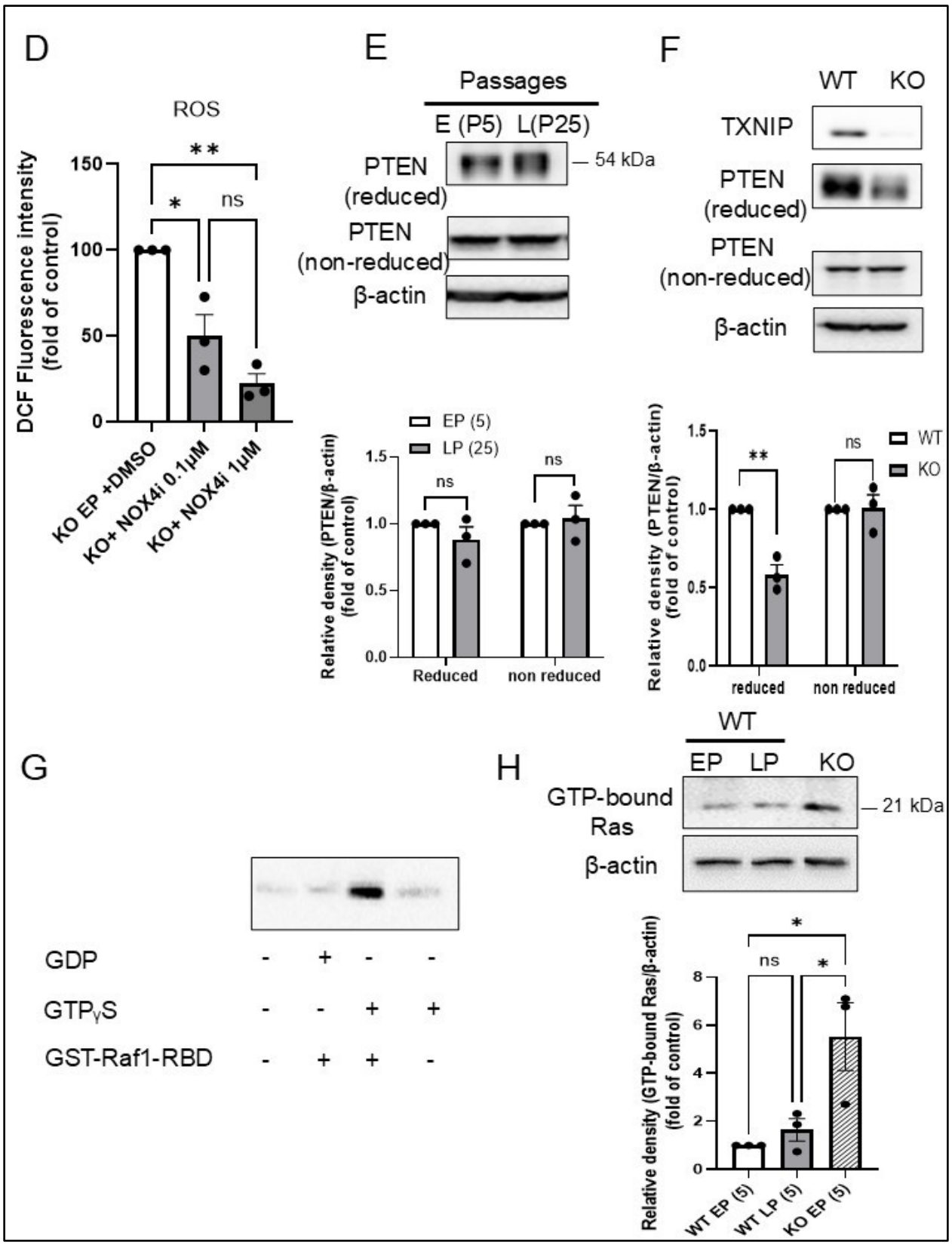

Figure 3.8 (*continued*)

Figure 3.8: TXNIP KO MC show features of OIS. (A) Representative image of mitochondrial ROS (red color) measured by mitosox assay by confocal microscopy (150-180 cells/condition were quantified) showing a significantly increased mitochondrial ROS in WT LP MC and a non-significant difference in TXNIP KO EP MC compared to WT EP MC. (B) Representative immunoblot of total cell lysate showing significantly increased NOX4 expression in WT LP MC and (C) TXNIP KO EP MC compared to WT EP MC. (D) ROS quantification by DCF showing significant reduction in TXNIP KO EP MC incubated with the NOX4 inhibitor (GKT136901) at 0.1 and 1 μM concentration for 48h. (E) Representative immunoblot of total cell lysate showing no difference in amount of reduced (active) PTEN in WT LP MC and (F) a significantly increased amount of reduced PTEN in TXNIP KO EP MC compared to WT EP MC. (G) A representative immunoblot showing the specific binding of GTP-bound Ras versus GDP, to the binding domain of Ras (control experiment) and (H) significantly increased GTP-bound (activated RAS) in TXNIP KO EP MC compared to WT EP MC. Graphs depict mean values ± SEM (n= 150-180 cells for mitosox assay, 3 separate experiments for W.B), *$p<0.05$, **$p<0.01$, ****$p<0.0001$

3.1.9 Inhibition of hyperactivated AKT rescues senescence in TXNIP KO EP MC

To investigate the contribution of AKT activation on senescence, WT and TXNIP KO MC were treated with the AKT inhibitor GSK690693 for 72 hr. Validation of the inhibitor's activity was confirmed by measuring the phosphorylation of the AKT target FOXO1 (Figure 3.9 A). Treatment with the AKT inhibitor effectively rescued the senescence phenotype in TXNIP KO MC, as evidenced by significant reductions in P53 and P16 protein levels (Figure 3.9 B) and decreased β-galactosidase staining (Figure 3.9 C).

To evaluate the relationship between AKT hyperactivation and ROS production in TXNIP KO MC, the cells were also treated with the AKT inhibitor GSK690693. This led to a significant reduction in NOX4 expression and ROS levels (Figure 3.9 D, E). Furthermore, AKT inhibition resulted in reduced DDR activation, as indicated by decreased histone H2AX phosphorylation in TXNIP KO MC (Figure 3.9 F). These findings indicate the pivotal role of AKT hyperactivation in mediating senescence, oxidative stress, and DDR activation in TXNIP-deficient MC.

AKT activation is recognized for its role in promoting cell survival in the presence of elevated ROS levels, particularly observed in cancer cells by upregulating endogenous antioxidants [370]. In EP KO MC, there was a significant increase in the expression of the central regulator of ROS detoxification, Nrf-2, along with its downstream targets SOD2 and catalase. Conversely, inhibition of AKT in TXNIP KO MC lowered the expression levels of Nrf-2, SOD2, and catalase (Figure 3.9 G). To validate the critical involvement of AKT in senescence linked to TXNIP loss in MC, LY 294002 was employed to inhibit its upstream activator PI3K. Phosphorylation of AKT was used to confirm the effectiveness of the inhibition (Figure 3.9 H). Treatment with LY 294002 led to a significant reduction of levels of senescence markers P53 and histone H2AX phosphorylation

(Figure 3.9 I). Taken together, these data demonstrate that inhibiting hyperactivated AKT can decrease ROS levels and revert the senescence phenotype in TXNIP KO MC.

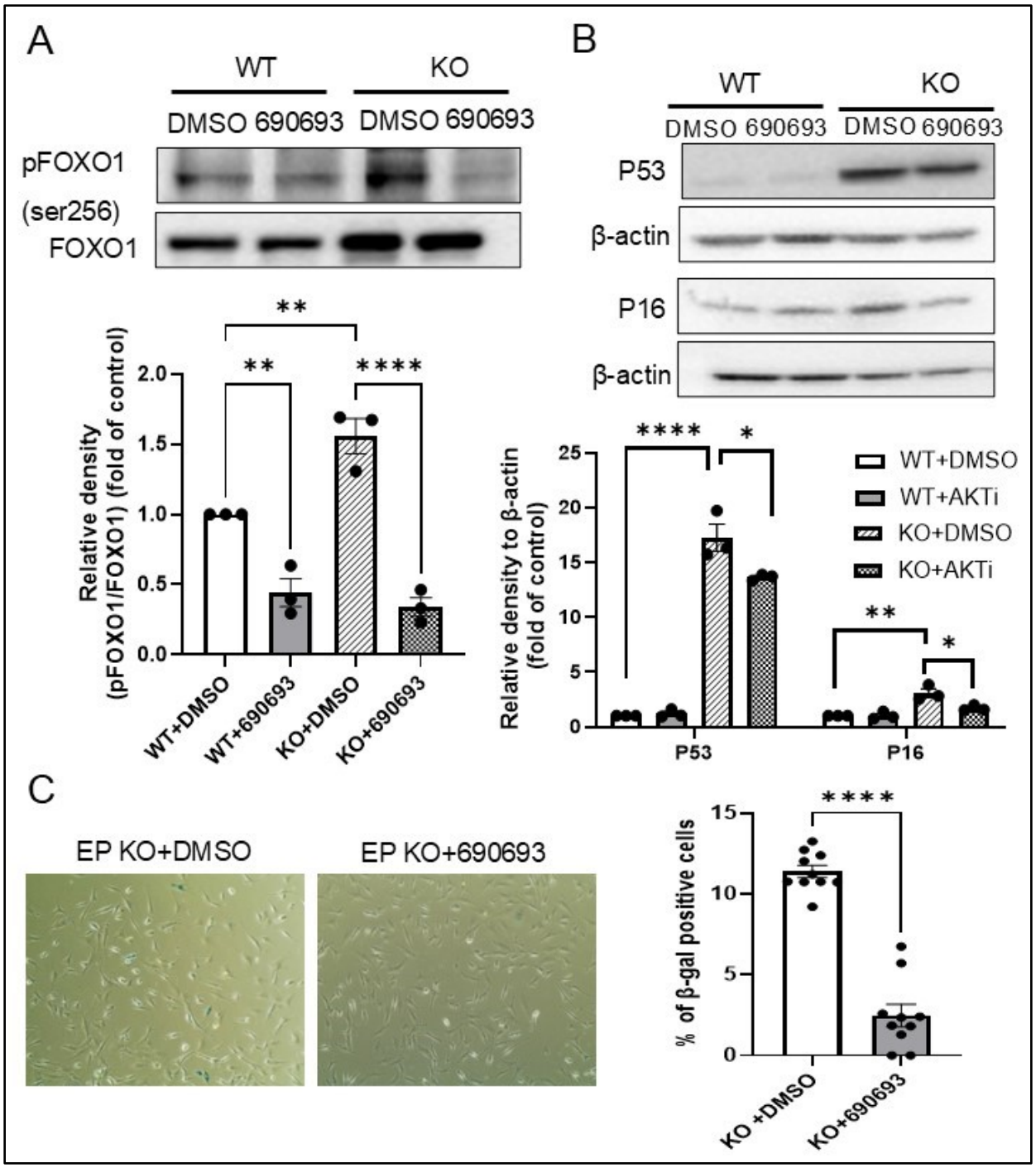

Figure 3.9

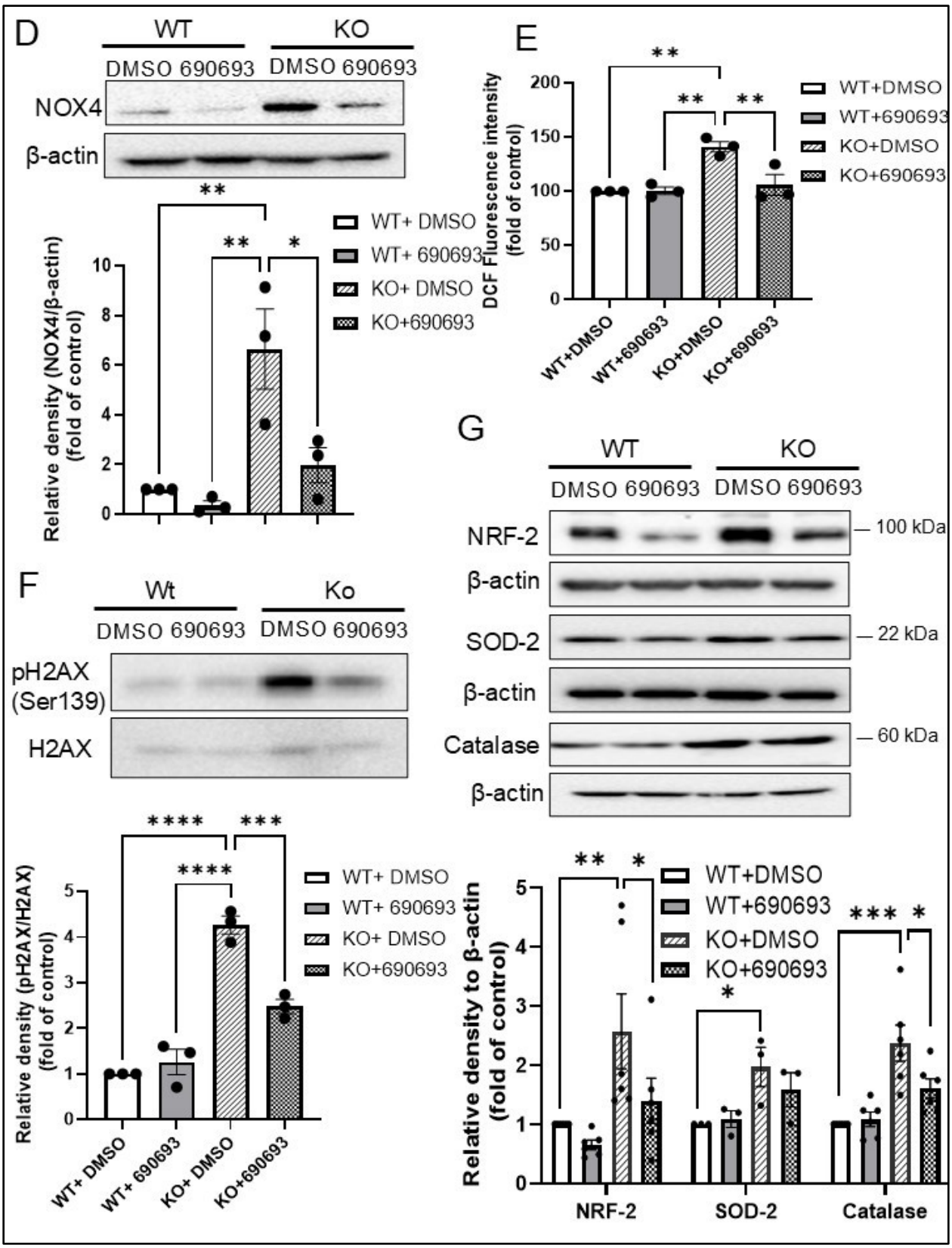

Figure 3.9 *(continued)*

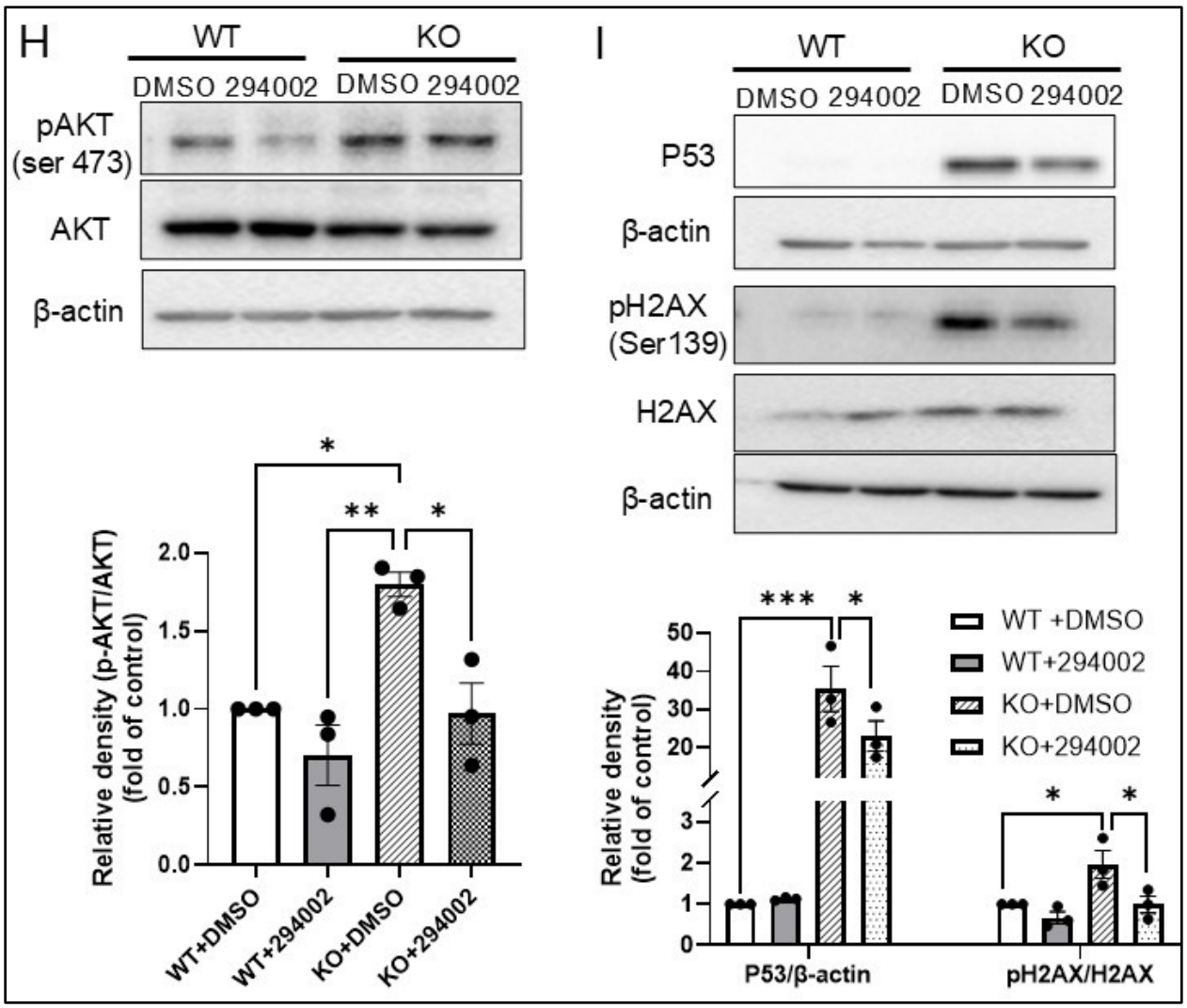

Figure 3.9 *(continued)*

Figure 3.9: AKT inhibition rescued the senescence phenotype of TXNIP KO EP MC and reduced ROS, NOX4, Nrf2 and its antioxidant targets SOD2 and catalase. (A) Representative western blot of total cell lysate showing the significantly reduced expression of phosphorylated FOXO1, a target of AKT, after exposure to GSK690693 at 5μM concentration for 72h in TXNIP KO EP MC compared to WT EP MC. (B) Exposure to GSK690693 significantly reduced the senescence markers P53 and P16 and (C) SA-β-gal in TXNIP KO EP MC compared to DMSO-containing controls. (D) GSK690693 exposure significantly reduced levels of NOX4, (E) ROS, and (F) phosphorylated H2AX in TXNIP KO MC compared to DMSO-containing controls. (G) GSK690693 treated TXNIP KO EP MC showed a significant reduction in levels of Nrf2 and catalase. (H) PI3K inhibitor (LY294002) at 25μM concentration for 72h significantly reduced Ser473 phosphorylated AKT in both WT EP MC and TXNIP KO EP MC compared to DMSO-containing controls. (I) TXNIP KO EP MC exposed to LY294002 showed a significant reduction in senescence markers P53 and phosphorylation of H2AX. Graphs depict mean values ± SEM (n=3-6 for W.B, n=10 for SA-β-gal), *$p<0.05$, **$p<0.01$, ***$p<0.001$, ****$p<0.0001$

3.1.10 Reconstitution of TXNIP rescues senescence in TXNIP KO MC

To confirm that the observed cellular senescence associated with a reduction or absence of TXNIP was directly caused by TXNIP deficiency, TXNIP KO MC. were transduced with GFP-tagged TXNIP lentiviral particles to re-introduce TXNIP expression into cells lacking endogenous TXNIP. Additionally, a mutated TXNIP variant (247 Cys to Ser) was utilized to assess the role of the thioredoxin binding function of TXNIP in its protective role against senescence.

Confirmation of successful transfection was determined by fluorescence microscopy, which visualized GFP fluorescence within transduced cells (Figure 3.10 A). Immunoblotting for TXNIP confirmed successful TXNIP reconstitution (Figure 3.10 B).

Comparative analysis of cellular senescence markers in TXNIP KO MC, revealed that lentivirus-mediated re-introduction of wildtype TXNIP led to a significant reduction in senescence markers, including P53 and P16 expression, as well as a significant decrease in NOX4 levels (Figure 3.10 C). Furthermore, the reconstitution of wildtype TXNIP correlated with a marked reduction in the percentage of β-galactosidase-positive cells (Figure 3.10 D).

Interestingly, re-expression of the mutant TXNIP variant did not significantly decrease senescence markers and NOX4 levels. However, both WT and mutant TXNIP significantly reduced P53 expression compared to TXNIP KO MC (Figure 3.10 C,D).

These findings indicate a critical role of TXNIP in regulating senescence and highlight the importance of its thioredoxin binding site in mediating this protective effect against cellular aging.

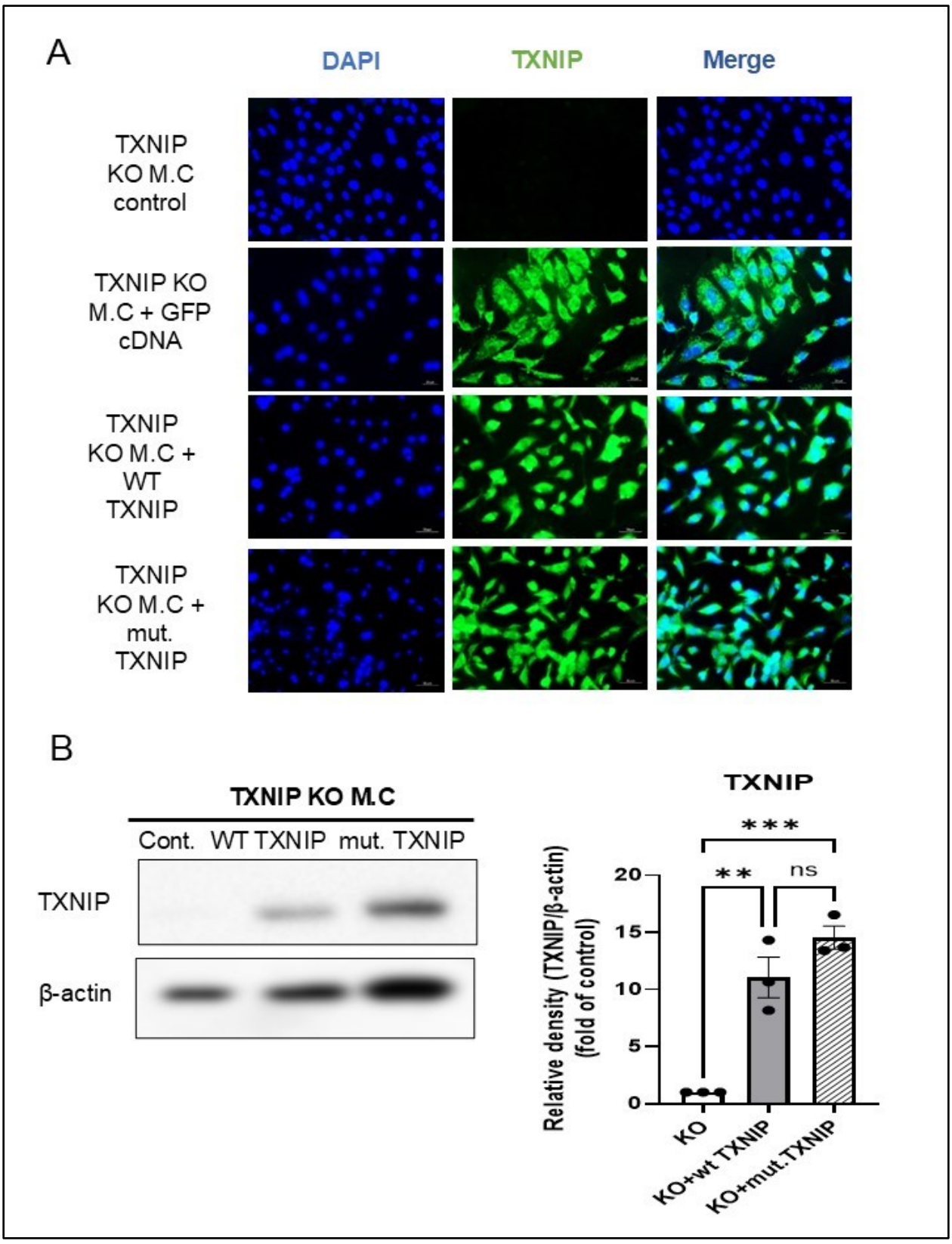
A
DAPI
TXNIP
Merge
TXNIP KO M.C control
TXNIP KO M.C + GFP cDNA
TXNIP KO M.C + WT TXNIP
TXNIP KO M.C + mut. TXNIP
B
TXNIP KO M.C
Cont.
WT TXNIP
mut. TXNIP
TXNIP
β-actin
TXNIP
***
**
ns
Relative density (TXNIP/β-actin) (fold of control)
20
15
10
5
0
KO
KO+wt.TXNIP
KO+mut.TXNIP

Figure 3.10

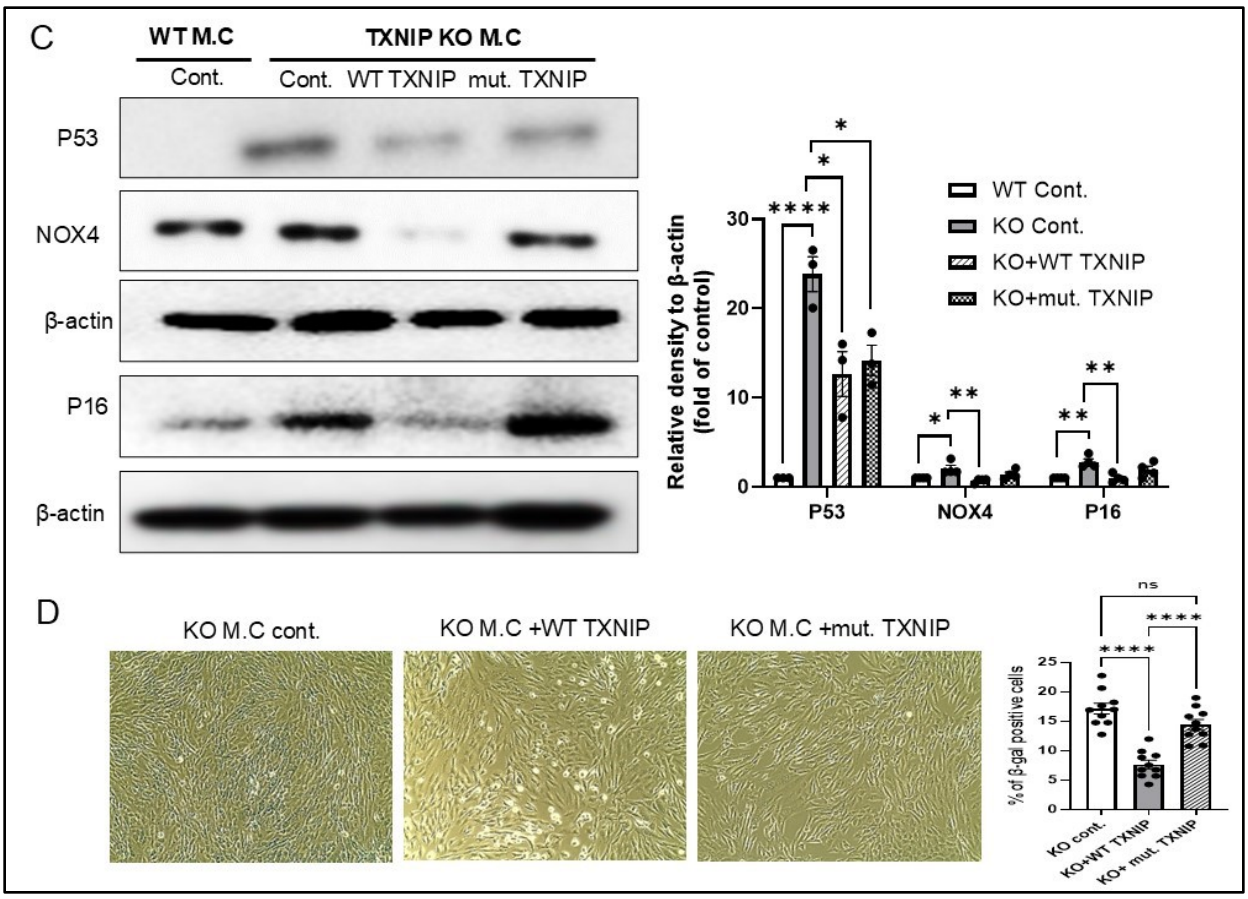

Figure 3.10 *(continued)*

Figure 3.10: WT TXNIP reconstitution in TXNIP KO MC rescued senescence phenotype while Cys247Ser mutant TXNIP was less effective. (A) Representative images (20X) taken by fluorescence microscope showing the lentivirus-mediated transduction of GFP-tagged (green color) WT and mutant TXNIP in addition to the GFP alone cDNA in TXNIP KO EP MC. (B) Representative immunoblot showing re-expression of both WT and mutant TXNIP in TXNIP KO EP MC. (C) Representative western blots of total cell lysates showing that re-expression of WT TXNIP (at 2 MOI concentration for 48h) significantly reduced P53, NOX4 and P16 expression, whereas mutant TXNIP reduced only P53 expression. (C) Representative images (20X) showing that re-expression of WT TXNIP in TXNIP KO EP MC significantly reduced the percentage of SA-β-gal -positive cells, while mutant TXNIP showed a non-significant reduction of SA-β-gal-positive cells (as described in methods). Graphs depict mean values ± SEM (n=3-4 for W.B, n=10 for SA-β-gal), *p<0.05, **p<0.01, ***p<0.001, ****p<0.0001

3.2 In vivo studies

3.2.1 TXNIP deficiency correlates with age-related cognitive and motor function decline in old male mice

Aging is commonly associated with a decline of cognitive and motor coordination functions [377, 378]. To evaluate cognitive function and spatial memory in male and female TXNIP KO mice compared to WT controls at ages 15 and 21 months, we utilized the Y-maze test. At 15 months, there were no significant differences between WT and KO mice in either males or females (Figure 3.11 A, B). However, at 21 months, male TXNIP KO mice exhibited significantly reduced cognitive function, as indicated by decreased spontaneous alteration behavior in the Y-maze (Figure 3.11 A). In contrast, there was no significant difference observed in female TXNIP KO mice compared to WT females at the same age (Figure 3.11 B).

To assess motor function, we employed the Rotarod test to measure latency to fall. At 15 months, there were no significant differences between WT and KO mice in either males or females (Figure 3.11 C, D). Surprisingly, at 21 months, male TXNIP KO mice demonstrated significantly impaired motor performance on the Rotarod compared to WT mice (Figure 3.11 C). Conversely, female TXNIP KO mice exhibited slightly better motor performance than WT females at 21 months, although this difference was not statistically significant (Figure 3.11 D).

These findings suggest that TXNIP deficiency may contribute to old age-related cognitive decline and motor impairments, particularly in male mice.

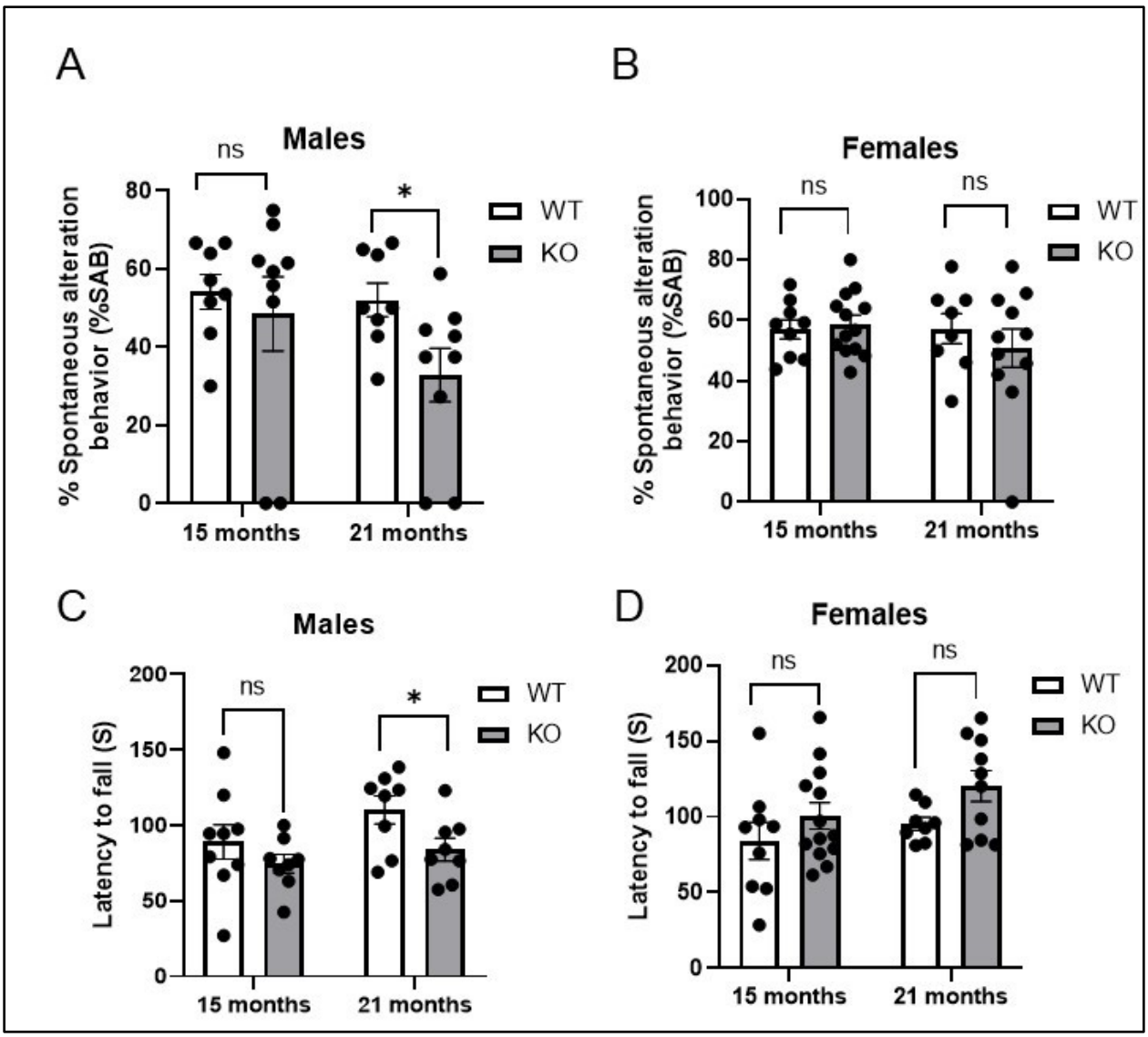
A
Males
ns
*
% Spontaneous alteration behavior (%SAB)
80
60
40
20
0
15 months
21 months
WT
KO
B
Females
ns
ns
100
80
60
40
20
0
15 months
21 months
WT
KO
C
Males
ns
*
Latency to fall (S)
200
150
100
50
0
15 months
21 months
WT
KO
D
Females
ns
ns
200
150
100
50
0
15 months
21 months
WT
KO

Figure 3.11

Figure 3.11: Y-maze and Rota-rod behavioral tests. (A) Male TXNIP KO 15 month old mice showed no difference in memory function measured by SAB % in a Y-maze, whereas 21 month old TXNIP KO males showed a significant reduction in memory function compared to WT littermates. (B) TXNIP KO females showed no significant change in memory function at 15 and 21 months old compared to their WT littermates. (C) TXNIP KO males show no difference in motor function (measured by latency to fall in a Rota-rod apparatus) at 15 months old, whereas at 21 months, male TXNIP KO mice showed significantly reduced motor function compared to WT littermates. (D) TXNIP KO female mice showed no significant difference compared to WT female littermates at both 15 and 21 months. Graphs depict mean values ± SEM (n=8-13), *$p<0.05$

3.2.2 Lack of TXNIP correlates with heightened lean mass, especially in aged female mice

To investigate whether the observed sex-related differences in motor function performance on the rotarod between old WT and TXNIP KO male mice could be linked to variations in lean body mass and body weight, we monitored animal body weights monthly from 15 to 21 months old and conducted body composition analysis for 21 months old mice using MRI.

In male KO mice, no significant differences were observed in body weight between 15 and 21 months old versus WT littermates (Figure 3.12 A). In contrast, female KO mice displayed a declining trend in body weight over time, with significant reduction noted starting from 19 months old compared to their WT littermates (Figure 3.12 B). Body composition analysis at 21 months old revealed that male and female KO mice were significantly leaner than age and sex-matched WT mice (Figure 3.12 C,D). Interestingly, the reduction in fat content and the increase in lean content both were found to be more significant in female KO mice ($P<0.0001$) than male KO mice ($P<0.01$) when compared to the age and sex-matched WT mice.

These findings suggest that the impaired motor performance in the male KO mice at 21 month was not due to a decrease in lean body mass. In addition, it is possible that the maintained motor performance observed in female KO mice on the rotarod may be attributed, at least in part, to increased muscle mass (lean body content) in KO females at 21 months old.

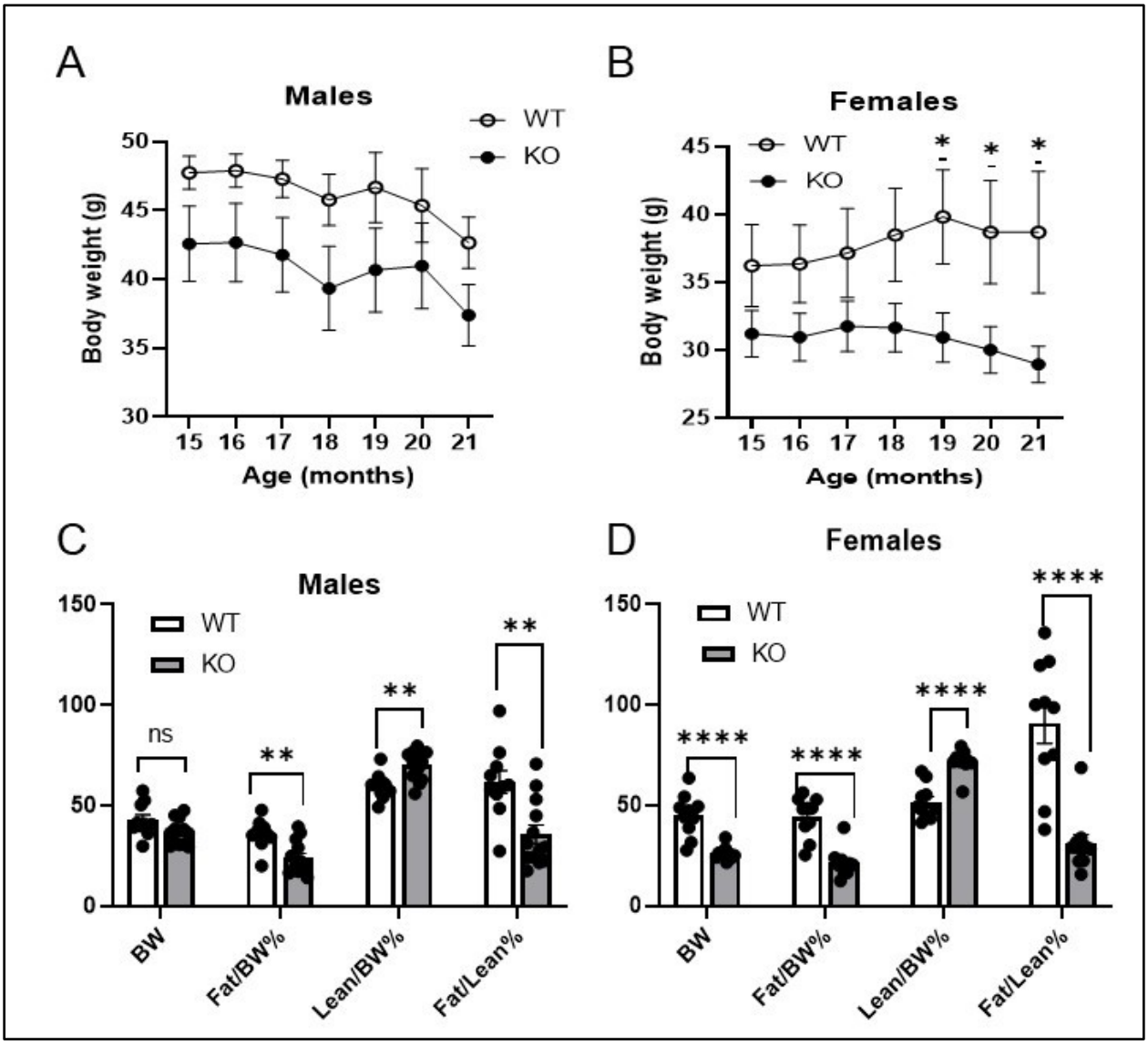
A
Males
WT
KO
Body weight (g)
50
45
40
35
30
15 16 17 18 19 20 21
Age (months)
B
Females
WT
KO
Body weight (g)
45
40
35
30
25
15 16 17 18 19 20 21
Age (months)
C
Males
WT
KO
150
100
50
0
ns
**
**
**
BW
Fat/BW%
Lean/BW%
Fat/Lean%
D
Females
WT
KO
150
100
50
0
****
****
****
****
BW
Fat/BW%
Lean/BW%
Fat/Lean%

Figure 3.12

Figure 3.12: Body weight and body composition comparison between WT and TXNIP KO male and female mice. (A) Male TXNIP KO mice show no difference in total body weight (BW) over time (between 15 and 21 months old), while (B) female TXNIP KO mice show progressive weight loss over time with significant difference in BW started from 19 months old and continued to 21 months old compared to WT sex-matched littermates. (C) TXNIP KO male mice show significantly reduced fat/BW %, fat/lean % and significantly increased lean/BW % ($P<0.01$), while (D) TXNIP KO female mice showed similar results with a more significant difference ($p<0.0001$) all compared to sex-matched WT littermates. Graphs depict mean values ± SEM (n=5-13), *$p<0.05$, **$p<0.01$, ****$p<0.0001$

3.2.3 TXNIP is downregulated with aging in vivo and lack of TXNIP is associated with senescent cell accumulation in the kidney cortex and brain hippocampus

To investigate the impact of natural aging on TXNIP expression in mice, we quantified TXNIP levels in the kidney cortex and brain hippocampal region of young (6 months old) and old (21 months old) WT male mice. Results demonstrate a significant downregulation of TXNIP expression in both organs of 21-month-old mice compared to their younger counterparts (Figures 3.13 A,F).

The accumulation of senescent cells is a key characteristic of organismal aging [130]. To assess whether the observed cognitive and motor function decline in 21-month-old TXNIP knockout (KO) male mice (in Figure 3.11) is associated with senescent cell accumulation, we evaluated markers of cellular senescence in the kidney cortex and brain hippocampal region of WT and KO male mice at 21 months of age. We observed significant increases in P53 and phosphorylated H2AX (pH2AX) levels in the 21-month-old KO mice compared to age-matched WT littermates in the kidney cortex (Figures 3.13 B,C) and in the brain hippocampal region (Figure 3.13 G,H). Additionally, immunohistochemical (IHC) analysis of kidney samples revealed a notably higher percentage of P16-positive cells in the glomeruli of 21-month-old KO mice compared to age-matched WT controls (Figure 3.13 D)). Moreover, the kidneys of 21-month-old TXNIP KO mice exhibited increased SA β-gal staining compared to age-matched WT controls (Figure 3.13 E). These findings indicate that aging is characterized by TXNIP downregulation, and lack of TXNIP is associated with enhanced cellular senescence in male mice.

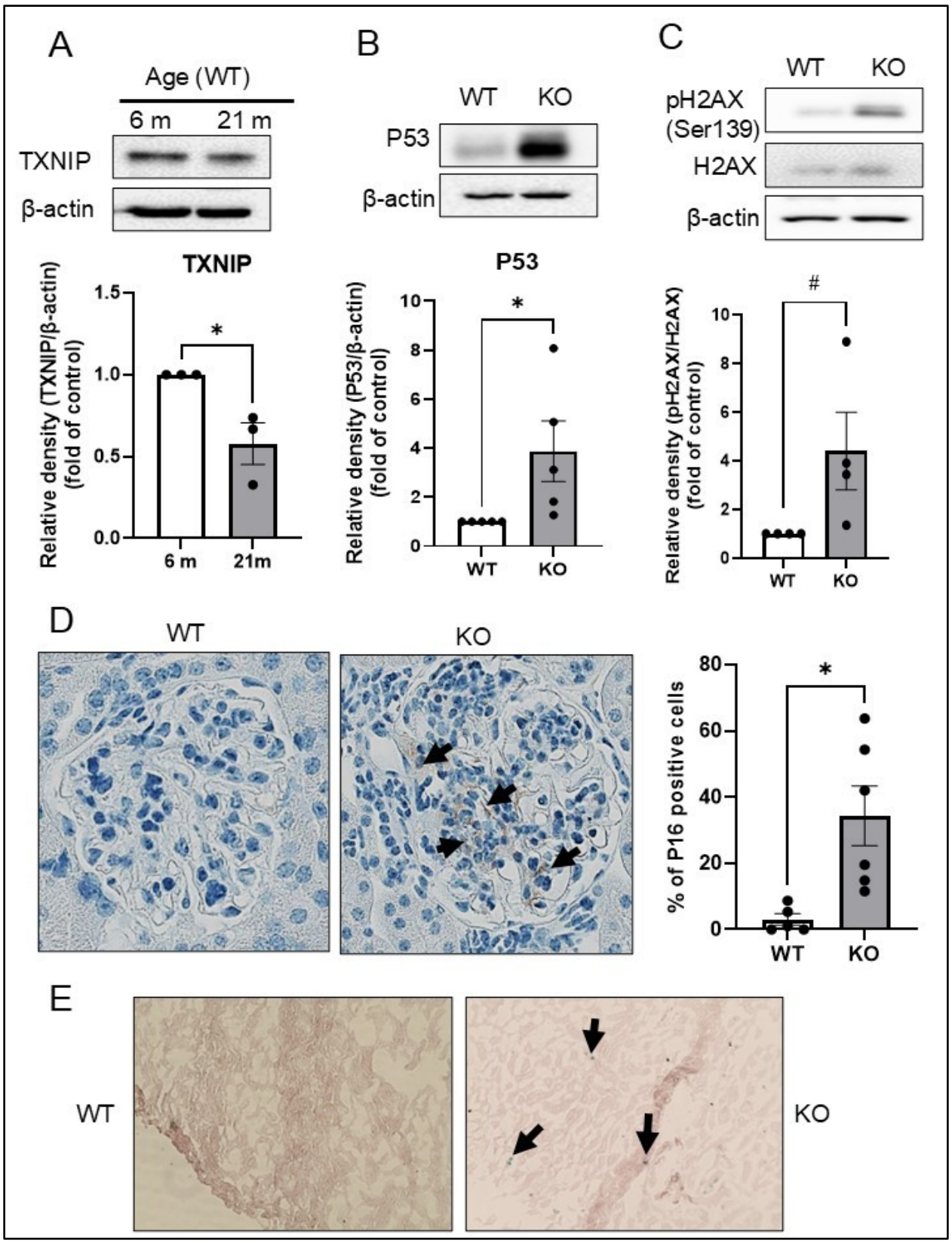

Figure 3.13 (kidney cortex)

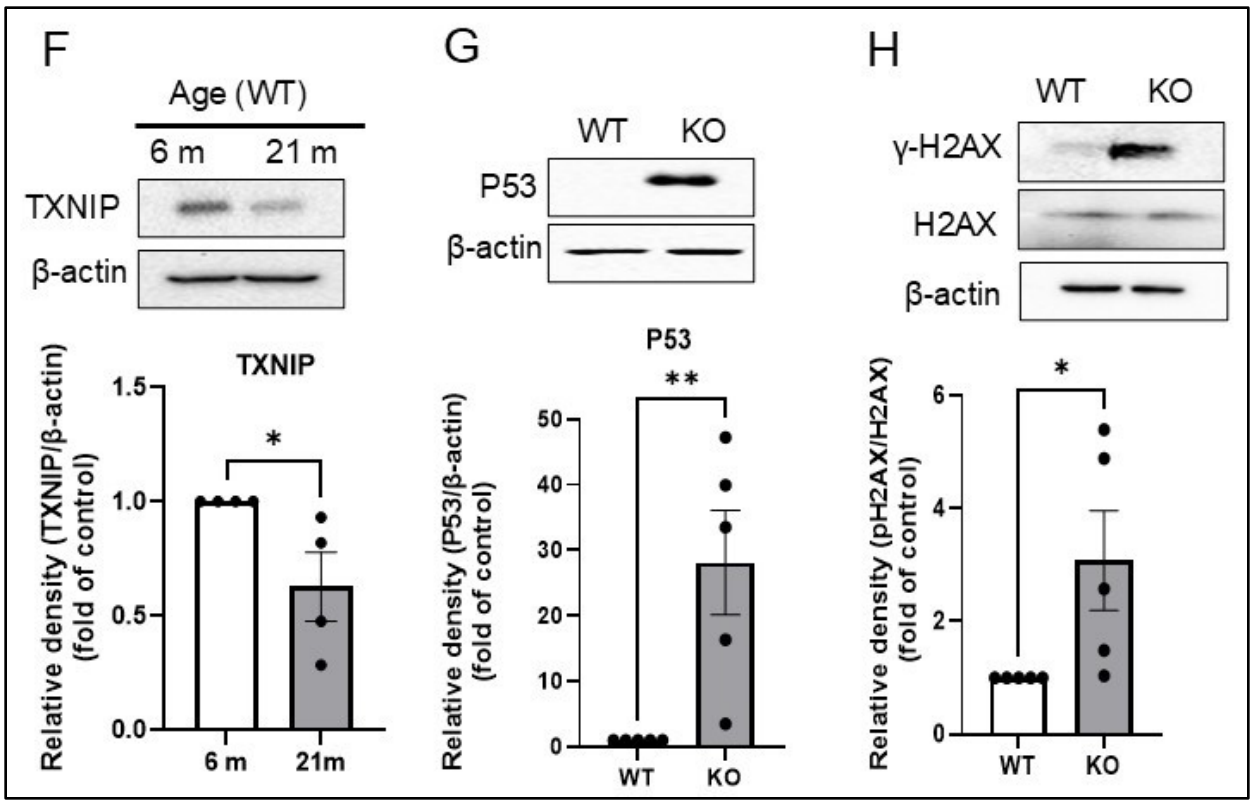

Figure 3.13 *(continued)* (hippocampus)

Figure 3.13: TXNIP is downregulated in aging mice and lack of TXNIP is associated with cellular senescence in kidney cortex and hippocampus. (A) Representative blot of total lysate of kidney cortex showing that TXNIP is significantly downregulated in 21-month-old male WT mice compared to 6-month-old mice. (B,C) P53 and phosphorylated histone H2AX (markers of senescence) are significantly upregulated in TXNIP KO 21-month-old male mice kidney cortex compared to WT littermates. (D) Representative images of P16 staining (IHC, 4μm sections); arrows indicate glomerular P16 staining (brown color). The data in the graph are expressed as a mean of P16-positive cells in at least 50 glomeruli/mouse. (E) Representative images of frozen kidney sections showing more SA-β-gal -positive cells (indicated by arrows) in TXNIP KO 21-month-old mice compared to WT littermates. (F) A representative blot showing that TXNIP expression is significantly downregulated in 21-month-old compared to 6-month-old WT male mice in the brain hippocampal region. (G,H) P53 and phosphorylated histone H2AX are significantly increased in TXNIP KO 21-month-old mice versus WT littermates in the brain hippocampal region. Graphs depict mean values ± SEM (n=3-5 mice for WB, 5-6 mice for IHC and SA-β-gal for each condition), *$p<0.05$, **$p<0.01$, # $p<0.05$ (one tail t-test)

3.2.4 Lack of TXNIP is associated with increased AKT activation and enhanced tumor formation

To validate the observations made in the in vitro model using MC, we quantified the levels of activated AKT in the kidney cortex and hippocampal region of 21-month-old TXNIP KO mice compared to WT controls. Our results demonstrated a significant increased activation of AKT in the kidney (Figure 3.14 A) and hippocampal area (Figure 3.14 B) of TXNIP KO mice.

Furthermore, in alignment with TXNIP's role as a tumor suppressor and the observed AKT hyperactivation, TXNIP KO mice exhibited organ abnormalities characterized by enlargement and/or tumor-like growth in various tissues, including the liver, colon, cecum, eyes, testes, lymph nodes, salivary glands and neck. Representative examples of these abnormal masses are illustrated in Figure 3.14 C. There was no specific age at which TXNIP KO mice started to develop these organ abnormalities, however, most of them began between 15 and 18 months of age.

To elucidate the nature of these tumors, we conducted immunohistochemistry (IHC) with dual staining using CD45 and CK20 on selected tumor samples. Microscopic examination of the tissue morphology revealed the presence of blood breakdown products and inflammatory cells within the tumors. Specifically, the tumors exhibited positive staining for CD45 (green color) and negative staining for CK20 (brown color) (indicating absence of epithelial cells), effectively ruling out epithelial-related lesions (Figure 3.14 D).

Collectively, these findings support the tumor suppressor function of TXNIP and potential tumorigenesis, in particular for lymphomas in TXNIP KO mice. The in vivo findings also support the key role of PI3K/AKT pathway in this process. These data indicate a pivotal role of TXNIP in senescence regulation, tumor suppression and cellular homeostasis.

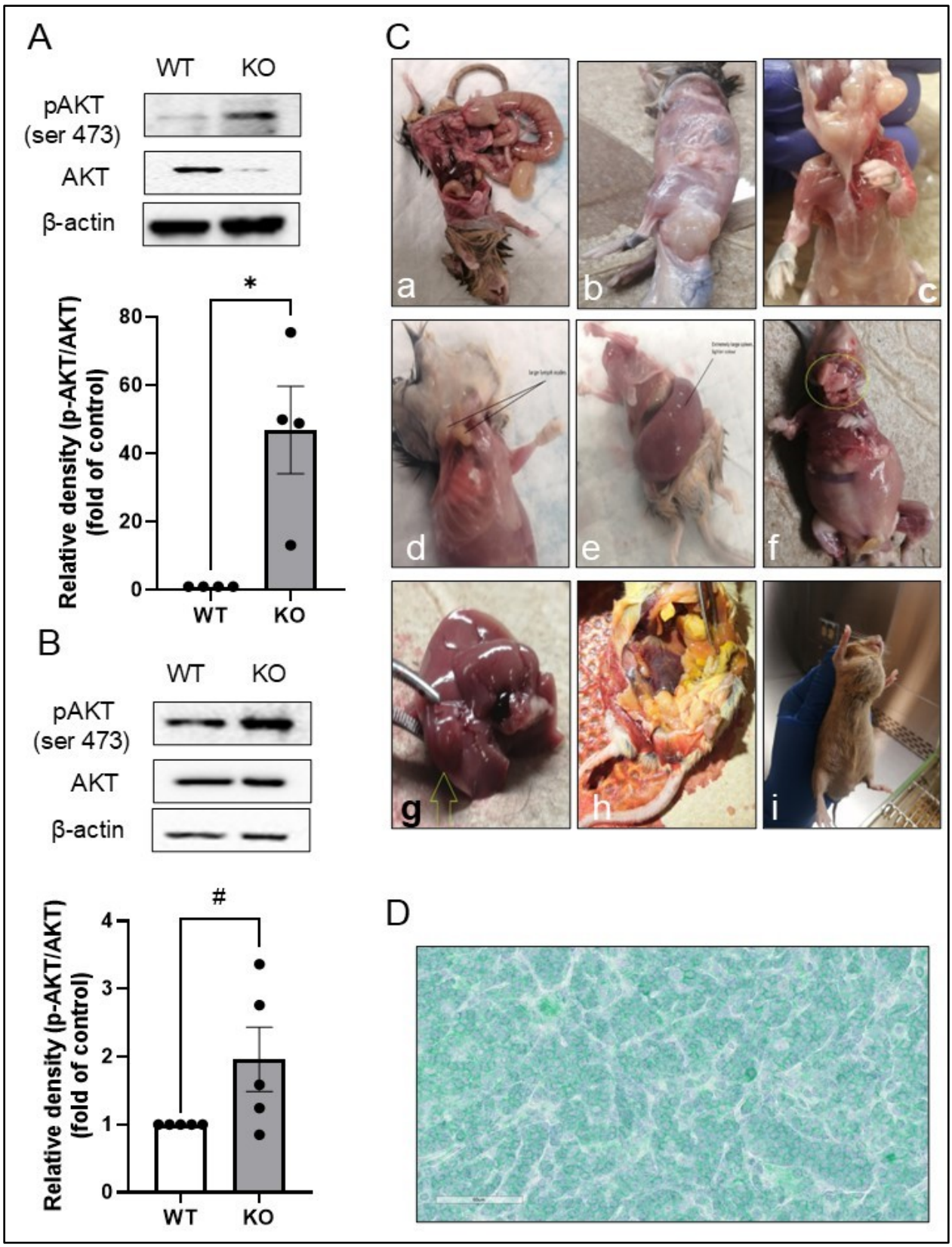
A
WT
KO
pAKT
(ser 473)
AKT
β-actin
Relative density (p-AKT/AKT)
(fold of control)
*
80
60
40
20
0
WT
KO
B
WT
KO
pAKT
(ser 473)
AKT
β-actin
Relative density (p-AKT/AKT)
(fold of control)
#
4
3
2
1
0
WT
KO
C
a
b
c
d
e
f
g
h
i
D

Figure 3.14

Figure 3.14: Lack of TXNIP is associated with increased AKT activation and tumor formation in old mice. (A) A representative blot showing increased AKT phosphorylation in kidney cortex and (B) brain hippocampal region of 21 months old TXNIP KO male mice compared to their WT littermates. (C) TXNIP KO mice have increased incidence of uncontrolled masses growth at different organs; a: enlarged colon, b: testicular mass, c: salivary glands masses, d: lymph nodes masses, e: enlarged spleen, f: salivary glands mass, g: abnormally enlarged liver, h: mass in right inguinal area, i: mass in the neck area. (D) A representative image (IHC, 4μm section, CD45 (green) and CK20 (brown) dual staining) of a mass in the neck area showing positive CD45 staining and lack of CK20 staining, characteristics of lymphoma. Graphs depict mean values ± SEM (n=4-5 mice for WB), *$p<0.05$, **$p<0.01$, # $p<0.05$ (one tail t-test).

3.2.5 Absence of TXNIP Shortens Mice Lifespan

To investigate the correlation between increased cellular senescence, declined cognitive and motor functions in TXNIP KO mice, and lifespan, we conducted a comprehensive lifespan analysis using the Kaplan-Meier curve under standard animal facility conditions. The results revealed a significantly shorter lifespan in TXNIP KO mice compared to their WT counterparts ($p<0.0001$). The maximum lifespan was 38 months in WT mice versus 29.5 months in KO mice, and the median survival was 28 months for WT mice versus 20.3 months for KO mice (Figure 3.15 A). Further analysis by sex showed that male TXNIP KO mice exhibited significantly shorter lifespans compared to male WT mice ($p<0.0001$). The maximum lifespan was 38 months in WT males versus 29.5 months in KO males, and the median survival was 28 months in WT males versus 21.9 months in KO males (Figure 3.15 B). Similarly, female TXNIP KO mice lived significantly shorter lives compared to female WT mice ($p<0.0001$), with a maximum lifespan of 38 months in WT females versus 25 months in KO females. The median survival was 28 months in WT females versus 19.23 months in KO females (Figure 3.15 C). These findings demonstrate for the first time the impact of TXNIP deficiency on lifespan and suggest a potential link between accelerated senescence and reduced longevity in TXNIP KO mice.

Figure 3.15: Lack of TXNIP is associated with reduced longevity in male and female mice.

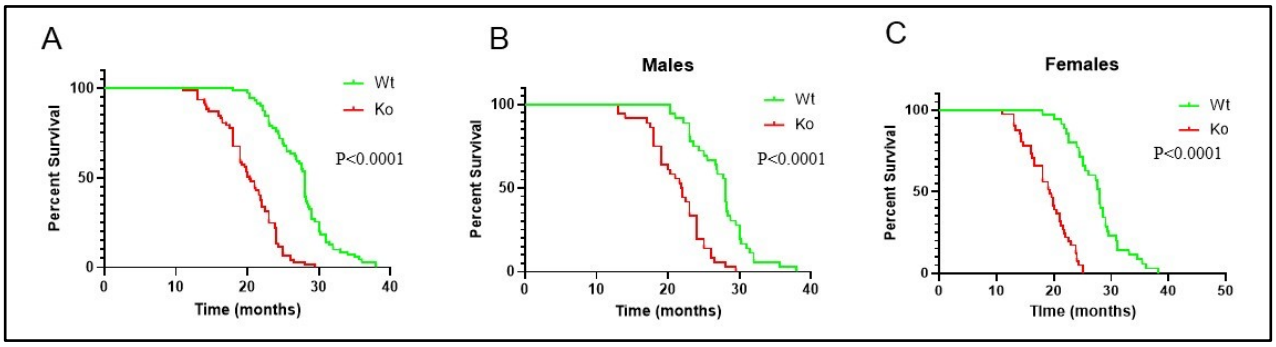

(A) Kaplan-Meier curves showing a significantly reduced lifespan of TXNIP KO mice with a median lifespan of 20.8 months for KO compared to 28 months for WT mice, (B) male KO mice showing reduced lifespan compared to WT males and (C) female KO mice showing decreased lifespan compared to female WT mice. n= 72 WT (36 males, 36 females), 77 KO (36 males, 41 females) mice.

Chapter 4 Discussion and Conclusions

4.1 Discussion

TXNIP is a multifunctional protein and a member of the arrestin superfamily, specifically belonging to the 'α-arrestin' or Arrestin Domain Containing proteins (ARRDC) [198, 379]. It shares essential structural features with α-arrestins, including five SH3 domains and two PPxY motifs [201].

TXNIP was identified as an inhibitor of thioredoxin, a critical antioxidant, as reported by Nishiyama et al. in 1999 [207]. However, apart from its involvement in redox processes, TXNIP was also found to play a notable role in suppressing glucose uptake, as demonstrated by Parikh et al. in 2007 [303], that appears to be mediated by its α-arrestin domain that promotes GLUT1 degradation [304].

In the context of cellular senescence and aging, some evidence has suggested a role for TXNIP in attenuating cellular senescence. TXNIP downregulation has been observed in age-related macular degeneration [344] and in various cancers [342]. Conversely, several studies in mouse models have shown that TXNIP is upregulated in response to longevity-promoting pathways such as calorie restriction [299, 305, 353]. Moreover, in murine models, loss of TXNIP has been linked to increased susceptibility and reduced survival under oxidative stress induced by paraquat exposure [345]. These findings suggest a potential role of TXNIP in mitigating cellular senescence and aging.

In vitro studies:

1. Evidence for a role of TXNIP in senescence:

We found that sequential passaging of primary WT MC culminates in the emergence of a senescence phenotype that is associated with the progressive attrition of telomeres (Figures 3.1 and 3.5), which has been documented to activate a cascade of events through the DNA Damage

Response (DDR). MC at LP showed induction of P53, cyclin-dependent kinase inhibitor, P16, and augmentation of senescence-associated beta-galactosidase staining (SA-β-gal) (Figure 3.1).

Associated with this senescence phenotype, we found downregulation of TXNIP at both the mRNA and protein levels in late passage cells (Figure 3.2), suggesting the involvement of TXNIP in the senescence process. Notably, we found that LP MC have attenuated levels of ChREBP and MondoA (Figure 3.3), known enhancers of TXNIP transcription. Incubating the LP MC in a high glucose-containing medium (for the purpose of activating ChREBP and MondoA), that consequently upregulates TXNIP was able to restore TXNIP expression and downregulate the senescence marker P53 (Figure 3.3). In line with our observations, Yamamoto-Imoto et al. demonstrated that MondoA is downregulated with aging. In that study, MondoA played a protective role against cellular senescence, whereas loss of MondoA exacerbated senescence in human retinal pigment epithelial (hRPE) cells [365]. Notably, TXNIP was identified as an associated molecule in the MondoA pathway regulating senescence where TXNIP was significantly downregulated in MondoA knockdown cells. These authors proposed that MondoA's protective effect against senescence involves maintaining autophagy function and inhibiting the autophagy negative regulator Rubicon [365].

The role of TXNIP in cellular homeostasis was further underscored in our study by investigating TXNIP KO cells. Intriguingly, we found that these cells exhibited a robust senescence phenotype that is characterized by upregulated expression of senescence markers including P16, P53 and senescence-associated β-galactosidase staining in early passage cells (Figure 3.4).

In support of the potential involvement of ChREBP and MondoA in upregulating TXNIP expression and mitigating senescence, TXNIP KO MC exhibited significantly increased

accumulation of both ChREBP and MondoA (Figure 3.4). Although the cause of the increased amounts of these transcription factors was not studied, we speculate that a negative feedback by TXNIP may be absent in the KO cells. Furthermore, when TXNIP KO MC were exposed to high glucose conditions, there was no significant alteration in the level of the senescence marker P53 protein (Figure 3.4). The lack of change in P53 levels under high glucose conditions in TXNIP KO MC as opposed to that observed in LP WT MC, implicates a potential importance of ChREBP and MondoA in mitigating senescence mediated through TXNIP expression within the replicative senescence model of LP WT MC. While TXNIP is not present in the KO MC, other targets of ChREBP and MondoA should still be present.

Our studies represent, as far as we know, the first demonstration that MC lacking TXNIP display a shorter replicative time to senescence compared to WT MC (Figure 3.5). Of significance, the induction of senescence in TXNIP-deficient EP MC was found to be unrelated to telomere shortening (Figure 3.5), supporting the notion that the replicative senescence observed in WT LP MC differs in some respects from that observed in the absence of TXNIP.

2. Role of ROS

Our data demonstrated that LP WT MC and EP TXNIP KO MC both exhibit increased levels of cellular ROS, as measured by DCF fluorescence. This elevation in ROS correlated with a significant increase in the phosphorylation of histone H2AX, a well-established marker of the DDR, in both WT LP MC and EP KO MC (Figure 3.6). These findings align with existing literature indicating that replicative senescence is associated with ROS overproduction, that has been attributed to multiple mechanisms such as mitochondrial dysfunction and reduced ATP

production, activation of P38 MAP kinase, diminished FOXO activity, loss of telomerase reverse transcriptase activity, and increased AKT activity [380-384].

Of note, published data have documented that lack of TXNIP in mouse embryonic fibroblasts (MEF) [343] and hematopoietic stem cells [345] is associated with elevated ROS production. Furthermore, mice lacking TXNIP demonstrate increased susceptibility to paraquat-induced mortality [345], highlighting a vulnerability to oxidative stress. These findings indicate an important role for TXNIP in mitigating oxidative stress-associated damage. The increase of ROS in the absence of TXNIP suggests a protective mechanism by which TXNIP modulates cellular redox homeostasis, thereby attenuating oxidative stress. The mechanism by which TXNIP promotes protection against acute oxidative stress is not clear. One possibility is that acute/short-term oxidative stress results in the dissociation of TXNIP from Trx resulting in free Trx to act as an antioxidant [214]. A lack of TXNIP may result in a lower expression of Trx and decreased antioxidant activity. This potential explanation will require further experimental testing.

To understand mechanisms underlying ROS overproduction and to identify the sources of ROS in both WT LP MC and EP KO MC, we utilized the MitoSOX assay to specifically quantify mitochondrial ROS (superoxide) in these cells. Interestingly, only the WT LP MC exhibited a significant increase in mitochondrial ROS production, while the EP KO MC did not show such an increase (Figure 3.8). This is consistent with a decreased TCA cycle flux and lack of increase in mitochondrial membrane potential in TXNIP KO cells upon high glucose exposure as we previously documented [313].We also measured the levels of NOX4, a major source of ROS, and found it to be significantly upregulated in both WT LP MC and EP KO MC (Figure 3.8).

These observations suggest a second difference between the two models of senescence (EP KO MC and the WT LP MC), specifically in the potential sources of ROS. Based on these results, we propose that in WT LP MC, mitochondrial ROS are a primary activator of the AKT pathway, consistent with the literature indicating that replicative senescence is associated with increased mitochondrial ROS [125, 385-389], documented drivers of AKT activation [390, 391]. Once AKT is activated, this creates a positive feedback loop producing more ROS via different mechanisms including FOXO transcription factor inactivation, increased oxygen consumption and increased NOX4 [384].

In EP KO MC, we suggest that the observed upregulation of NOX4 (in both WT LP and EP KO MC) is a downstream effect of AKT activation, as PI3K/AKT pathway-mediated induction of NOX4 has been extensively reported in the literature [370, 392-395]. These findings suggest distinct molecular mechanisms underlying senescence in these two models, highlighting the role of mitochondrial ROS in WT LP MC and the more important role of increased AKT activity in EP MC lacking TXNIP.

Our data also showed that despite the heightened ROS and NOX4 expression in EP KO MC, these cells exhibited significantly less apoptosis (Figure 3.8). To understand the regulatory mechanisms that maintain cell survival in oxidative stress environments and under conditions of hyperactive AKT, we investigated the potential role of the prominent antioxidant transcription factor nuclear factor erythroid 2–related factor 2 (Nrf2) in cells deficient in TXNIP.

A study by He and Ma, demonstrated that Nrf2 significantly suppresses both basal and high glucose-induced TXNIP expression in murine hearts [396]. Nrf2 exerts its effects through major endogenous antioxidant gene targets, to sustain cellular survival and counteract apoptosis under

oxidative stress [370, 396]. Furthermore, a study by Katsu-Jiménez et al. identified a family with a mutation in the TXNIP gene resulting in undetectable expression of the TXNIP protein. This group isolated primary myoblasts from members of this family and conducted quantitative RT-PCR on these cells. They observed a strong basal activation of Nrf2 and its target gene SOD1 in primary TXNIP-null myoblasts. This observation supports the role of Nrf2 and its target antioxidant genes in mediating cellular responses in the absence of TXNIP [397].

Under normal redox conditions, Nrf2 is sequestered in the cytoplasm by Kelch-like ECH associating protein 1 (Keap1). As reviewed above (Introduction), ROS induce dissociation of the Nrf2-Keap1to promote Nrf2 nuclear localization and transcription of genes involved in cellular defense mechanisms, including antioxidant enzymes such as manganese superoxide dismutase (MnSOD) and catalase [281, 285].

3. Role of AKT in senescence

AKT plays a critical role in modulating glucose uptake and metabolism in insulin-sensitive cells by regulating the expression and translocation of GLUT4, thereby facilitating glucose uptake [398, 399]. The PI3K/AKT pathway is also implicated in promoting cellular glucose uptake in other cell types via downregulation of TXNIP expression thereby inhibiting GLUT degradation [305, 400]. TXNIP KO mice demonstrate enhanced AKT signaling, insulin sensitivity, and glycolysis in oxidative tissues compared to WT mice, which coincides with impaired mitochondrial fuel oxidation and accumulation of oxidized PTEN [306]. Activated AKT leads to premature senescence through mechanisms involving inhibition of FOXO family transcriptional activity and activation of mTOR pathways in addition to increased ROS [401-404].

Our data support these concepts, showing that both WT LP MC and EP KO MC display increased AKT activation and consequently heightened AKT-mediated phosphorylation of FOXO1 and FOXO3 transcription factors (Figure 3.7). Additionally, measuring the active (reduced form) level of the AKT negative regulator PTEN phosphatase was found to be higher in EP KO MC but not in WT LP MC (Figure 3.8).

Importantly, PI3K/AKT activation is essential for Nrf2 nuclear translocation, and inhibitors of PI3K, such as LY294002 and wortmannin, have been shown to reduce Nrf2 transcriptional activation of antioxidant genes in neuroblastoma SH-SY5Y cells [405]. PI3K-mediated upregulation of Nrf2 signaling plays a critical role in promoting cell survival by providing protection against excessive oxidative stress [406, 407]. Thus, despite the increased ROS observed in TXNIP KO MC, these data suggest that the level of ROS may be limited and the extent of oxidative stress is reduced to inhibit apoptosis. Further experiments abrogating the activation of Nrf2 are necessary to investigate this possibility.

A significant advancement in our understanding is highlighted by the use of AKT inhibitor (GSK690693), which effectively rescued senescence markers (P53, P16, SA-β-gal), DNA damage response (phosphorylation of histone H2AX, ROS, and NOX4), as well as Nrf2 and its antioxidant target genes (SOD2 and catalase) in TXNIP KO cells (Figure 3.9). To further corroborate the data obtained with the AKT inhibitor, we inhibited the upstream activator PI3K with a different chemical inhibitor, LY294002. Our results demonstrated that inhibition of PI3K significantly reduced the levels of the senescence marker P53 and the DDR marker, phosphorylation of histone H2AX, in TXNIP KO MC (Figure 3.9). These data demonstrate a pivotal role of the PI3K/AKT pathway and its downstream signaling in driving the observed cellular senescence and the associated DDR in the absence of TXNIP. The role of AKT is consistent with the results of

Fuhrmann-Stroissnigg et al., who reported that the HSP90 inhibitor 17-DMAG, a novel senolytic drug, downregulates AKT activity and induces apoptosis in senescent murine mesenchymal stem cells and human fibroblasts [408]. Additionally, the widely recognized senolytic drug Quercetin has been reported to inhibit the PI3K/AKT pathway, targeting senescence and the antiapoptotic features of senescent cells [409-411].

4. Evidence for TXNIP deficiency as a model of OIS

Based on the established role of TXNIP as a tumor suppressor protein and its observed downregulation in multiple cancers, including breast, renal, gastric, and hepatocellular carcinomas [342], our findings provide further insight into the molecular mechanisms underlying cellular senescence in TXNIP-deficient conditions. Specifically, we observed distinct differences in the senescence phenotype between EP KO MC and WT LP MC. One notable difference was the significant downregulation of active PTEN phosphatase in EP KO MC (Figure 3.8), and the telomere attrition-independent nature of the observed senescence in KO EP MC (Figure 3.5).

These observations support the hypothesis that the senescence phenotype in EP KO MC may reflect oncogene-induced senescence (OIS) rather than replicative senescence. This hypothesis is supported by our findings of elevated levels of active Ras (GTP-bound) in EP KO MC, whereas no significant difference in Ras activation was observed in WT LP MC (Figure 3.8). The increased Ras activity in EP KO MC suggests that the loss of TXNIP leads to the activation of oncogenic pathways, driving the senescence phenotype observed in these cells.

The decreased PTEN activity in EP KO MC likely contributes to this oncogenic signaling, given PTEN's role as a tumor suppressor and its involvement in regulating the PI3K/AKT pathway [412]. The interplay between PTEN loss and RAS activation has been recognized as a critical factor in

melanoma pathogenesis. Tsao et al. proposed that the loss of PTEN and the activation of RAS are redundant events that synergistically contribute to melanoma development. This redundancy highlights the complementary roles these alterations play in promoting oncogenesis [413].

Further supporting this notion, Nogueira et al. demonstrated that HRAS activation cooperates with Pten+/- and Ink4a/Arf-/- genotypes to significantly increase melanoma penetrance and facilitate metastasis [414].

In a different study, Vasudevan et al. provided insight into the functional importance of PTEN's phosphatase activity. They found that the restoration of wild-type PTEN, but not a phosphatase-defective mutant of PTEN, was capable of inducing apoptosis in Jun+/+ mouse embryonic fibroblast (MEF) cells [415].

The lack of telomere attrition in EP KO MC further supports the notion that their senescence is not driven by replicative exhaustion but rather by oncogene activation. Independence of telomere attrition was reported as a feature of OIS [156, 162].

These findings align with the broader context of TXNIP's function in cancer biology, where its loss facilitates oncogenic processes and impairs cellular mechanisms that counteract tumorigenesis [416]. In contrast to the replicative senescence model of LP WT MC, in EP KO MC lacking TXNIP, we hypothesize that reduced PTEN activity is the main driver of AKT activation. This reduction in PTEN activity has been previously reported in the literature and attributed to an increased NADH/NADPH ratio in cells lacking TXNIP [306].

5. TXNIP re-expression reverses senescence

To provide direct evidence of TXNIP's role in mitigating senescence, we reintroduced GFP-labelled TXNIP into TXNIP KO MC using lentiviral particles. The re-expression of TXNIP significantly rescued the senescence phenotype in these cells, as evidenced by the downregulation of P53, P16, beta-galactosidase staining, and NOX4 levels (Figure 3.10). These results support our hypothesis and extend previous findings. Cho et al. demonstrated that lentivirus-mediated re-expression of TXNIP in TXNIP-depleted ARPE-19 cells reduced the elevated levels of P53, suggesting that TXNIP regulates P53 stability or degradation [344]. Additionally, Jung et al. have found that reintroducing TXNIP rescued hematopoietic stem cell (HSC) frequency and significantly increased survival in mice subjected to paraquat-induced oxidative stress [345].

To investigate the importance of the thioredoxin binding site of TXNIP, we re-expressed a mutant form of TXNIP with a cysteine-to-serine mutation at position 247 (C247S). Interestingly, this mutant TXNIP exhibited only a very minor effect on the senescence markers compared to the wild-type TXNIP (Figure 3.10). Only P53 upregulation, but not P16, NOX4 and β-galactosidase staining was reversed. This finding aligns with those of Jung et al., who reported that re-expression of a double-mutant TXNIP (C247S/C267S) failed to restore the frequency of TXNIP KO donor hematopoietic cells and did not improve mouse survival following paraquat exposure [345]. These results confirm the critical role of TXNIP binding Trx or possibly a similar Cys247 binding protein in mitigating cellular senescence.

<u>In vivo studies</u>

1. TXNIP and memory and motor function impairment

As cellular senescence is a critical hallmark of organismal aging [130], we extended our studies to assess aging in TXNIP KO mice. One well-documented functional impairment in aging is

cognitive impairment [377]. In mice this can be assessed using a Y-maze apparatus that measures the ability to learn. Utilizing the Y-maze apparatus, our results demonstrated that TXNIP KO old male mice (21 months old) exhibited significantly reduced cognitive function as measured by spontaneous alternation behavior (SAB), whereas females showed no significant difference compared to age- and sex-matched WT mice (Figure 3.11). Interestingly, motor coordination, which also deteriorates with aging [417] assessed via the latency to fall on the rota-rod apparatus, revealed a similar pattern: old TXNIP KO males exhibited significantly reduced performance compared to WT males, while old KO females showed a tendency towards better performance on the rota-rod, though this difference was not statistically significant (Figure 3.11).

Based on a thorough review of the available literature up to the time of writing this thesis, we are the first to apply these behavioral tests in TXNIP KO old mice and to identify changes in cognitive and motor function and differences between males and females.

2. TXNIP and body weight and composition

Regarding body weight, TXNIP KO male mice displayed a tendency towards reduced body weight with aging, but this trend was not statistically significant compared to age-matched WT male mice. However, female KO mice exhibited a progressive body weight reduction that was statistically significant observed at 19 months old and continuing to the study's endpoint (21 months of age) compared to their age-matched WT female mice (Figure 3.12). Further investigation of body composition using MRI in 21-month-old male and female TXNIP KO mice revealed that both were significantly leaner than their age-matched WT counterparts, with KO females showing a more significant difference ($p<0.0001$) compared to males ($p<0.01$) (Figure 3.12).

These results support the concept that the rota-rod data indicate an age-related motor coordination impairment rather than a greater loss of lean muscle mass in the KO mice. A decreased muscle mass could have contributed to the lower scores observed in the KO mice.

Some of these findings align with existing literature. In a study by Chutkow et al., male mice were used exclusively to compare standard chow diet (SCD) to high-fat diet (HFD) in WT and TXNIP KO mice. It was found that on SCD, KO male mice had more lean mass and a lower ratio of fat to total body weight compared to WT, assessed via magnetic resonance spectroscopy (MRS) [418]. In another study, researchers focused on neuronal TXNIP and its function as a nutrient sensor by creating Agrp neuron-specific TXNIP gain-of-function and loss-of-function mouse models, using both male and female mice. They discovered that overexpressing TXNIP in these neurons predisposed animals to diet-induced obesity and adipose tissue storage by diminishing energy expenditure, whereas TXNIP loss conferred protection from diet-induced obesity and adipose tissue storage by enhancing energy expenditure. Specifically, deletion of TXNIP in Agrp neurons decreased the rate of body weight gain and fat mass in both male and female mice [298]. In a third study, researchers used prolonged fasting to induce liver steatosis in TXNIP WT and KO mice. As expected, TXNIP KO mice were highly sensitive to fasting and developed hypoglycemia as well as weight loss. Notably, they found that female TXNIP KO mice were more susceptible to fasting and developed more severe phenotypes, losing more weight than WT male and female mice, as well as TXNIP KO male mice [353]. It is important to mention that none of these studies investigated differences between male and female mice at an older age (21 months old).

The findings in the present study provide novel insights into the differential impact of TXNIP deficiency on aging parameters between male and female mice, highlighting the importance of sex-specific analyses in aging research.

3. TXNIP and senescence in vivo

To begin to further elucidate the role of TXNIP in in vivo aging, we quantified TXNIP levels in the kidney cortex and the hippocampal area of the brain in male mice, focusing on these two organs due to their susceptibility to age-associated impaired function. Comparing young (6 months old) and old (21 months old) WT mice, our results revealed a significant downregulation of TXNIP in the kidneys and hippocampal areas of the older mice (Figure 3.13).

These findings align with existing literature. In a study that quantified TXNIP in both mice and human brains, significant downregulation of TXNIP with advanced aging was observed. This study also examined the expression profile of TXNIP in the prefrontal cortex (PFC) of healthy mice from E14.5 (Embryonic 14.5 days) to P405 (postnatal 405 days), thus encompassing stages from embryonic development to middle age. They reported that TXNIP levels decreased progressively as the mice aged. Furthermore, analysis of TXNIP mRNA in human brains via the BrainSpan atlas demonstrated a similar trend, with TXNIP mRNA levels decreasing progressively with aging [419].

Extending our in vitro findings, we compared cellular senescence in the kidney cortex and hippocampal area of 21-month-old male WT and TXNIP KO mice. The results corroborated our in vitro data, demonstrating significantly upregulated senescence markers in the aged TXNIP KO mice compared to their age-matched WT counterparts (Figure 3.13). This observation is consistent with one previous report, which showed that the loss of TXNIP was associated with increased beta-galactosidase staining in the kidneys of 12 months old TXNIP KO mice compared to WT age-matched mice [343].

4. TXNIP, longevity and tumorigenesis

Consistent with the established role of TXNIP as a tumor suppressor and its downregulation in various cancers [420], our studies revealed an apparent increased incidence of tumor formation and abnormal organ growth in TXNIP KO mice. Affected tissues included the liver, colon, salivary glands, lymph nodes, testes, and spleen (Figure 3.14). Previous studies reported increased hepatocellular carcinoma and lymphomas in TXNIP KO mice [421, 422]. Preliminary data (not shown) in 4 of these tumor-like masses indicate cells of hematopoietic origin consistent with lymphoma. These findings were accompanied by hyperactivated AKT in the kidney cortex and brain hippocampal area (Figure 3.14), which supports the data obtained in the in vitro MC model (Figure 3.7).

Senescence is closely associated with aging [423]. There are no published studies of lifespan in TXNIP KO mice. Thus in the present study, we measured lifespan of these mice housed under standard conditions. Importantly, TXNIP KO mice demonstrated significantly reduced longevity compared to WT mice, with a maximum lifespan of 38 months in WT mice versus 29.5 months in KO mice, and median survival of 28 months for WT mice versus 20.3 months for KO mice (Figure 3.15). These data represent the first documented evidence of reduced lifespan in TXNIP KO mice and indicate a powerful effect of TXNIP in the control of longevity.

Importantly, during the longevity study, many TXNIP KO mice were euthanized at the end of life due to a weight loss exceeding 20%, which was considered an endpoint by the standard operation procedures (SOP) of the animal facility of the Research Institute of McGill University Health Center (RI-MUHC) (data not shown). This substantial weight loss in TXNIP KO mice during their late life stages, along with the increased tumor incidence and mass formation, suggest the possibly that these mice may suffer from cancer-related cachexia, contributing to the observed weight loss. While these data are preliminary, these observations underscore an important role of TXNIP in

preventing tumorigenesis and maintaining longevity, further emphasizing the potential implications of TXNIP suppression in aging and cancer-related pathologies.

In conclusion, our comprehensive in vitro and in vivo studies underscore the pivotal role of TXNIP in mitigating cellular senescence and aging. Our study demonstrates that the cell senescence observed in the absence of TXNIP is intricately linked to AKT hyperactivation and ROS overproduction and accompanied by activation of NRF2. The reintroduction of TXNIP in TXNIP KO cells effectively reversed senescence markers, highlighting its critical function in cellular homeostasis and the regulation of oxidative stress. The observed downregulation of TXNIP in aged tissues, coupled with increased cellular senescence markers in TXNIP KO mice, further confirms its significance in vivo and indicates a role in the aging processes. Moreover, the pronounced susceptibility of TXNIP-deficient mice to tumor formation, cognitive and motor dysfunction in aged male mice, and reduced lifespan in both sexes indicate the broad implications of TXNIP in aging-related pathologies and cancer. These findings collectively establish TXNIP as a critical regulator of cellular and organismal aging, providing valuable insights for potential therapeutic strategies targeting age-associated diseases and cancers.

4.2 Summary and Conclusions

This thesis has elucidated the critical role of TXNIP in regulating cellular senescence and organismal aging. Our in vitro and in vivo studies collectively reveal that TXNIP is a key modulator of oxidative stress responses and senescence pathways, with significant implications for aging and age-related diseases.

In our in vitro experiments, we discovered that replicative senescence in WT MC is associated with the downregulation of TXNIP. Our data suggest that this downregulation may be mediated

by the decreased expression of the carbohydrate-response element-binding protein (ChREBP) and/or MondoA in late-passage (25) WT MC. Notably, upregulating TXNIP by incubating LP MC in a high-glucose-containing medium was found to mitigate the senescence marker P53. Further studies are required to determine the extent to which these decreased transcription factors are the regulators of TXNIP and senescence as well as the cause of their decreased protein levels.

Further investigation into the underlying mechanisms revealed that AKT hyperactivation, increased ROS formation, and reduced PTEN activity are significant drivers of the senescence observed in the absence of TXNIP. This was corroborated by the use of AKT and PI3K inhibitors.

Three important distinctions that we observed between replicative senescence and TXNIP-deficiency-mediated senescence in EP MC are the involvement of decreased PTEN activity, absence of telomere shortening, and mitochondrial ROS production in the TXNIP KO cells. We propose that the senescence phenotype in EP TXNIP KO MC presents features similar to oncogene-induced senescence (OIS) and appears to mimic this model. Indeed, since TXNIP has been classified as a tumor suppressor, its absence may induce cell response similar to that of oncogenes. Reintroducing TXNIP into TXNIP KO cells effectively reversed markers of senescence, including P53, P16, and NOX4 levels, and reduced beta-galactosidase staining indicating that TXNIP is a direct mediator of these changes rather than a secondary effect of the KO.

The limited rescue observed with the mutant TXNIP (lacking thioredoxin binding function) emphasizes the importance of TXNIP's thioredoxin binding activity in preventing cellular senescence. Since it has been proposed that the PTEN inhibition is mediated by metabolic changes (NADH/NADPH ratio), our data imply that TXNIP binding to Trx is a key mechanism of

regulating TCA cycle versus glycolytic flux. Further work is needed to probe this question and mechanism(s).

Extending our investigation to in vivo models, we observed that aged TXNIP KO mice exhibited significantly upregulated senescence markers in the kidney cortex and hippocampal area, aligning with our in vitro findings. Functional assays, i.e. behavioral tests demonstrated a pronounced decline in cognitive and motor functions in aged male TXNIP KO mice, with a notable reduction in body weight, especially in females. Significantly, we also documented a marked decrease in maximum and median lifespan in TXNIP KO male and female mice. These results, to our knowledge, are the first to demonstrate evidence of decreased longevity in TXNIP KO mice indicating a significant role of TXNIP in the control of senescence, longevity and potentially age-related diseases.

The increased incidence of tumor formation and abnormal organ growth in various tissues of TXNIP KO mice, coupled with hyperactivated AKT signaling, supports a tumor-suppressive function of TXNIP. The reduced longevity and significant weight loss in aged TXNIP KO mice, may be mediated at least in part by malignancy and/or cancer-related cachexia.

In conclusion, our findings establish TXNIP as a crucial regulator of cellular senescence and organismal aging, with significant roles in oxidative stress response, tumor suppression, and maintenance of cognitive and motor functions. These insights pave the way for potential therapeutic strategies targeting TXNIP to combat age-associated diseases and improve healthspan and lifespan. Future research should continue to explore the molecular mechanisms underlying TXNIP's protective effects and its potential as a therapeutic target in age-related pathologies and cancer.

4.3 Future directions

Building on the findings of this thesis, several potential avenues for future research can be pursued to further elucidate the role of TXNIP in cellular senescence, aging, and related pathologies.

Mechanistic Studies on TXNIP and Senescence Pathways:

Elucidation of Downstream Targets: Future research should focus on identifying and characterizing the specific downstream targets of TXNIP in the context of cellular senescence. This includes detailed investigation of the interactions between TXNIP, Nrf2, and other key regulators of oxidative stress and cellular homeostasis.

Role of TXNIP in DNA Damage Response (DDR): Further studies are needed to explore how TXNIP influences the DDR pathway, particularly the mechanisms by which it modulates p53 stability and activity under different stress conditions.

Role of TXNIP in mechanism(s) relating cell metabolism, senescence and tumor suppression: Our data implicated a TXNIP-Trx interaction as critical to the maintenance of cellular homeostasis in the face of stressors. The detailed mechanism of this process and the proteins involved are not completely identified. Thus, further studies of the determinants of TCA cycle versus glycolytic (lactate production) flux are necessary to elucidate these TXNIP-regulated functions.

In Vivo Functional Studies:

Longitudinal Aging Studies: Conducting long-term studies on the aging process in TXNIP KO mice, including detailed histopathological analyses, could provide deeper insights into the age-dependent physiological changes and the development of age-related diseases.

Tissue-Specific Knockout Models: Developing tissue-specific TXNIP knockout models will help to delineate the role of TXNIP in different organs and systems. This can uncover how TXNIP deficiency impacts various tissues differently and contribute to aging and disease.

Tumor suppression: The mechanisms of the tumor suppression role of TXNIP are also incompletely understood. Whether the Trx binding is essential or the α-arrestin domain contributes to this action will require reconstitution of WT and mutant TXNIP and also possibly in a tissue-specific manner.

Therapeutic Potential and Intervention Studies:

Pharmacological Activation of TXNIP: Investigate small molecules or other pharmacological agents that can enhance TXNIP expression or block degradation. These studies could evaluate the potential of TXNIP regulators in preventing or reversing senescence and improving healthspan.

Gene Therapy Approaches: Explore the feasibility of using gene therapy to restore TXNIP function in vivo, particularly in models of age-related diseases or cancer and in a targeted manner to specific cells and tissues. This includes assessing the safety, efficacy, and delivery methods for gene therapy targeting of TXNIP.

Role of TXNIP in Cancer:

Cancer Susceptibility and Progression: Future studies should investigate the precise role of TXNIP in tumor initiation, progression, and metastasis. This includes exploring how TXNIP interacts with other tumor suppressors and oncogenes, such as PTEN and RAS, in various cancer models.

Senescence-Associated Secretory Phenotype (SASP): Understanding how TXNIP influences the SASP and its impact on the tumor microenvironment could provide new insights into cancer biology and potential therapeutic targets.

Sex-Specific Differences in TXNIP Function:

Investigate Sex Differences: Given the observed differences in the functional consequences of aging and senescence between male and female TXNIP KO mice, future research should focus on elucidating the underlying mechanisms modifying these sex-specific effects. A limitation of this study was that only male mice were evaluated in the in vivo senescence marker experiments. Therefore, future investigation should include female KO mice as well as potential hormonal regulation, metabolic differences, and their impact on TXNIP function and expression.

Metabolic and Mitochondrial Function:

Mitochondrial Dysfunction and Mitophagy: Further exploration of how TXNIP deficiency affects mitochondrial function, dynamics, and mitophagy could shed light on the metabolic aspects of aging and senescence.

Nutrient Sensing and Energy Metabolism: Studies should continue to investigate the role of TXNIP in nutrient sensing pathways and energy metabolism, particularly in relation to calorie restriction and fasting, which are known to influence aging and longevity.

In summary, these future directions are suggestions aiming to deepen our understanding of TXNIP's multifaceted role in cellular and organismal aging, with the ultimate goal of developing novel interventions to enhance healthspan and treat age-related diseases.

Chapter 5 References

References

1. Martínez, D.E., *Mortality patterns suggest lack of senescence in hydra.* Experimental gerontology, 1998. **33**(3): p. 217-225.
2. Terman, A. and U.T. Brunk, *Oxidative stress, accumulation of biological'garbage', and aging.* Antioxidants & redox signaling, 2006. **8**(1-2): p. 197-204.
3. Harman, D., *The aging process.* Proceedings of the National Academy of Sciences, 1981. **78**(11): p. 7124-7128.
4. Uhlenberg, P., *International handbook of population aging*. Vol. 1. 2009: Springer Science & Business Media.
5. United Nations Department of Economic and Social Affairs, P.D., *World Population Prospects 2022: Summary of Results. UN DESA/POP/2022/TR/NO. 3*.
6. https://doi.org/10.25318/1710000501-eng.
7. https://population.un.org/wpp/Graphs/Probabilistic/EX/MaleAndFemale/124.
8. https://doi.org/10.25318/1310083701-eng.
9. Schulz, R., et al., *Older adults who need caregiving and the family caregivers who help them*, in *Families caring for an aging America*. 2016, National Academies Press (US).
10. Chen, J., et al., *How heavy is the medical expense burden among the older adults and what are the contributing factors? A literature review and problem-based analysis.* Frontiers in Public Health, 2023. **11**: p. 1165381.
11. Sciences, N.A.o., et al., *Social isolation and loneliness in older adults: Opportunities for the health care system*. 2020: National Academies Press.
12. Jones, C.H. and M. Dolsten, *Healthcare on the brink: navigating the challenges of an aging society in the United States.* npj Aging, 2024. **10**(1): p. 22.

13. De Grey, A.D., *Life span extension research and public debate: societal considerations.* Studies in Ethics, Law, and Technology, 2007. **1**(1).

14. Dillin, A., D.E. Gottschling, and T. Nyström, *The good and the bad of being connected: the integrons of aging.* Current opinion in cell biology, 2014. **26**: p. 107-112.

15. MacNee, W., R.A. Rabinovich, and G. Choudhury, *Ageing and the border between health and disease.* European Respiratory Journal, 2014. **44**(5): p. 1332-1352.

16. Jousilahti, P., et al., *Sex, age, cardiovascular risk factors, and coronary heart disease: a prospective follow-up study of 14 786 middle-aged men and women in Finland.* Circulation, 1999. **99**(9): p. 1165-1172.

17. Pencina, M.J., et al., *Quantifying importance of major risk factors for coronary heart disease.* Circulation, 2019. **139**(13): p. 1603-1611.

18. Doruk, H., et al., *The relationship between body mass index and incidental mild cognitive impairment, Alzheimer's disease, and Vascular Dementia in elderly.* The journal of nutrition, health & aging, 2010. **14**: p. 834-838.

19. Herrup, K., *Reimagining Alzheimer's disease—an age-based hypothesis.* Journal of Neuroscience, 2010. **30**(50): p. 16755-16762.

20. Harris, R.E., *Epidemiology of chronic disease: global perspectives*. 2019: Jones & Bartlett Learning.

21. Miwa, S., et al., *Mitochondrial dysfunction in cell senescence and aging.* The Journal of Clinical Investigation, 2022. **132**(13).

22. Mailloux, R.J. and M.-E. Harper, *Uncoupling proteins and the control of mitochondrial reactive oxygen species production.* Free Radical Biology and Medicine, 2011. **51**(6): p. 1106-1115.

23. Leutner, S., A. Eckert, and W. Müller, *ROS generation, lipid peroxidation and antioxidant enzyme activities in the aging brain.* Journal of neural transmission, 2001. **108**: p. 955-967.

24. Mallajosyula, J.K., et al., *MAO-B elevation in mouse brain astrocytes results in Parkinson's pathology.* PloS one, 2008. **3**(2): p. e1616.

25. Poljšak, B., R.G. Dahmane, and A. Godić, *Intrinsic skin aging: the role of oxidative stress.* Acta Dermatovenerol Alp Pannonica Adriat, 2012. **21**(2): p. 33-36.

26. Smith, C., et al., *Excess brain protein oxidation and enzyme dysfunction in normal aging and in Alzheimer disease.* Proceedings of the National Academy of Sciences, 1991. **88**(23): p. 10540-10543.

27. Pansarasa, O., et al., *Age and sex differences in human skeletal muscle: role of reactive oxygen species.* Free radical research, 2000. **33**(3): p. 287-293.

28. Rizvi, S.I., R. Jha, and P.K. Maurya, *Erythrocyte plasma membrane redox system in human aging.* Rejuvenation research, 2006. **9**(4): p. 470-474.

29. Droge, W., *Free radicals in the physiological control of cell function. Physiology Review, v. 82.* 2002.

30. Short, K.R., et al., *Decline in skeletal muscle mitochondrial function with aging in humans.* Proceedings of the National Academy of Sciences, 2005. **102**(15): p. 5618-5623.

31. Harkema, L., S.A. Youssef, and A. de Bruin, *Pathology of mouse models of accelerated aging.* Veterinary pathology, 2016. **53**(2): p. 366-389.

32. Evans, G.W. and E. Kantrowitz, *Socioeconomic status and health: the potential role of environmental risk exposure.* Annual review of public health, 2002. **23**(1): p. 303-331.

33. Harman, D., *Ageing: a theory based on free radical and radiation chemistry.* J. Gerontal, 1956. **11**: p. 293-3.

34. Beckman, K.B. and B.N. Ames, *The free radical theory of aging matures.* Physiological reviews, 1998.

35. Barja, G., et al., *Low mitochondrial free radical production per unit O2 consumption can explain the simultaneous presence of high longevity and high aerobic metabolic rate in birds.* Free radical research, 1994. **21**(5): p. 317-327.

36. Csiszar, A., et al., *Testing the oxidative stress hypothesis of aging in primate fibroblasts: is there a correlation between species longevity and cellular ROS production?* Journals of Gerontology Series A: Biomedical Sciences and Medical Sciences, 2012. **67**(8): p. 841-852.

37. Ku, H.-H., U.T. Brunk, and R.S. Sohal, *Relationship between mitochondrial superoxide and hydrogen peroxide production and longevity of mammalian species.* Free Radical Biology and Medicine, 1993. **15**(6): p. 621-627.

38. Ku, H.-H. and R. Sohal, *Comparison of mitochondrial pro-oxidant generation and anti-oxidant defenses between rat and pigeon: possible basis of variation in longevity and metabolic potential.* Mechanisms of ageing and development, 1993. **72**(1): p. 67-76.

39. Delhaye, J., et al., *Interspecific correlation between red blood cell mitochondrial ROS production, cardiolipin content and longevity in birds.* Age, 2016. **38**: p. 433-443.

40. Allen, C., et al., *Isolation of quiescent and nonquiescent cells from yeast stationary-phase cultures.* The Journal of cell biology, 2006. **174**(1): p. 89-100.

41. Fabrizio, P., et al., *SOD2 functions downstream of Sch9 to extend longevity in yeast.* Genetics, 2003. **163**(1): p. 35-46.

42. Longo, V. and P. Fabrizio, *Visions & Reflections¶ Regulation of longevity and stress resistance: a molecular strategy conserved from yeast to humans?* Cellular and Molecular Life Sciences CMLS, 2002. **59**: p. 903-908.

43. Fabrizio, P. and V.D. Longo, *The chronological life span of Saccharomyces cerevisiae.* Aging cell, 2003. **2**(2): p. 73-81.

44. Unlu, E.S. and A. Koc, *Effects of deleting mitochondrial antioxidant genes on life span.* Annals of the New York Academy of Sciences, 2007. **1100**(1): p. 505-509.

45. Longo, V.D., et al., *Mitochondrial superoxide decreases yeast survival in stationary phase.* Archives of biochemistry and biophysics, 1999. **365**(1): p. 131-142.

46. Kumsta, C., M. Thamsen, and U. Jakob, *Effects of oxidative stress on behavior, physiology, and the redox thiol proteome of Caenorhabditis elegans.* Antioxidants & redox signaling, 2011. **14**(6): p. 1023-1037.

47. Honda, Y. and S. Honda, *The daf-2 gene network for longevity regulates oxidative stress resistance and Mn-superoxide dismutase gene expression in Caenorhabditis elegans.* The FASEB journal, 1999. **13**(11): p. 1385-1393.

48. Murakami, S. and T.E. Johnson, *A genetic pathway conferring life extension and resistance to UV stress in Caenorhabditis elegans.* Genetics, 1996. **143**(3): p. 1207-1218.

49. Oláhová, M., et al., *A redox-sensitive peroxiredoxin that is important for longevity has tissue-and stress-specific roles in stress resistance.* Proceedings of the national academy of sciences, 2008. **105**(50): p. 19839-19844.

50. Taub, J., et al., *A cytosolic catalase is needed to extend adult lifespan in C. elegans daf-C and clk-1 mutants.* Nature, 1999. **399**(6732): p. 162-166.

51. Tiller, G.R. and D.A. Garsin, *The SKPO-1 peroxidase functions in the hypodermis to protect Caenorhabditis elegans from bacterial infection.* Genetics, 2014. **197**(2): p. 515-526.

52. Sun, J. and J. Tower, *FLP recombinase-mediated induction of Cu/Zn-superoxide dismutase transgene expression can extend the life span of adult Drosophila melanogaster flies.* Molecular and cellular biology, 1999.

53. Sun, J., et al., *Induced overexpression of mitochondrial Mn-superoxide dismutase extends the life span of adult Drosophila melanogaster.* Genetics, 2002. **161**(2): p. 661-672.

54. Orr, W.C. and R.S. Sohal, *Extension of life-span by overexpression of superoxide dismutase and catalase in Drosophila melanogaster.* Science, 1994. **263**(5150): p. 1128-1130.

55. Parkes, T.L., et al., *Extension of Drosophila lifespan by overexpression of human SOD1 in motorneurons.* Nature genetics, 1998. **19**(2): p. 171-174.

56. Izuo, N., et al., *Brain-specific superoxide dismutase 2 deficiency causes perinatal death with spongiform encephalopathy in mice.* Oxidative medicine and cellular longevity, 2015. **2015**.

57. Elchuri, S., et al., *CuZnSOD deficiency leads to persistent and widespread oxidative damage and hepatocarcinogenesis later in life.* Oncogene, 2005. **24**(3): p. 367-380.

58. Fischer, L.R., et al., *Absence of SOD1 leads to oxidative stress in peripheral nerve and causes a progressive distal motor axonopathy.* Experimental Neurology, 2012. **233**(1): p. 163-171.

59. Flood, D.G., et al., *Hindlimb motor neurons require Cu/Zn superoxide dismutase for maintenance of neuromuscular junctions.* The American journal of pathology, 1999. **155**(2): p. 663-672.

60. Garratt, M., et al., *Superoxide dismutase deficiency impairs olfactory sexual signaling and alters bioenergetic function in mice.* Proceedings of the National Academy of Sciences, 2014. **111**(22): p. 8119-8124.

61. Imamura, Y., et al., *Drusen, choroidal neovascularization, and retinal pigment epithelium dysfunction in SOD1-deficient mice: a model of age-related macular degeneration.* Proceedings of the National Academy of Sciences, 2006. **103**(30): p. 11282-11287.

62. Iuchi, Y., et al., *Spontaneous skin damage and delayed wound healing in SOD1-deficient mice.* Molecular and cellular biochemistry, 2010. **341**: p. 181-194.

63. Matzuk, M.M., et al., *Ovarian function in superoxide dismutase 1 and 2 knockout mice.* Endocrinology, 1998. **139**(9): p. 4008-4011.

64. Muller, F.L., et al., *Absence of CuZn superoxide dismutase leads to elevated oxidative stress and acceleration of age-dependent skeletal muscle atrophy.* Free Radical Biology and Medicine, 2006. **40**(11): p. 1993-2004.

65. Shi, Y., et al., *The lack of CuZnSOD leads to impaired neurotransmitter release, neuromuscular junction destabilization and reduced muscle strength in mice.* PLoS One, 2014. **9**(6): p. e100834.

66. Zhang, Y., et al., *Dietary restriction attenuates the accelerated aging phenotype of Sod1−/− mice.* Free Radical Biology and Medicine, 2013. **60**: p. 300-306.

67. Yoshihara, D., et al., *The absence of the SOD1 gene causes abnormal monoaminergic neurotransmission and motivational impairment-like behavior in mice.* Free Radical Research, 2016. **50**(11): p. 1245-1256.

68. Ghimire, S. and M.S. Kim, *Enhanced locomotor activity is required to exert dietary restriction-dependent increase of stress resistance in Drosophila.* Oxidative medicine and cellular longevity, 2015. **2015**.

69. Alugoju, P., K.S. VKD, and L. Periyasamy, *Effect of short-term quercetin, caloric restriction and combined treatment on age-related oxidative stress markers in the rat cerebral cortex.* CNS & Neurological Disorders-Drug Targets (Formerly Current Drug Targets-CNS & Neurological Disorders), 2018. **17**(2): p. 119-131.

70. David, C.E.B., et al., *Calorie restriction attenuates hypertrophy-induced redox imbalance and mitochondrial ATP-sensitive K+ channel repression.* The Journal of Nutritional Biochemistry, 2018. **62**: p. 87-94.

71. Lee, C.-K., et al., *Gene expression profile of aging and its retardation by caloric restriction.* Science, 1999. **285**(5432): p. 1390-1393.

72. Li, D., et al., *Caloric restriction attenuates C57BL/6 J mouse lung injury and extra-pulmonary toxicity induced by real ambient particulate matter exposure.* Particle and fibre toxicology, 2020. **17**(1): p. 1-17.

73. Zainal, T.A., et al., *Caloric restriction of rhesus monkeys lowers oxidative damage in skeletal muscle.* The FASEB Journal, 2000. **14**(12): p. 1825-1836.

74. López-Domènech, S., et al., *Dietary weight loss intervention improves subclinical atherosclerosis and oxidative stress markers in leukocytes of obese humans.* International Journal of Obesity, 2019. **43**(11): p. 2200-2209.

75. Gonsette, R., *Neurodegeneration in multiple sclerosis: the role of oxidative stress and excitotoxicity.* Journal of the neurological sciences, 2008. **274**(1-2): p. 48-53.

76. Mitosek-Szewczyk, K., et al., *Free radical peroxidation products in cerebrospinal fluid and serum of patients with multiple sclerosis after glucocorticoid therapy.* Folia Neuropathologica, 2010. **48**(2): p. 116-122.

77. Thylefors, B., et al., *Global data on blindness.* Bulletin of the world health organization, 1995. **73**(1): p. 115.

78. Beebe, D.C., N.M. Holekamp, and Y.-B. Shui, *Oxidative damage and the prevention of age-related cataracts.* Ophthalmic research, 2010. **44**(3): p. 155-165.

79. Berthoud, V.M. and E.C. Beyer, *Oxidative stress, lens gap junctions, and cataracts.* Antioxidants & redox signaling, 2009. **11**(2): p. 339-353.

80. Ansari, N.H., L. Wang, and S.K. Srivastava, *Role of lipid aldehydes in cataractogenesis: 4-hydroxynonenal-induced cataract.* Biochemical and molecular medicine, 1996. **58**(1): p. 25-30.

81. Chang, D., et al., *Serum antioxidative enzymes levels and oxidative stress products in age-related cataract patients.* Oxidative medicine and cellular longevity, 2013. **2013**.

82. Teng, H., et al., *Senescence marker protein30 protects lens epithelial cells against oxidative damage by restoring mitochondrial function.* Bioengineered, 2022. **13**(5): p. 12955-12971.

83. Santiago-López, D., et al., *Oxidative stress, progressive damage in the substantia nigra and plasma dopamine oxidation, in rats chronically exposed to ozone.* Toxicology letters, 2010. **197**(3): p. 193-200.

84. Buffenstein, R. and W. Craft, *The idiosyncratic physiological traits of the naked mole-rat; a resilient animal model of aging, longevity, and healthspan.* The extraordinary biology of the naked mole-rat, 2021: p. 221-254.

85. Ruby, J.G., M. Smith, and R. Buffenstein, *Naked mole-rat mortality rates defy Gompertzian laws by not increasing with age.* elife, 2018. **7**: p. e31157.

86. Andziak, B. and R. Buffenstein, *Disparate patterns of age-related changes in lipid peroxidation in long-lived naked mole-rats and shorter-lived mice.* Aging cell, 2006. **5**(6): p. 525-532.

87. Andziak, B., et al., *High oxidative damage levels in the longest-living rodent, the naked mole-rat.* Aging cell, 2006. **5**(6): p. 463-471.

88. Pérez, V.I., et al., *Protein stability and resistance to oxidative stress are determinants of longevity in the longest-living rodent, the naked mole-rat.* Proceedings of the National Academy of Sciences, 2009. **106**(9): p. 3059-3064.

89. Marbois, B.N. and C.F. Clarke, *The COQ7 Gene Encodes a Protein in Saccharomyces cerevisiae Necessary for Ubiquinone Biosynthesis (∗).* Journal of Biological Chemistry, 1996. **271**(6): p. 2995-3004.

90. Nakai, D., et al., *coq7/clk-1 regulates mitochondrial respiration and the generation of reactive oxygen species via coenzyme Q.* Aging Cell, 2004. **3**(5): p. 273-281.

91. Do, T.Q., J.R. Schultz, and C.F. Clarke, *Enhanced sensitivity of ubiquinone-deficient mutants of Saccharomyces cerevisiae to products of autoxidized polyunsaturated fatty acids.* Proceedings of the National Academy of Sciences, 1996. **93**(15): p. 7534-7539.

92. Lapointe, J. and S. Hekimi, *Early mitochondrial dysfunction in long-lived Mclk1+/-mice.* Journal of Biological Chemistry, 2008. **283**(38): p. 26217-26227.

93. Doonan, R., et al., *Against the oxidative damage theory of aging: superoxide dismutases protect against oxidative stress but have little or no effect on life span in Caenorhabditis elegans.* Genes & development, 2008. **22**(23): p. 3236-3241.

94. Van Raamsdonk, J.M. and S. Hekimi, *Deletion of the mitochondrial superoxide dismutase sod-2 extends lifespan in Caenorhabditis elegans.* PLoS genetics, 2009. **5**(2): p. e1000361.

95. Braeckman, B.P., et al., *Apparent uncoupling of energy production and consumption in long-lived Clk mutants of Caenorhabditis elegans.* Current Biology, 1999. **9**(9): p. 493-497.

96. Yang, W., J. Li, and S. Hekimi, *A measurable increase in oxidative damage due to reduction in superoxide detoxification fails to shorten the life span of long-lived mitochondrial mutants of Caenorhabditis elegans.* Genetics, 2007. **177**(4): p. 2063-2074.

97. Felkai, S., et al., *CLK-1 controls respiration, behavior and aging in the nematode Caenorhabditis elegans.* The EMBO journal, 1999. **18**(7): p. 1783-1792.

98. Feng, J., F. Bussière, and S. Hekimi, *Mitochondrial electron transport is a key determinant of life span in Caenorhabditis elegans.* Developmental cell, 2001. **1**(5): p. 633-644.

99. Falk, M.J., et al., *Mitochondrial complex I function modulates volatile anesthetic sensitivity in C. elegans.* Current biology, 2006. **16**(16): p. 1641-1645.

100. Yang, W. and S. Hekimi, *A mitochondrial superoxide signal triggers increased longevity in Caenorhabditis elegans.* PLoS biology, 2010. **8**(12): p. e1000556.

101. Sohal, R.S. and W.C. Orr, *The redox stress hypothesis of aging.* Free Radical Biology and Medicine, 2012. **52**(3): p. 539-555.

102. Luo, Z., et al., *ROS-induced autophagy regulates porcine trophectoderm cell apoptosis, proliferation, and differentiation.* American Journal of Physiology-Cell Physiology, 2019. **316**(2): p. C198-C209.

103. Mittler, R., *ROS are good.* Trends in plant science, 2017. **22**(1): p. 11-19.

104. Redza-Dutordoir, M. and D.A. Averill-Bates, *Activation of apoptosis signalling pathways by reactive oxygen species.* Biochimica et Biophysica Acta (BBA)-Molecular Cell Research, 2016. **1863**(12): p. 2977-2992.

105. Hekimi, S., J. Lapointe, and Y. Wen, *Taking a "good" look at free radicals in the aging process.* Trends in cell biology, 2011. **21**(10): p. 569-576.

106. Veal, E.A., A.M. Day, and B.A. Morgan, *Hydrogen peroxide sensing and signaling.* Molecular cell, 2007. **26**(1): p. 1-14.

107. Groeger, G., C. Quiney, and T.G. Cotter, *Hydrogen peroxide as a cell-survival signaling molecule.* Antioxidants & redox signaling, 2009. **11**(11): p. 2655-2671.

108. Van Raamsdonk, J.M. and S. Hekimi, *Reactive oxygen species and aging in Caenorhabditis elegans: causal or casual relationship?* Antioxidants & redox signaling, 2010. **13**(12): p. 1911-1953.

109. Cypser, J.R. and T.E. Johnson, *Multiple stressors in Caenorhabditis elegans induce stress hormesis and extended longevity.* The Journals of Gerontology Series A: Biological Sciences and Medical Sciences, 2002. **57**(3): p. B109-B114.

110. Heidler, T., et al., *Caenorhabditis elegans lifespan extension caused by treatment with an orally active ROS-generator is dependent on DAF-16 and SIR-2.1.* Biogerontology, 2010. **11**: p. 183-195.

111. Schulz, T.J., et al., *Glucose restriction extends Caenorhabditis elegans life span by inducing mitochondrial respiration and increasing oxidative stress.* Cell metabolism, 2007. **6**(4): p. 280-293.

112. Caldeira da Silva, C.C., et al., *Mild mitochondrial uncoupling in mice affects energy metabolism, redox balance and longevity.* Aging cell, 2008. **7**(4): p. 552-560.

113. Cox, C.S., et al., *Mitohormesis in mice via sustained basal activation of mitochondrial and antioxidant signaling.* Cell metabolism, 2018. **28**(5): p. 776-786. e5.

114. Campisi, J., *From cells to organisms: can we learn about aging from cells in culture?* Experimental gerontology, 2001. **36**(4-6): p. 607-618.

115. Hernandez-Segura, A., J. Nehme, and M. Demaria, *Hallmarks of cellular senescence.* Trends in cell biology, 2018. **28**(6): p. 436-453.

116. Baker, D.J., et al., *Clearance of p16Ink4a-positive senescent cells delays ageing-associated disorders.* Nature, 2011. **479**(7372): p. 232-236.

117. Burd, C.E., et al., *Monitoring tumorigenesis and senescence in vivo with a p16INK4a-luciferase model.* Cell, 2013. **152**(1): p. 340-351.

118. Demaria, M., et al., *An essential role for senescent cells in optimal wound healing through secretion of PDGF-AA.* Developmental cell, 2014. **31**(6): p. 722-733.

119. Gorgoulis, V., et al., *Cellular senescence: defining a path forward.* Cell, 2019. **179**(4): p. 813-827.

120. Shiloh, Y., *The ATM-mediated DNA-damage response: taking shape.* Trends in biochemical sciences, 2006. **31**(7): p. 402-410.

121. Zou, L., *Single-and double-stranded DNA: building a trigger of ATR-mediated DNA damage response.* Genes & development, 2007. **21**(8): p. 879-885.

122. Bent, E.H., L.A. Gilbert, and M.T. Hemann, *A senescence secretory switch mediated by PI3K/AKT/mTOR activation controls chemoprotective endothelial secretory responses.* Genes & development, 2016. **30**(16): p. 1811-1821.

123. Druelle, C., et al., *ATF6α regulates morphological changes associated with senescence in human fibroblasts.* Oncotarget, 2016. **7**(42): p. 67699.

124. Cormenier, J., et al., *The ATF6α arm of the Unfolded Protein Response mediates replicative senescence in human fibroblasts through a COX2/prostaglandin E2 intracrine pathway.* Mechanisms of Ageing and Development, 2018. **170**: p. 82-91.

125. Passos, J.F., et al., *Mitochondrial dysfunction accounts for the stochastic heterogeneity in telomere-dependent senescence.* PLoS biology, 2007. **5**(5): p. e110.

126. Tai, H., et al., *Autophagy impairment with lysosomal and mitochondrial dysfunction is an important characteristic of oxidative stress-induced senescence.* Autophagy, 2017. **13**(1): p. 99-113.

127. Studencka, M. and J. Schaber, *Senoptosis: non-lethal DNA cleavage as a route to deep senescence.* Oncotarget, 2017. **8**(19): p. 30656.

128. Lee, B.Y., et al., *Senescence-associated β-galactosidase is lysosomal β-galactosidase.* Aging cell, 2006. **5**(2): p. 187-195.

129. Kurz, D.J., et al., *Senescence-associated β-galactosidase reflects an increase in lysosomal mass during replicative ageing of human endothelial cells.* Journal of cell science, 2000. **113**(20): p. 3613-3622.

130. Borghesan, M., et al., *A senescence-centric view of aging: implications for longevity and disease.* Trends in cell biology, 2020. **30**(10): p. 777-791.

131. López-Otín, C., et al., *The hallmarks of aging.* Cell, 2013. **153**(6): p. 1194-1217.

132. Krishnamurthy, J., et al., *p16INK4a induces an age-dependent decline in islet regenerative potential.* Nature, 2006. **443**(7110): p. 453-457.

133. Sousa-Victor, P., et al., *Geriatric muscle stem cells switch reversible quiescence into senescence.* Nature, 2014. **506**(7488): p. 316-321.

134. Cosgrove, B.D., et al., *Rejuvenation of the muscle stem cell population restores strength to injured aged muscles.* Nature medicine, 2014. **20**(3): p. 255-264.

135. Braun, H., et al., *Cellular senescence limits regenerative capacity and allograft survival.* Journal of the American Society of Nephrology: JASN, 2012. **23**(9): p. 1467.

136. Franceschi, C. and J. Campisi, *Chronic inflammation (inflammaging) and its potential contribution to age-associated diseases.* Journals of Gerontology Series A: Biomedical Sciences and Medical Sciences, 2014. **69**(Suppl_1): p. S4-S9.

137. Rea, I.M., et al., *Age and age-related diseases: role of inflammation triggers and cytokines.* Frontiers in immunology, 2018: p. 586.

138. Muñoz-Espín, D. and M. Serrano, *Cellular senescence: from physiology to pathology.* Nature reviews Molecular cell biology, 2014. **15**(7): p. 482-496.

139. Di Micco, R., et al., *Cellular senescence in ageing: from mechanisms to therapeutic opportunities.* Nature reviews Molecular cell biology, 2021. **22**(2): p. 75-95.

140. Celeste, A., et al., *Genomic instability in mice lacking histone H2AX.* Science, 2002. **296**(5569): p. 922-927.

141. Turenne, G.A., et al., *Activation of p53 transcriptional activity requires ATM's kinase domain and multiple N-terminal serine residues of p53.* Oncogene, 2001. **20**(37): p. 5100-5110.

142. Hayflick, L. and P.S. Moorhead, *The serial cultivation of human diploid cell strains.* Experimental cell research, 1961. **25**(3): p. 585-621.

143. Dunham, M.A., et al., *Telomere maintenance by recombination in human cells.* Nature genetics, 2000. **26**(4): p. 447-450.

144. Roake, C.M. and S.E. Artandi, *Telomere-lengthening mechanism revealed.* Nature, 2016. **539**(7627): p. 35-36.

145. Vaziri, H. and S. Benchimol, *Reconstitution of telomerase activity in normal human cells leads to elongation of telomeres and extended replicative life span.* Current Biology, 1998. **8**(5): p. 279-282.

146. Martin, H., et al., *Telomere shortening causes distinct cell division regimes during replicative senescence in Saccharomyces cerevisiae.* Cell & Bioscience, 2021. **11**(1): p. 1-10.

147. Shay, J.W. and W.E. Wright, *Telomeres and telomerase: three decades of progress.* Nature Reviews Genetics, 2019. **20**(5): p. 299-309.

148. D'adda Di Fagagna, F., *Living on a break: cellular senescence as a DNA-damage response.* Nature Reviews Cancer, 2008. **8**(7): p. 512-522.

149. Petrova, N.V., et al., *Small molecule compounds that induce cellular senescence.* Aging Cell, 2016. **15**(6): p. 999-1017.

150. Maity, A., W.G. McKenna, and R.J. Muschel, *The molecular basis for cell cycle delays following ionizing radiation: a review.* Radiotherapy and oncology, 1994. **31**(1): p. 1-13.

151. Kang, H.T., et al., *Chemical screening identifies ATM as a target for alleviating senescence.* Nature chemical biology, 2017. **13**(6): p. 616-623.

152. Ye, C., et al., *Radiation-induced cellular senescence results from a slippage of long-term G2 arrested cells into G1 phase.* Cell cycle, 2013. **12**(9): p. 1424-1432.

153. Correia-Melo, C., et al., *Mitochondria are required for pro-ageing features of the senescent phenotype.* The EMBO journal, 2016. **35**(7): p. 724-742.

154. Sharpless, N.E. and C.J. Sherr, *Forging a signature of in vivo senescence.* Nature Reviews Cancer, 2015. **15**(7): p. 397-408.

155. Sarkisian, C.J., et al., *Dose-dependent oncogene-induced senescence in vivo and its evasion during mammary tumorigenesis.* Nature cell biology, 2007. **9**(5): p. 493-505.

156. Rattanavirotkul, N., K. Kirschner, and T. Chandra, *Induction and transmission of oncogene-induced senescence.* Cellular and Molecular Life Sciences, 2021. **78**: p. 843-852.

157. Gorgoulis, V.G., et al., *Integrating the DNA damage and protein stress responses during cancer development and treatment.* The Journal of pathology, 2018. **246**(1): p. 12-40.

158. Hills, S.A. and J.F. Diffley, *DNA replication and oncogene-induced replicative stress.* Current biology, 2014. **24**(10): p. R435-R444.

159. Gorgoulis, V.G. and T.D. Halazonetis, *Oncogene-induced senescence: the bright and dark side of the response.* Current opinion in cell biology, 2010. **22**(6): p. 816-827.

160. Kamijo, T., et al., *Tumor suppression at the mouse INK4a locus mediated by the alternative reading frame product p19 ARF.* Cell, 1997. **91**(5): p. 649-659.

161. Ventura, A., et al., *Restoration of p53 function leads to tumour regression in vivo.* Nature, 2007. **445**(7128): p. 661-665.

162. Xue, W., et al., *Senescence and tumour clearance is triggered by p53 restoration in murine liver carcinomas.* Nature, 2007. **445**(7128): p. 656-660.

163. Terzi, M.Y., M. Izmirli, and B. Gogebakan, *The cell fate: senescence or quiescence.* Molecular biology reports, 2016. **43**: p. 1213-1220.

164. Rao, S.G. and J.G. Jackson, *SASP: tumor suppressor or promoter? Yes!* Trends in cancer, 2016. **2**(11): p. 676-687.

165. Coppé, J.-P., et al., *Secretion of vascular endothelial growth factor by primary human fibroblasts at senescence.* Journal of Biological Chemistry, 2006. **281**(40): p. 29568-29574.

166. Sparmann, A. and D. Bar-Sagi, *Ras-induced interleukin-8 expression plays a critical role in tumor growth and angiogenesis.* Cancer cell, 2004. **6**(5): p. 447-458.

167. Badache, A. and N.E. Hynes, *Interleukin 6 inhibits proliferation and, in cooperation with an epidermal growth factor receptor autocrine loop, increases migration of T47D breast cancer cells.* Cancer research, 2001. **61**(1): p. 383-391.

168. Ritschka, B., et al., *The senescence-associated secretory phenotype induces cellular plasticity and tissue regeneration.* Genes & development, 2017. **31**(2): p. 172-183.

169. Pazolli, E., et al., *Chromatin remodeling underlies the senescence-associated secretory phenotype of tumor stromal fibroblasts that supports cancer progression.* Cancer research, 2012. **72**(9): p. 2251-2261.

170. Tchkonia, T., et al., *Cellular senescence and the senescent secretory phenotype: therapeutic opportunities.* The Journal of clinical investigation, 2013. **123**(3): p. 966-972.

171. Admasu, T.D., M.J. Rae, and A. Stolzing, *Dissecting primary and secondary senescence to enable new senotherapeutic strategies.* Ageing Research Reviews, 2021. **70**: p. 101412.

172. Gonzalez-Meljem, J.M., et al., *Paracrine roles of cellular senescence in promoting tumourigenesis.* British journal of cancer, 2018. **118**(10): p. 1283-1288.

173. Kojima, H., et al., *IL-6-STAT3 signaling and premature senescence.* Jak-stat, 2013. **2**(4): p. e25763.

174. Kojima, H., et al., *The STAT3-IGFBP5 axis is critical for IL-6/gp130-induced premature senescence in human fibroblasts.* Cell Cycle, 2012. **11**(4): p. 730-739.

175. Borghesan, M., et al., *Small extracellular vesicles are key regulators of non-cell autonomous intercellular communication in senescence via the interferon protein IFITM3.* Cell Reports, 2019. **27**(13): p. 3956-3971. e6.

176. Sies, H., *Oxidative stress: from basic research to clinical application.* The American journal of medicine, 1991. **91**(3): p. S31-S38.

177. Höhn, A., et al., *Happily (n) ever after: Aging in the context of oxidative stress, proteostasis loss and cellular senescence.* Redox biology, 2017. **11**: p. 482-501.

178. Ogrodnik, M., et al., *Cellular senescence drives age-dependent hepatic steatosis.* Nature communications, 2017. **8**(1): p. 15691.

179. Sharma, V., et al., *Oxidative stress at low levels can induce clustered DNA lesions leading to NHEJ mediated mutations.* Oncotarget, 2016. **7**(18): p. 25377.

180. Ohanna, M., et al., *Senescent cells develop a PARP-1 and nuclear factor-κB-associated secretome (PNAS).* Genes & development, 2011. **25**(12): p. 1245-1261.

181. Le Gal, K., E.E. Schmidt, and V.I. Sayin, *Cellular redox homeostasis.* Antioxidants, 2021. **10**(9): p. 1377.

182. Dröge, W., *Free radicals in the physiological control of cell function.* Physiological reviews, 2002.

183. Sies, H. and W. Stahl, *Vitamins E and C, beta-carotene, and other carotenoids as antioxidants.* The American journal of clinical nutrition, 1995. **62**(6): p. 1315S-1321S.

184. Tainer, J.A., et al., *Structure and mechanism of copper, zinc superoxide dismutase.* Nature, 1983. **306**(5940): p. 284-287.

185. Shields, H.J., A. Traa, and J.M. Van Raamsdonk, *Beneficial and detrimental effects of reactive oxygen species on lifespan: a comprehensive review of comparative and experimental studies.* Frontiers in Cell and Developmental Biology, 2021. **9**: p. 181.

186. Fukai, T. and M. Ushio-Fukai, *Superoxide dismutases: role in redox signaling, vascular function, and diseases.* Antioxidants & redox signaling, 2011. **15**(6): p. 1583-1606.

187. Lee, S., S.M. Kim, and R.T. Lee, *Thioredoxin and thioredoxin target proteins: from molecular mechanisms to functional significance.* Antioxidants & redox signaling, 2013. **18**(10): p. 1165-1207.

188. Hanschmann, E.-M., et al., *Thioredoxins, glutaredoxins, and peroxiredoxins—molecular mechanisms and health significance: from cofactors to antioxidants to redox signaling.* Antioxidants & redox signaling, 2013. **19**(13): p. 1539-1605.

189. Matés, J.M., C. Pérez-Gómez, and I.N. De Castro, *Antioxidant enzymes and human diseases.* Clinical biochemistry, 1999. **32**(8): p. 595-603.

190. Flohé, L., *The glutathione peroxidase reaction: molecular basis of the antioxidant function of selenium in mammals*, in *Current topics in cellular regulation*. 1985, Elsevier. p. 473-478.

191. Birben, E., et al., *Oxidative stress and antioxidant defense.* World allergy organization journal, 2012. **5**: p. 9-19.

192. Wu, G., et al., *Glutathione metabolism and its implications for health.* The Journal of nutrition, 2004. **134**(3): p. 489-492.

193. Aldini, G., et al., *N-Acetylcysteine as an antioxidant and disulphide breaking agent: the reasons why.* Free radical research, 2018. **52**(7): p. 751-762.

194. Šalamon, Š., et al., *Medical and dietary uses of N-acetylcysteine.* Antioxidants, 2019. **8**(5): p. 111.

195. Chen, K.-S. and H.F. DeLuca, *Isolation and characterization of a novel cDNA from HL-60 cells treated with 1, 25-dihydroxyvitamin D-3.* Biochimica et Biophysica Acta (BBA)-Gene Structure and Expression, 1994. **1219**(1): p. 26-32.

196. Ludwig, D.L., et al., *Cloning, genetic characterization, and chromosomal mapping of the mouse VDUP1 gene.* Gene, 2001. **269**(1-2): p. 103-112.

197. Alvarez, C.E., *On the origins of arrestin and rhodopsin.* BMC evolutionary biology, 2008. **8**(1): p. 1-13.

198. Patwari, P., et al., *Thioredoxin-independent regulation of metabolism by the α-arrestin proteins.* Journal of Biological Chemistry, 2009. **284**(37): p. 24996-25003.

199. Patwari, P., et al., *The interaction of thioredoxin with Txnip: evidence for formation of a mixed disulfide by disulfide exchange.* Journal of Biological Chemistry, 2006. **281**(31): p. 21884-21891.

200. Masutani, H., et al., *Thioredoxin binding protein (TBP)-2/Txnip and α-arrestin proteins in cancer and diabetes mellitus.* Journal of clinical biochemistry and nutrition, 2011. **50**(1): p. 23-34.

201. Spindel, O.N., C. World, and B.C. Berk, *Thioredoxin interacting protein: redox dependent and independent regulatory mechanisms.* Antioxidants & redox signaling, 2012. **16**(6): p. 587-596.

202. Zhang, P., et al., *The ubiquitin ligase itch regulates apoptosis by targeting thioredoxin-interacting protein for ubiquitin-dependent degradation.* Journal of Biological Chemistry, 2010. **285**(12): p. 8869-8879.

203. Spindel, O.N., C. Yan, and B.C. Berk, *Thioredoxin-Interacting Protein Mediates Nuclear–to–Plasma Membrane Communication: Role in Vascular Endothelial Growth Factor 2 Signaling.* Arteriosclerosis, thrombosis, and vascular biology, 2012. **32**(5): p. 1264-1270.

204. Shin, D., et al., *VDUP1 mediates nuclear export of HIF1α via CRM1-dependent pathway.* Biochimica et Biophysica Acta (BBA)-Molecular Cell Research, 2008. **1783**(5): p. 838-848.

205. Cao, X., et al., *Redox-dependent and independent effects of thioredoxin interacting protein.* Biological chemistry, 2020. **401**(11): p. 1215-1231.

206. Jiang, N., et al., *Thioredoxin-interacting protein: A new therapeutic target in bone metabolism disorders?* Frontiers in Immunology, 2022. **13**: p. 955128.

207. Nishiyama, A., et al., *Identification of thioredoxin-binding protein-2/vitamin D3 up-regulated protein 1 as a negative regulator of thioredoxin function and expression.* Journal of Biological Chemistry, 1999. **274**(31): p. 21645-21650.

208. Yoshihara, E., et al., *Thioredoxin/Txnip: redoxisome, as a redox switch for the pathogenesis of diseases.* Frontiers in immunology, 2014. **4**: p. 514.

209. Saxena, G., J. Chen, and A. Shalev, *Intracellular Shuttling and Mitochondrial Function of Thioredoxin-interacting Protein 2.* Journal of Biological Chemistry, 2010. **285**(6): p. 3997-4005.

210. Park, S.-J., et al., *Blocking CHOP-dependent TXNIP shuttling to mitochondria attenuates albuminuria and mitigates kidney injury in nephrotic syndrome.* Proceedings of the National Academy of Sciences, 2022. **119**(35): p. e2116505119.

211. Masson, E., et al., *High β-cell mass prevents streptozotocin-induced diabetes in thioredoxin-interacting protein-deficient mice.* American Journal of Physiology-Endocrinology and Metabolism, 2009. **296**(6): p. E1251-E1261.

212. Zhou, R., et al., *Thioredoxin-interacting protein links oxidative stress to inflammasome activation.* Nature immunology, 2010. **11**(2): p. 136-140.

213. Schroder, K., R. Zhou, and J. Tschopp, *The NLRP3 inflammasome: a sensor for metabolic danger?* Science, 2010. **327**(5963): p. 296-300.

214. Hwang, J., et al., *The structural basis for the negative regulation of thioredoxin by thioredoxin-interacting protein.* Nature communications, 2014. **5**(1): p. 2958.

215. Bronner, D.N., et al., *Endoplasmic reticulum stress activates the inflammasome via NLRP3-and caspase-2-driven mitochondrial damage.* Immunity, 2015. **43**(3): p. 451-462.

216. Glasauer, A. and N.S. Chandel, *Ros.* Current Biology, 2013. **23**(3): p. R100-R102.

217. Santos, A.L., S. Sinha, and A.B. Lindner, *The good, the bad, and the ugly of ROS: new insights on aging and aging-related diseases from eukaryotic and prokaryotic model organisms.* Oxidative medicine and cellular longevity, 2018. **2018**.

218. Pham-Huy, L.A., H. He, and C. Pham-Huy, *Free radicals, antioxidants in disease and health.* International journal of biomedical science: IJBS, 2008. **4**(2): p. 89.

219. Winterbourn, C.C., *Reconciling the chemistry and biology of reactive oxygen species.* Nature chemical biology, 2008. **4**(5): p. 278-286.

220. Phaniendra, A., D.B. Jestadi, and L. Periyasamy, *Free radicals: properties, sources, targets, and their implication in various diseases.* Indian journal of clinical biochemistry, 2015. **30**: p. 11-26.

221. Stanton, R.C., *Oxidative stress and diabetic kidney disease.* Current diabetes reports, 2011. **11**: p. 330-336.

222. De Jager, T., A. Cockrell, and S. Du Plessis, *Ultraviolet light induced generation of reactive oxygen species.* Ultraviolet Light in Human Health, Diseases and Environment, 2017: p. 15-23.

223. Ganguly, B., M. Hota, and J. Pradhan, *Skin aging: implications of UV radiation, reactive oxygen species and natural antioxidants.* Reactive Oxygen Species, 2021: p. 1-21.

224. MohanKumar, S.M., et al., *Role of cytokines and reactive oxygen species in brain aging.* Mechanisms of Ageing and Development, 2023: p. 111855.

225. Bashan, N., et al., *Positive and negative regulation of insulin signaling by reactive oxygen and nitrogen species.* Physiological reviews, 2009.

226. Travasso, R.D., et al., *Localized redox relays as a privileged mode of cytoplasmic hydrogen peroxide signaling.* Redox biology, 2017. **12**: p. 233-245.

227. Di Marzo, N., E. Chisci, and R. Giovannoni, *The role of hydrogen peroxide in redox-dependent signaling: homeostatic and pathological responses in mammalian cells.* Cells, 2018. **7**(10): p. 156.

228. de Almeida, A.J.P.O., et al., *ROS: Basic concepts, sources, cellular signaling, and its implications in aging pathways.* Oxidative Medicine and Cellular Longevity, 2022. **2022**.

229. Holmström, K.M. and T. Finkel, *Cellular mechanisms and physiological consequences of redox-dependent signalling.* Nature reviews Molecular cell biology, 2014. **15**(6): p. 411-421.

230. Daiber, A., et al., *Crosstalk of mitochondria with NADPH oxidase via reactive oxygen and nitrogen species signalling and its role for vascular function.* British journal of pharmacology, 2017. **174**(12): p. 1670-1689.

231. Canugovi, C., et al., *Increased mitochondrial NADPH oxidase 4 (NOX4) expression in aging is a causative factor in aortic stiffening.* Redox biology, 2019. **26**: p. 101288.

232. Chocron, E.S., E. Munkácsy, and A.M. Pickering, *Cause or casualty: The role of mitochondrial DNA in aging and age-associated disease.* Biochimica et Biophysica Acta (BBA)-Molecular Basis of Disease, 2019. **1865**(2): p. 285-297.

233. Dai, D.-F., et al., *Mitochondrial oxidative stress in aging and healthspan.* Longevity & healthspan, 2014. **3**(1): p. 1-22.

234. Serino, A. and G. Salazar, *Protective role of polyphenols against vascular inflammation, aging and cardiovascular disease.* Nutrients, 2018. **11**(1): p. 53.

235. Sfeir, A., et al., *Mammalian telomeres resemble fragile sites and require TRF1 for efficient replication.* Cell, 2009. **138**(1): p. 90-103.

236. Wiley, C.D., et al., *Mitochondrial dysfunction induces senescence with a distinct secretory phenotype.* Cell metabolism, 2016. **23**(2): p. 303-314.

237. Chance, B., H. Sies, and A. Boveris, *Hydroperoxide metabolism in mammalian organs.* Physiological reviews, 1979. **59**(3): p. 527-605.

238. Staniek, K. and H. Nohl, *H2O2 detection from intact mitochondria as a measure for one-electron reduction of dioxygen requires a non-invasive assay system.* Biochimica et Biophysica Acta (BBA)-Bioenergetics, 1999. **1413**(2): p. 70-80.

239. Brand, M.D., *Mitochondrial generation of superoxide and hydrogen peroxide as the source of mitochondrial redox signaling.* Free Radical Biology and Medicine, 2016. **100**: p. 14-31.

240. Jastroch, M., et al., *Mitochondrial proton and electron leaks.* Essays in biochemistry, 2010. **47**: p. 53-67.

241. Hardeland, R., *Melatonin and the electron transport chain.* Cellular and Molecular Life Sciences, 2017. **74**: p. 3883-3896.

242. Haythorne, E., et al., *Diabetes causes marked inhibition of mitochondrial metabolism in pancreatic β-cells.* Nature communications, 2019. **10**(1): p. 2474.

243. Vermot, A., et al., *NADPH oxidases (NOX): an overview from discovery, molecular mechanisms to physiology and pathology.* Antioxidants, 2021. **10**(6): p. 890.

244. Paik, Y.-H., et al., *Role of NADPH oxidases in liver fibrosis.* Antioxidants & redox signaling, 2014. **20**(17): p. 2854-2872.

245. Bedard, K. and K.-H. Krause, *The NOX family of ROS-generating NADPH oxidases: physiology and pathophysiology.* Physiological reviews, 2007. **87**(1): p. 245-313.

246. Schroder, K., *NADPH oxidases: current aspects and tools. Redox Biol 34: 101512*. 2020.

247. Shanmugasundaram, K., et al., *NOX4 functions as a mitochondrial energetic sensor coupling cancer metabolic reprogramming to drug resistance.* Nature communications, 2017. **8**(1): p. 997.

248. Ogboo, B.C., et al., *Architecture of the NADPH oxidase family of enzymes.* Redox Biology, 2022. **52**: p. 102298.

249. Sedeek, M., et al., *NADPH oxidases, reactive oxygen species, and the kidney: friend and foe.* Journal of the American Society of Nephrology: JASN, 2013. **24**(10): p. 1512.

250. Lambeth, J.D., T. Kawahara, and B. Diebold, *Regulation of Nox and Duox enzymatic activity and expression.* Free Radical Biology and Medicine, 2007. **43**(3): p. 319-331.

251. McCrann, D., et al., *Upregulation of Nox4 in the aging vasculature and its association with smooth muscle cell polyploidy.* Cell cycle, 2009. **8**(6): p. 902-908.

252. Elko, E.A., et al., *Age-dependent dysregulation of redox genes may contribute to fibrotic pulmonary disease susceptibility.* Free Radical Biology and Medicine, 2019. **141**: p. 438-446.

253. Ghatak, S., et al., *Transforming growth factor β1 (TGFβ1)-induced CD44V6-NOX4 signaling in pathogenesis of idiopathic pulmonary fibrosis.* Journal of Biological Chemistry, 2017. **292**(25): p. 10490-10519.

254. Meijles, D.N., et al., *The matricellular protein TSP1 promotes human and mouse endothelial cell senescence through CD47 and Nox1.* Science signaling, 2017. **10**(501): p. eaaj1784.

255. Li, Y., et al., *Forestalling age-impaired angiogenesis and blood flow by targeting NOX: Interplay of NOX1, IL-6, and SASP in propagating cell senescence.* Proceedings of the National Academy of Sciences, 2021. **118**(42): p. e2015666118.

256. Lee, H.-Y., et al., *Nox4 regulates the eNOS uncoupling process in aging endothelial cells.* Free Radical Biology and Medicine, 2017. **113**: p. 26-35.

257. Weyemi, U., et al., *ROS-generating NADPH oxidase NOX4 is a critical mediator in oncogenic H-Ras-induced DNA damage and subsequent senescence.* Oncogene, 2012. **31**(9): p. 1117-1129.

258. Kodama, R., et al., *ROS-generating oxidases N ox1 and N ox4 contribute to oncogenic R as-induced premature senescence.* Genes to Cells, 2013. **18**(1): p. 32-41.

259. Kim, Y.Y., et al., *Cooperation between p21 and Akt is required for p53-dependent cellular senescence.* Aging cell, 2017. **16**(5): p. 1094-1103.

260. Diebold, I., et al., *The NADPH oxidase subunit NOX4 is a new target gene of the hypoxia-inducible factor-1.* Molecular biology of the cell, 2010. **21**(12): p. 2087-2096.

261. Manea, A., et al., *Transcriptional regulation of NADPH oxidase isoforms, Nox1 and Nox4, by nuclear factor-κB in human aortic smooth muscle cells.* Biochemical and biophysical research communications, 2010. **396**(4): p. 901-907.

262. Pendyala, S., et al., *Nrf2 regulates hyperoxia-induced Nox4 expression in human lung endothelium: identification of functional antioxidant response elements on the Nox4 promoter.* Free Radical Biology and Medicine, 2011. **50**(12): p. 1749-1759.

263. Tang, P., et al., *NADPH oxidase NOX4 is a glycolytic regulator through mROS-HIF1α axis in thyroid carcinomas.* Scientific reports, 2018. **8**(1): p. 15897.

264. Averill-Bates, D.A., *The antioxidant glutathione*, in *Vitamins and hormones*. 2023, Elsevier. p. 109-141.

265. Sies, H. and D.P. Jones, *Reactive oxygen species (ROS) as pleiotropic physiological signalling agents.* Nature reviews Molecular cell biology, 2020. **21**(7): p. 363-383.

266. Averill-Bates, D., *Reactive oxygen species and cell signaling. Review.* Biochimica et Biophysica Acta (BBA)-Molecular Cell Research, 2023: p. 119573.

267. Lambeth, J.D., *NOX enzymes and the biology of reactive oxygen.* Nature Reviews Immunology, 2004. **4**(3): p. 181-189.

268. Morgan, M.J. and Z.-g. Liu, *Crosstalk of reactive oxygen species and NF-κB signaling.* Cell research, 2011. **21**(1): p. 103-115.

269. Wenqi, Z., et al., *"Double-Edged Sword" Effect of Reactive Oxygen Species (ROS) in Tumor Development and Carcinogenesis.* Physiological Research, 2023. **72**(3): p. 301.

270. Dharshini, L.C.P., et al., *Oxidative stress responsive transcription factors in cellular signalling transduction mechanisms.* Cellular Signalling, 2020. **72**: p. 109670.

271. Barford, D., *The role of cysteine residues as redox-sensitive regulatory switches.* Current opinion in structural biology, 2004. **14**(6): p. 679-686.

272. Jones, D.P., *Redox sensing: orthogonal control in cell cycle and apoptosis signalling.* Journal of internal medicine, 2010. **268**(5): p. 432-448.

273. Paulsen, C.E. and K.S. Carroll, *Cysteine-mediated redox signaling: chemistry, biology, and tools for discovery.* Chemical reviews, 2013. **113**(7): p. 4633-4679.

274. Liu, R., et al., *PI3K/AKT pathway as a key link modulates the multidrug resistance of cancers.* Cell Death & Disease, 2020. **11**(9): p. 797.

275. Aslan, M. and T. Özben, *Oxidants in receptor tyrosine kinase signal transduction pathways.* Antioxidants and Redox Signaling, 2003. **5**(6): p. 781-788.

276. Lou, Y.W., et al., *Redox regulation of the protein tyrosine phosphatase PTP1B in cancer cells.* The FEBS journal, 2008. **275**(1): p. 69-88.

277. Lee, S.-R., et al., *Reversible inactivation of the tumor suppressor PTEN by H2O2.* Journal of Biological Chemistry, 2002. **277**(23): p. 20336-20342.

278. Chalhoub, N. and S.J. Baker, *PTEN and the PI3-kinase pathway in cancer.* Annual Review of Pathology: Mechanisms of Disease, 2009. **4**: p. 127-150.

279. Tobiume, K., M. Saitoh, and H. Ichijo, *Activation of apoptosis signal-regulating kinase 1 by the stress-induced activating phosphorylation of pre-formed oligomer.* Journal of cellular physiology, 2002. **191**(1): p. 95-104.

280. Saitoh, M., et al., *Mammalian thioredoxin is a direct inhibitor of apoptosis signal-regulating kinase (ASK) 1.* The EMBO journal, 1998. **17**(9): p. 2596-2606.

281. Bellezza, I., et al., *Nrf2-Keap1 signaling in oxidative and reductive stress.* Biochimica et Biophysica Acta (BBA)-Molecular Cell Research, 2018. **1865**(5): p. 721-733.

282. Suzuki, T., J. Takahashi, and M. Yamamoto, *Molecular Basis of the KEAP1-NRF2 Signaling Pathway.* Molecules and Cells, 2023. **46**(3): p. 133.

283. Yamamoto, M., T.W. Kensler, and H. Motohashi, *The KEAP1-NRF2 system: a thiol-based sensor-effector apparatus for maintaining redox homeostasis.* Physiological reviews, 2018. **98**(3): p. 1169-1203.

284. Adinolfi, S., et al., *The KEAP1-NRF2 pathway: Targets for therapy and role in cancer.* Redox Biology, 2023: p. 102726.

285. Blank, V., *Small Maf proteins in mammalian gene control: mere dimerization partners or dynamic transcriptional regulators?* Journal of molecular biology, 2008. **376**(4): p. 913-925.

286. Glory, A. and D.A. Averill-Bates, *The antioxidant transcription factor Nrf2 contributes to the protective effect of mild thermotolerance (40 C) against heat shock-induced apoptosis.* Free radical biology and medicine, 2016. **99**: p. 485-497.

287. Chen, R., et al., *Reactive oxygen species formation in the brain at different oxygen levels: the role of hypoxia inducible factors.* Frontiers in cell and developmental biology, 2018. **6**: p. 132.

288. Brunelle, J.K., et al., *Oxygen sensing requires mitochondrial ROS but not oxidative phosphorylation.* Cell metabolism, 2005. **1**(6): p. 409-414.

289. Celeste Simon, M., *Mitochondrial reactive oxygen species are required for hypoxic HIFα stabilization.* Hypoxia and Exercise, 2007: p. 165-170.

290. Guzy, R.D., et al., *Mitochondrial complex III is required for hypoxia-induced ROS production and cellular oxygen sensing.* Cell metabolism, 2005. **1**(6): p. 401-408.

291. Liu, Y., et al., *Hypoxia-inducible factor-1: a potential target to treat acute lung injury.* Oxidative medicine and cellular longevity, 2020. **2020**.

292. Ma, Z., et al., *Targeting hypoxia-inducible factor-1-mediated metastasis for cancer therapy.* Antioxidants & Redox Signaling, 2021. **34**(18): p. 1484-1497.

293. Papandreou, I., et al., *HIF-1 mediates adaptation to hypoxia by actively downregulating mitochondrial oxygen consumption.* Cell metabolism, 2006. **3**(3): p. 187-197.

294. Mohammad Alhawiti, N., et al., *TXNIP in metabolic regulation: physiological role and therapeutic outlook.* Current drug targets, 2017. **18**(9): p. 1095-1103.

295. Levendusky, M.C., et al., *Expression and regulation of vitamin D3 upregulated protein 1 (VDUP1) is conserved in mammalian and insect brain.* Journal of Comparative Neurology, 2009. **517**(5): p. 581-600.

296. Aon-Bertolino, M.L., et al., *Thioredoxin and glutaredoxin system proteins—immunolocalization in the rat central nervous system.* Biochimica et Biophysica Acta (BBA)-General Subjects, 2011. **1810**(1): p. 93-110.

297. Blouet, C. and G.J. Schwartz, *Nutrient-sensing hypothalamic TXNIP links nutrient excess to energy imbalance in mice.* Journal of Neuroscience, 2011. **31**(16): p. 6019-6027.

298. Blouet, C., et al., *TXNIP in Agrp neurons regulates adiposity, energy expenditure, and central leptin sensitivity.* Journal of Neuroscience, 2012. **32**(29): p. 9870-9877.

299. Hand, L.E., et al., *Induction of the metabolic regulator Txnip in fasting-induced and natural torpor.* Endocrinology, 2013. **154**(6): p. 2081-2091.

300. Minn, A.H., C. Hafele, and A. Shalev, *Thioredoxin-interacting protein is stimulated by glucose through a carbohydrate response element and induces β-cell apoptosis.* Endocrinology, 2005. **146**(5): p. 2397-2405.

301. Cha-Molstad, H., et al., *Glucose-stimulated expression of Txnip is mediated by carbohydrate response element-binding protein, p300, and histone H4 acetylation in pancreatic beta cells.* Journal of Biological Chemistry, 2009. **284**(25): p. 16898-16905.

302. Yu, F.-X. and Y. Luo, *Tandem ChoRE and CCAAT motifs and associated factors regulate Txnip expression in response to glucose or adenosine-containing molecules.* PloS one, 2009. **4**(12): p. e8397.

303. Parikh, H., et al., *TXNIP regulates peripheral glucose metabolism in humans.* PLoS medicine, 2007. **4**(5): p. e158.

304. Wu, N., et al., *AMPK-dependent degradation of TXNIP upon energy stress leads to enhanced glucose uptake via GLUT1.* Molecular cell, 2013. **49**(6): p. 1167-1175.

305. Waldhart, A.N., et al., *Phosphorylation of TXNIP by AKT mediates acute influx of glucose in response to insulin.* Cell reports, 2017. **19**(10): p. 2005-2013.

306. Hui, S.T., et al., *Txnip balances metabolic and growth signaling via PTEN disulfide reduction.* Proceedings of the National Academy of Sciences, 2008. **105**(10): p. 3921-3926.

307. Pelicano, H., et al., *Mitochondrial respiration defects in cancer cells cause activation of Akt survival pathway through a redox-mediated mechanism.* The Journal of cell biology, 2006. **175**(6): p. 913-923.

308. Hui, T.Y., et al., *Mice lacking thioredoxin-interacting protein provide evidence linking cellular redox state to appropriate response to nutritional signals.* Journal of Biological Chemistry, 2004. **279**(23): p. 24387-24393.

309. Farrell, M.R., et al., *Thioredoxin-interacting protein inhibits hypoxia-inducible factor transcriptional activity.* Free Radical Biology and Medicine, 2010. **49**(9): p. 1361-1367.

310. Cantley, J., et al., *The hypoxia response pathway and β-cell function.* Diabetes, Obesity and Metabolism, 2010. **12**: p. 159-167.

311. Marin-Hernandez, A., et al., *HIF-1α modulates energy metabolism in cancer cells by inducing over-expression of specific glycolytic isoforms.* Mini reviews in medicinal chemistry, 2009. **9**(9): p. 1084-1101.

312. Yoshioka, J., et al., *Deletion of thioredoxin-interacting protein in mice impairs mitochondrial function but protects the myocardium from ischemia-reperfusion injury.* The Journal of clinical investigation, 2012. **122**(1): p. 267-279.

313. Shah, A., et al., *Thioredoxin-interacting protein mediates high glucose-induced reactive oxygen species generation by mitochondria and the NADPH oxidase, Nox4, in mesangial cells.* Journal of Biological Chemistry, 2013. **288**(10): p. 6835-6848.

314. Carmeliet, P., et al., *Role of HIF-1α in hypoxia-mediated apoptosis, cell proliferation and tumour angiogenesis.* Nature, 1998. **394**(6692): p. 485-490.

315. Vaupel, P., *The role of hypoxia-induced factors in tumor progression.* The oncologist, 2004. **9**(S5): p. 10-17.

316. Burke-Gaffney, A., M.E. Callister, and H. Nakamura, *Thioredoxin: friend or foe in human disease?* Trends in pharmacological sciences, 2005. **26**(8): p. 398-404.

317. Watanabe, R., et al., *Anti-oxidative, anti-cancer and anti-inflammatory actions by thioredoxin 1 and thioredoxin-binding protein-2.* Pharmacology & therapeutics, 2010. **127**(3): p. 261-270.

318. Park, J.W., et al., *Downregulation of TXNIP leads to high proliferative activity and estrogen-dependent cell growth in breast cancer.* Biochemical and biophysical research communications, 2018. **498**(3): p. 566-572.

319. Kwon, H.-J., et al., *Vitamin D3 upregulated protein 1 deficiency promotes N-methyl-N-nitrosourea and Helicobacter pylori-induced gastric carcinogenesis in mice.* Gut, 2012. **61**(1): p. 53-63.

320. Kwon, H.-J., et al., *Vitamin D3 upregulated protein 1 suppresses TNF-α–induced NF-κB activation in hepatocarcinogenesis.* The Journal of Immunology, 2010. **185**(7): p. 3980-3989.

321. Yuan, Y., et al., *TXNIP inhibits the progression of osteosarcoma through DDIT4-mediated mTORC1 suppression.* American Journal of Cancer Research, 2022. **12**(8): p. 3760.

322. Chen, J.L.-Y., et al., *Lactic acidosis triggers starvation response with paradoxical induction of TXNIP through MondoA.* PLoS genetics, 2010. **6**(9): p. e1001093.

323. Li, J., et al., *TXNIP overexpression suppresses proliferation and induces apoptosis in SMMC7221 cells through ROS generation and MAPK pathway activation.* Oncology reports, 2017. **37**(6): p. 3369-3376.

324. Zhou, Y., et al., *BET Bromodomain inhibition promotes De-repression of TXNIP and activation of ASK1-MAPK pathway in acute myeloid leukemia.* BMC cancer, 2018. **18**: p. 1-11.

325. Morrison, J.A., et al., *Thioredoxin interacting protein (TXNIP) is a novel tumor suppressor in thyroid cancer.* Molecular cancer, 2014. **13**: p. 1-13.

326. Shin, K.-H., et al., *hnRNP G elicits tumor-suppressive activity in part by upregulating the expression of Txnip.* Biochemical and biophysical research communications, 2008. **372**(4): p. 880-885.

327. Oka, S.i., et al., *Impaired fatty acid utilization in thioredoxin binding protein-2 (TBP-2)-deficient mice: a unique animal model of Reye syndrome.* The FASEB journal, 2006. **20**(1): p. 121-123.

328. Yoshioka, J., et al., *Targeted deletion of thioredoxin-interacting protein regulates cardiac dysfunction in response to pressure overload.* Circulation research, 2007. **101**(12): p. 1328-1338.

329. Lee, K.N., et al., *VDUP1 is required for the development of natural killer cells.* Immunity, 2005. **22**(2): p. 195-208.

330. Sheth, S.S., et al., *Thioredoxin-interacting protein deficiency disrupts the fasting-feeding metabolic transition.* Journal of lipid research, 2005. **46**(1): p. 123-134.

331. Chau, G.C., et al., *mTOR controls ChREBP transcriptional activity and pancreatic β cell survival under diabetic stress.* Journal of Cell Biology, 2017. **216**(7): p. 2091-2105.

332. Thielen, L. and A. Shalev, *Diabetes pathogenic mechanisms and potential new therapies based upon a novel target called TXNIP.* Current opinion in endocrinology, diabetes, and obesity, 2018. **25**(2): p. 75.

333. Chen, J., et al., *Thioredoxin-interacting protein: a critical link between glucose toxicity and β-cell apoptosis.* Diabetes, 2008. **57**(4): p. 938-944.

334. Chen, J., et al., *Thioredoxin-interacting protein deficiency induces Akt/Bcl-xL signaling and pancreatic beta-cell mass and protects against diabetes.* The FASEB Journal, 2008. **22**(10): p. 3581.

335. Sun, H., et al., *Role of thioredoxin-interacting protein in diabetic fatty kidney induced by advanced glycation end-products.* Journal of Agricultural and Food Chemistry, 2021. **69**(40): p. 11982-11991.

336. Shah, A., et al., *Thioredoxin-interacting protein deficiency protects against diabetic nephropathy.* Journal of the American Society of Nephrology: JASN, 2015. **26**(12): p. 2963.

337. Cunningham, G.M., et al., *The paradoxical role of thioredoxin on oxidative stress and aging.* Archives of Biochemistry and Biophysics, 2015. **576**: p. 32-38.

338. Miranda-Vizuete, A., et al., *Lifespan decrease in a Caenorhabditis elegans mutant lacking TRX-1, a thioredoxin expressed in ASJ sensory neurons.* FEBS letters, 2006. **580**(2): p. 484-490.

339. Mitsui, A., et al., *Overexpression of human thioredoxin in transgenic mice controls oxidative stress and life span.* Antioxidants and Redox Signaling, 2002. **4**(4): p. 693-696.

340. Pérez, V.I., et al., *Thioredoxin 1 overexpression extends mainly the earlier part of life span in mice.* Journals of Gerontology Series A: Biomedical Sciences and Medical Sciences, 2011. **66**(12): p. 1286-1299.

341. Tsuda, M., et al., *Loss of Trx-2 enhances oxidative stress-dependent phenotypes in Drosophila.* FEBS letters, 2010. **584**(15): p. 3398-3401.

342. Zhou, J., Q. Yu, and W.-J. Chng, *TXNIP (VDUP-1, TBP-2): a major redox regulator commonly suppressed in cancer by epigenetic mechanisms.* The international journal of biochemistry & cell biology, 2011. **43**(12): p. 1668-1673.

343. Huy, H., et al., *TXNIP regulates AKT-mediated cellular senescence by direct interaction under glucose-mediated metabolic stress.* Aging cell, 2018. **17**(6): p. e12836.

344. Ji Cho, M., et al., *Oxidative stress-mediated TXNIP loss causes RPE dysfunction.* Experimental & Molecular Medicine, 2019. **51**(10): p. 1-13.

345. Jung, H., et al., *TXNIP maintains the hematopoietic cell pool by switching the function of p53 under oxidative stress.* Cell metabolism, 2013. **18**(1): p. 75-85.

346. Jung, H., et al., *Thioredoxin-interacting protein regulates haematopoietic stem cell ageing and rejuvenation by inhibiting p38 kinase activity.* Nature Communications, 2016. **7**(1): p. 13674.

347. Lim, T.-Y., et al., *TXNIP loss expands Myc-dependent transcriptional programs by increasing Myc genomic binding.* PLoS Biology, 2023. **21**(3): p. e3001778.

348. Persyn, E., et al., *TXNIP promotes human NK cell development but is dispensable for NK cell functionality.* International Journal of Molecular Sciences, 2022. **23**(19): p. 11345.

349. Mizuno, K., et al., *Genes associated with the formation of germ cells from embryonic stem cells in cultures containing different glucose concentrations.* Molecular reproduction and development, 2006. **73**(4): p. 437-445.

350. Testa, G., et al., *Calorie restriction and dietary restriction mimetics: a strategy for improving healthy aging and longevity.* Current pharmaceutical design, 2014. **20**(18): p. 2950-2977.

351. Yu, B.P. and H.Y. Chung, *Stress resistance by caloric restriction for longevity.* Annals of the New York Academy of Sciences, 2001. **928**(1): p. 39-47.

352. Barja, G., *Endogenous oxidative stress: relationship to aging, longevity and caloric restriction.* Ageing research reviews, 2002. **1**(3): p. 397-411.

353. Miyahara, H., et al., *Thioredoxin interacting protein protects mice from fasting induced liver steatosis by activating ER stress and its downstream signaling pathways.* Scientific reports, 2022. **12**(1): p. 4819.

354. Menè, P. and A. Stoppacciaro, *Isolation and propagation of glomerular mesangial cells.* Kidney research: experimental protocols, 2009: p. 1-15.

355. Takemoto, M., et al., *A new method for large scale isolation of kidney glomeruli from mice.* The American journal of pathology, 2002. **161**(3): p. 799-805.

356. King, D.L. and G.W. Arendash, *Behavioral characterization of the Tg2576 transgenic model of Alzheimer's disease through 19 months.* Physiology & behavior, 2002. **75**(5): p. 627-642.

357. Luk, K.C., et al., *Pathological α-synuclein transmission initiates Parkinson-like neurodegeneration in nontransgenic mice.* Science, 2012. **338**(6109): p. 949-953.

358. Dai, Y., et al., *Striatal expression of a calmodulin fragment improved motor function, weight loss, and neuropathology in the R6/2 mouse model of Huntington's disease.* Journal of Neuroscience, 2009. **29**(37): p. 11550-11559.

359. Jaszczyk, A., A.M. Stankiewicz, and G.R. Juszczak, *Dissection of mouse hippocampus with its dorsal, intermediate and ventral subdivisions combined with molecular validation.* Brain sciences, 2022. **12**(6): p. 799.

360. Cazin, C., A. Chiche, and H. Li, *Evaluation of injury-induced senescence and in vivo reprogramming in the skeletal muscle.* JoVE (Journal of Visualized Experiments), 2017(128): p. e56201.

361. Hayflick, L., *The limited in vitro lifetime of human diploid cell strains.* Experimental cell research, 1965. **37**(3): p. 614-636.

362. Campisi, J. and F. d'Adda di Fagagna, *Cellular senescence: when bad things happen to good cells.* Nature reviews Molecular cell biology, 2007. **8**(9): p. 729-740.

363. Johmura, Y., et al., *Necessary and sufficient role for a mitosis skip in senescence induction.* Molecular cell, 2014. **55**(1): p. 73-84.

364. Stoltzman, C.A., et al., *Glucose sensing by MondoA: Mlx complexes: a role for hexokinases and direct regulation of thioredoxin-interacting protein expression.* Proceedings of the National Academy of Sciences, 2008. **105**(19): p. 6912-6917.

365. Yamamoto-Imoto, H., et al., *Age-associated decline of MondoA drives cellular senescence through impaired autophagy and mitochondrial homeostasis.* Cell Reports, 2022. **38**(9).

366. Chang, E. and C.B. Harley, *Telomere length and replicative aging in human vascular tissues.* Proceedings of the National Academy of Sciences, 1995. **92**(24): p. 11190-11194.

367. Chiu, C.-P. and C.B. Harley, *Replicative senescence and cell immortality: the role of telomeres and telomerase.* Proceedings of the Society for Experimental Biology and Medicine, 1997. **214**(2): p. 99-106.

368. Von Zglinicki, T., *Role of oxidative stress in telomere length regulation and replicative senescence.* Annals of the New York Academy of Sciences, 2000. **908**(1): p. 99-110.

369. Davalli, P., et al., *ROS, cell senescence, and novel molecular mechanisms in aging and age-related diseases.* Oxidative medicine and cellular longevity, 2016. **2016**.

370. Koundouros, N. and G. Poulogiannis, *Phosphoinositide 3-kinase/Akt signaling and redox metabolism in cancer.* Frontiers in oncology, 2018. **8**: p. 160.

371. Sanders, Y.Y., et al., *Histone modifications in senescence-associated resistance to apoptosis by oxidative stress.* Redox biology, 2013. **1**(1): p. 8-16.

372. Raffetto, J.D., et al., *Synopsis on cellular senescence and apoptosis.* Journal of vascular surgery, 2001. **34**(1): p. 173-177.

373. Nakanishi, A., et al., *Link between PI3K/AKT/PTEN pathway and NOX proteinin diseases.* Aging and disease, 2014. **5**(3): p. 203.

374. Noh, E.M., et al., *PTEN inhibits replicative senescence-induced MMP-1 expression by regulating NOX 4-mediated ROS in human dermal fibroblasts.* Journal of Cellular and Molecular Medicine, 2017. **21**(11): p. 3113-3116.

375. Maehama, T. and J.E. Dixon, *The tumor suppressor, PTEN/MMAC1, dephosphorylates the lipid second messenger, phosphatidylinositol 3, 4, 5-trisphosphate.* Journal of Biological Chemistry, 1998. **273**(22): p. 13375-13378.

376. Ogrunc, M., et al., *Oncogene-induced reactive oxygen species fuel hyperproliferation and DNA damage response activation.* Cell Death & Differentiation, 2014. **21**(6): p. 998-1012.

377. Murman, D.L. *The impact of age on cognition*. in *Seminars in hearing*. 2015. Thieme Medical Publishers.

378. Zapparoli, L., M. Mariano, and E. Paulesu, *How the motor system copes with aging: a quantitative meta-analysis of the effect of aging on motor function control.* Communications Biology, 2022. **5**(1): p. 79.

379. Alvarez, C.E., *On the origins of arrestin and rhodopsin.* BMC evolutionary biology, 2008. **8**: p. 1-13.

380. Haendeler, J., et al., *Antioxidants inhibit nuclear export of telomerase reverse transcriptase and delay replicative senescence of endothelial cells.* Circulation research, 2004. **94**(6): p. 768-775.

381. Jeong, S.-G. and G.-W. Cho, *Endogenous ROS levels are increased in replicative senescence in human bone marrow mesenchymal stromal cells.* Biochemical and biophysical research communications, 2015. **460**(4): p. 971-976.

382. Kim, J.-E., et al., *Vitamin C inhibits p53-induced replicative senescence through suppression of ROS production and p38 MAPK activity.* International journal of molecular medicine, 2008. **22**(5): p. 651-655.

383. Korolchuk, V.I., et al., *Mitochondria in cell senescence: is mitophagy the weakest link?* EBioMedicine, 2017. **21**: p. 7-13.

384. Nogueira, V., et al., *Akt determines replicative senescence and oxidative or oncogenic premature senescence and sensitizes cells to oxidative apoptosis.* Cancer cell, 2008. **14**(6): p. 458-470.

385. Ahmed, E.K., et al., *Protein modification and replicative senescence of WI-38 human embryonic fibroblasts.* Aging cell, 2010. **9**(2): p. 252-272.

386. Hutter, E., et al., *Senescence-associated changes in respiration and oxidative phosphorylation in primary human fibroblasts.* Biochemical Journal, 2004. **380**(3): p. 919-928.

387. Sitte, N., et al., *Lipofuscin accumulation in proliferating fibroblasts in vitro: an indicator of oxidative stress.* Experimental gerontology, 2001. **36**(3): p. 475-486.

388. Sitte, N., et al., *Protein oxidation and degradation during proliferative senescence of human MRC-5 fibroblasts.* Free Radical Biology and Medicine, 2000. **28**(5): p. 701-708.

389. Lawless, C., et al., *A stochastic step model of replicative senescence explains ROS production rate in ageing cell populations.* PloS one, 2012. **7**(2): p. e32117.

390. Cairns, R.A., I.S. Harris, and T.W. Mak, *Regulation of cancer cell metabolism.* Nature Reviews Cancer, 2011. **11**(2): p. 85-95.

391. Niwa, K., et al., *Redox regulation of PI3K/Akt and p53 in bovine aortic endothelial cells exposed to hydrogen peroxide.* Antioxidants and Redox Signaling, 2003. **5**(6): p. 713-722.

392. Chatterjee, S., et al., *Membrane depolarization is the trigger for PI3K/Akt activation and leads to the generation of ROS.* American Journal of Physiology-Heart and Circulatory Physiology, 2012. **302**(1): p. H105-H114.

393. Chen, J.s., et al., *Involvement of PI3K/PTEN/AKT/mTOR pathway in invasion and metastasis in hepatocellular carcinoma: association with MMP-9.* Hepatology Research, 2009. **39**(2): p. 177-186.

394. Chen, Q., et al., *Akt phosphorylates p47phox and mediates respiratory burst activity in human neutrophils.* The Journal of Immunology, 2003. **170**(10): p. 5302-5308.

395. Usatyuk, P.V., et al., *Role of c-Met/phosphatidylinositol 3-kinase (PI3k)/Akt signaling in hepatocyte growth factor (HGF)-mediated lamellipodia formation, reactive oxygen species (ROS) generation, and motility of lung endothelial cells.* Journal of Biological Chemistry, 2014. **289**(19): p. 13476-13491.

396. He, X. and Q. Ma, *Redox regulation by nuclear factor erythroid 2-related factor 2: gatekeeping for the basal and diabetes-induced expression of thioredoxin-interacting protein.* Molecular pharmacology, 2012. **82**(5): p. 887-897.

397. Katsu-Jiménez, Y., et al., *Absence of TXNIP in humans leads to lactic acidosis and low serum methionine linked to deficient respiration on pyruvate.* Diabetes, 2019. **68**(4): p. 709-723.

398. Hajduch, E., G.J. Litherland, and H.S. Hundal, *Protein kinase B (PKB/Akt)–a key regulator of glucose transport?* FEBS letters, 2001. **492**(3): p. 199-203.

399. Tan, S.-X., Y. Ng, and D.E. James, *Akt inhibitors reduce glucose uptake independently of their effects on Akt.* Biochemical Journal, 2010. **432**(1): p. 191-198.

400. Hong, S.Y., et al., *Oncogenic activation of the PI3K/Akt pathway promotes cellular glucose uptake by downregulating the expression of thioredoxin-interacting protein.* Cellular signalling, 2016. **28**(5): p. 377-383.

401. Dolado, I. and A.R. Nebreda, *AKT and oxidative stress team up to kill cancer cells.* Cancer cell, 2008. **14**(6): p. 427-429.

402. Johnson, S.C., P.S. Rabinovitch, and M. Kaeberlein, *mTOR is a key modulator of ageing and age-related disease.* Nature, 2013. **493**(7432): p. 338-345.

403. Sheu, M.L., et al., *Activation of phosphoinositide 3-kinase in response to high glucose leads to regulation of reactive oxygen species-related nuclear factor-κB activation and cyclooxygenase-2 expression in mesangial cells.* Molecular pharmacology, 2004. **66**(1): p. 187-196.

404. Zhao, Y., et al., *ROS signaling under metabolic stress: cross-talk between AMPK and AKT pathway.* Molecular cancer, 2017. **16**: p. 1-12.

405. Nakaso, K., et al., *PI3K is a key molecule in the Nrf2-mediated regulation of antioxidative proteins by hemin in human neuroblastoma cells.* FEBS letters, 2003. **546**(2-3): p. 181-184.

406. DeNicola, G.M., et al., *Oncogene-induced Nrf2 transcription promotes ROS detoxification and tumorigenesis.* Nature, 2011. **475**(7354): p. 106-109.

407. Sporn, M.B. and K.T. Liby, *NRF2 and cancer: the good, the bad and the importance of context.* Nature Reviews Cancer, 2012. **12**(8): p. 564-571.

408. Fuhrmann-Stroissnigg, H., et al., *Identification of HSP90 inhibitors as a novel class of senolytics.* Nature communications, 2017. **8**(1): p. 422.

409. Delenko, J.G., et al., *Quercetin, a senolytic, enhances endometrial stromal cell decidualization through AKT and p53 signaling and reveals the potential role of senescent stromal cells in endometriosis.* medRxiv, 2023: p. 2023.08. 30.23294800.

410. Zoico, E., et al., *Senolytic effects of quercetin in an in vitro model of pre-adipocytes and adipocytes induced senescence.* Scientific reports, 2021. **11**(1): p. 23237.

411. Hohmann, M.S., et al., *Quercetin enhances ligand-induced apoptosis in senescent idiopathic pulmonary fibrosis fibroblasts and reduces lung fibrosis in vivo.* American journal of respiratory cell and molecular biology, 2019. **60**(1): p. 28-40.

412. Luongo, F., et al., *PTEN tumor-suppressor: the dam of stemness in cancer.* Cancers, 2019. **11**(8): p. 1076.

413. Tsao, H., et al., *Relative reciprocity of NRAS and PTEN/MMAC1 alterations in cutaneous melanoma cell lines.* Cancer research, 2000. **60**(7): p. 1800-1804.

414. Nogueira, C., et al., *Cooperative interactions of PTEN deficiency and RAS activation in melanoma metastasis.* Oncogene, 2010. **29**(47): p. 6222-6232.

415. Vasudevan, K.M., et al., *Suppression of PTEN expression is essential for antiapoptosis and cellular transformation by oncogenic Ras.* Cancer research, 2007. **67**(21): p. 10343-10350.

416. Deng, J., et al., *The role of TXNIP in cancer: a fine balance between redox, metabolic, and immunological tumor control.* British Journal of Cancer, 2023. **129**(12): p. 1877-1892.

417. Seidler, R.D., et al., *Motor control and aging: links to age-related brain structural, functional, and biochemical effects.* Neuroscience & Biobehavioral Reviews, 2010. **34**(5): p. 721-733.

418. Chutkow, W.A., et al., *Deletion of the α-arrestin protein Txnip in mice promotes adiposity and adipogenesis while preserving insulin sensitivity.* Diabetes, 2010. **59**(6): p. 1424-1434.

419. Xue, T., et al., *Embryonic Deletion of TXNIP in GABAergic Neurons Enhanced Oxidative Stress in PV+ Interneurons in Primary Somatosensory Cortex of Aging Mice: Relevance to Schizophrenia.* Brain Sciences, 2022. **12**(10): p. 1395.

420. Katturajan, R., et al., *Immunomodulatory role of thioredoxin interacting protein in cancer's impediments: current understanding and therapeutic implications.* Vaccines, 2022. **10**(11): p. 1902.

421. Shao, Y., et al., *TXNIP regulates germinal center generation by suppressing BCL-6 expression.* Immunology letters, 2010. **129**(2): p. 78-84.

422. Sheth, S., et al., *Hepatocellular carcinoma in Txnip-deficient mice.* Oncogene, 2006. **25**(25): p. 3528-3536.

423. Lopez-Otin, C., et al., *The hallmarks of aging. Cell 153, 1194e1217*. 2013.